

**Development of Nickel-Catalyzed Cross-Electrophile Coupling of Aryl Chlorides and
Triflates with Alkyl Halides**

By

Seoyoung Kim

A dissertation submitted in partial fulfillment of
the requirements for the degree of

Doctor of Philosophy
(Chemistry)

at the

UNIVERSITY OF WISCONSIN-MADISON

2023

Date of final oral examination: 05/30/2023

The dissertation is approved by the following members of the Final Oral Committee:

Daniel J. Weix, Wayland E. Noland Distinguished Professor, Chemistry
John F. Berry, Lester R. McNall Professor, Chemistry
Jennifer M. Schomaker, Professor, Chemistry
Zachary K. Wickens, Assistant Professor

Dedication

To all those who have supported me throughout this journey.

사랑하는 하나님, 가족, 그리고 친구들에게

Biographical Sketch

Seoyoung Kim was born in Gwangju, South Korea, and raised in Mokpo, South Korea. After graduating from Woodstock School, in Mussoorie India in 2011, she enrolled in Bard College for her undergraduate studies. In the summer after her freshman year, she began researching through the Bard Summer Research Institute under the supervision of Professor Tanay Kesharwani, publishing an article on the development of a synthetic strategy to benzothiophenes via electrophilic cyclization. She then worked under the supervision of Professor Emily C. McLaughlin studying and completing her senior thesis on the efforts toward the synthesis of natural pigment violacein analogs.

After graduating with a Bachelor of Arts in Chemistry in 2015, she began her graduate studies at the University of Rochester. Under the supervision of Professor Daniel J. Weix, she worked on developing nickel-catalyzed cross-electrophile coupling reactions for the formation of carbon-carbon bonds. She received a Master's of Science from the University of Rochester in 2017. In the summer of 2017, she relocated with Professor Daniel J. Weix and his group to the University of Wisconsin-Madison where she continued to work on methods to engage inert electrophiles in nickel-catalyzed cross-coupling reactions.

The following publications were a result of work conducted during doctoral research:

Kim, S.; Goldfogel, M. J.; Gilbert, M. M.; Weix, D. J. "Nickel-Catalyzed Cross-Electrophile Coupling of Aryl Chlorides with Primary Alkyl Chlorides" *J. Am. Chem. Soc.* **2020**, *142*, 9902–9907.

Huihui, K. M. M.; Caputo, J. A.; Melchor, Z.; Olivares, A. M.; Spiewak, A. M.; Johnson, K. A.; DiBenedetto, T. A.; Kim, S.; Ackerman L. K. G.; Weix, D. J. "Decarboxylative Cross-Electrophile Coupling of N-Hydroxyphthalimide Esters with Aryl Iodides" *J. Am. Chem. Soc.* **2016**, *138*, 5016–5019.

Acknowledgments

First and foremost, I have to say my gratitude to my advisor Professor Daniel Weix. I cannot express enough how much I appreciate your support throughout my time at grad school. Your enthusiasm for science and discovery have always been inspiring. It is amazing how it takes just a conversation with you for me to be excited again to try new ideas when I am stuck. You have also shown me how to care for the individual, the group, the department, and furthermore, the scientific community by paying attention to details and continuously conversing. Your guidance has helped me grow as an experimentalist, a thinker, and a caring individual. I was able to keep at it despite the longer time at grad school thanks to your support.

I would like to thank my committee members, Professors Jen Schomaker, John Berry, and Zach Wickens. From the occasional, friendly nudge, “How is it going? Let me know if I can help with anything,” in front of the elevator to the insightful science and life conversations, I appreciate the honest feedback, encouragement, and support. Thank you all for our mentorship.

The move would have been extra difficult if it weren’t for the people in the Department of Chemistry at the UW-Madison. I would like to thank Karen Stephens for making settling down to Madison smoothly, warm conversations and baked goods, and memorable times spent together. I would also like to thank the Schomaker Group, Yoon Group, and Stahl Group for the kind welcomes and showing us the Chemistry Department and Madison.

It has been an honor and a pleasure to be a part of the Weix Group. I have had the privilege to overlap with so many amazing people. I am very grateful for all the past and present members of the Weix Group. Thank you for the support, all the conversations, and memories to cherish.

I would also like to thank my other friends inside and outside of the Chemistry Department. Finding a Korean church community is important to me, and I am thankful for communities both in

Rochester and Madison. I am especially grateful to Diana Wang, Jeehyae Son, Soobin Im, and Eunjin Kim for their continuous encouragement, prayer, and good times we have shared.

Finally, I would like to thank my family: mom, dad, Mokyoung, Aelin, and Sulin for their unconditional and endless love, support, and prayer. Thank you for always being there. I am very grateful for all of you.

Abstract

Cross-coupling is one of the most commonly used reactions in synthetic chemistry. While palladium-catalyzed cross-coupling is well-developed and established, cross-electrophile coupling is significantly younger field of study. In this approach two carbon electrophiles are directly coupled under reductive conditions, avoiding the need to prepare organometallic reagents. This is an attractive strategy because these reactions proceed through mild conditions, have high functional group tolerance, and employ readily available coupling partners. Nickel-catalyzed cross-electrophile couplings have seen considerable success in the past decade, initially in the coupling of organic iodides and later organic bromides. Despite these advances, the cross-coupling with the more abundant and inexpensive organic chlorides remain elusive due to their low reactivity. Furthermore the nickel-catalyzed cross-coupling of aryl triflates presents analogous challenges due to their differential reactivity. This thesis presents our studies to address these limitations. Through a combination of: (1) new ligand application, (2) fine tuning of alkyl electrophile reactivity through in situ halide exchange, (3) detailed mechanistic investigation of elementary steps, we demonstrate the nickel-catalyzed cross-electrophile coupling of these traditionally inert organic coupling partner. This dissertation is presented as follows:

Chapter 1 is an introduction to cross-coupling strategies. Common palladium-catalyzed cross-coupling methods are discussed and their origin of cross-selectivity is highlighted. This is contrasted to cross-electrophile approaches of which mechanism is less well-understood. Early reports on nickel-catalyzed cross-electrophile coupling are presented and how mechanistic studies have elucidated the origin of cross-selectivity in these processes. Finally, the challenges of applying aryl chlorides in these first generation approaches are briefly discussed.

Chapter 2 describes the development of nickel-catalyzed cross-electrophile coupling of aryl chlorides with primary alkyl chlorides to form C(sp²)–C(sp³) bonds. Investigation of ligands on selectivity and in situ halide exchange on the activation of C(sp³)–Cl bonds are detailed.

Chapter 3 discusses a strategy for nickel-catalyzed cross-electrophile coupling of aryl triflates with alkyl halides. The development of reaction conditions for differing aryl electronics and mechanistic insights are described in detail. Mechanistically driven optimization and the extent of halide exchange to modulate alkyl halide reactivity are also discussed.

Contributors and Funding Sources

This thesis was supervised by a dissertation committee consisting of Professors Daniel J. Weix (advisor), John F. Berry, Jennifer M. Schomaker, and Zachary K. Wickens of the Department of Chemistry. The author performed all experimental procedures in this dissertation unless specified below:

Chapter 2: The scope of the cross-electrophile coupling of aryl chlorides with alkyl chlorides was investigated by Dr. Matthew J. Goldfogel. Isolation and characterization of compounds synthesized using iodide as halide source were assisted by Dr. Michael M. Gilbert.

Chapter 3: The ligand and additive optimization, substrate scope investigation, and initial mechanistic studies were conducted by Dr. Matthew J. Goldfogel. Mechanistic studies and isolation and characterization of compounds synthesized using condition C were assisted by Dr. Daniel C. Salgueiro.

The reported work was supported by the University of Rochester, the University of Wisconsin-Madison, and the National Institutes of Health (R01GM097243).

Table of Contents

Dedication.....	i
Biographical Sketch	ii
Acknowledgments	iii
Abstract.....	v
Contributors and Funding Sources	vii
Table of Contents	viii
List of Figures	x
List of Tables	xi
List of Symbols and Abbreviations	xii
Chapter 1: An Introduction to Nickel-Catalyzed Cross-Electrophile Coupling Reactions	
1.....	
1.1. Significance of Developing Methods for the Formation of C(sp ²)–C(sp ³) Bonds.....	2
1.2. Nickel-Catalyzed Cross-Electrophile Coupling Reactions.....	4
1.3. General Proposal for Achieving Cross-Selectivity.....	7
1.4. References.....	10
Chapter 2: Nickel-Catalyzed Cross-Electrophile Coupling of Aryl Chlorides with Primary Alkyl Chlorides	12
2.1. Introduction.....	13
2.2. Reaction Optimization.....	14
2.3. Reaction Scope.....	17
2.4. Mechanistic Studies.....	19
2.5. Conclusions.....	35
2.6. Experimental.....	35
2.6.1. Reagents.....	35
2.6.2. Methods.....	37
2.6.3. General Procedures.....	39
2.6.3.1. General Procedure for Reaction Optimization.....	39
2.6.3.2. General Procedure A.....	41
2.6.3.3. General Procedure B.....	42
2.6.3.4. Preparative-Scale Benchtop Procedure.....	43
2.6.3.5. General procedure for equilibrium study.....	45
2.6.4. Specific Procedures and Product Characterization.....	45
2.7. References.....	70
Chapter 3: Nickel-Catalyzed Cross-Electrophile Coupling of Aryl Triflates with Alkyl Halides	77
3.1. Introduction.....	78
3.2. Reaction Optimization.....	82

3.2.1. Aryl Triflates and Alkyl Bromides.....	82
3.2.2. Aryl Triflates and Alkyl Chlorides.....	84
3.3. Reaction Scope.....	85
3.4. Mechanistic Studies.....	87
3.4.1. Comparisons of Reactions with Phen and PyBCam ^{CN}	88
3.4.2. Role of the Aryl Zinc Species.....	90
3.5. Complex Role of the Lithium Additives.....	92
3.6. Discussion.....	94
3.6.1. Ligand Trends.....	95
3.6.2. Transmetalation as a Side Reaction.....	95
3.6.3. Halide Exchange beyond Finkelstein.....	97
3.6.4. Proposed Mechanism.....	99
3.7. Conclusions.....	100
3.8. Experimental.....	100
3.8.1. General Information.....	100
3.8.1.1. Reagents.....	100
3.8.1.2. Methods.....	108
3.8.2. General Procedures.....	110
3.8.2.1. General Procedure for Reaction Optimization with Electron Poor Arenes.....	110
3.8.2.2. General Procedure for Electron Poor Arenes.....	112
3.8.2.3. General Procedure for Reaction Optimization with Electron Rich Arenes.....	113
3.8.2.4. General Procedure for Electron Rich Arenes.....	113
3.8.2.5. General Procedure for Preparative-Scale Benchtop Reactions.....	114
3.8.3. Product Characterization.....	116
3.9. References.....	144

List of Figures

Figure 1.1. Challenges of Using Alkyl Electrophiles with β -hydrogen atoms for Coupling Partners..2	
Figure 1.2. Cross-Coupling Reactions Using Nucleophilic Organometallic Reagents to Form C(sp ³)–C(sp ²) Bonds.....	3
Figure 1.3. Comparisons of Selectivity Challenges of Cross-Coupling and Cross-Electrophile Coupling.....	5
Figure 1.4. Cross-Electrophile Coupling of Aryl Halides with Alkyl Halides.....	6
Figure 1.5. Initial Report on Aryl Chlorides in Cross-Electrophile Coupling	6
Figure 1.6. Proposed Route for Cross-Selectivity	7
Figure 1.7. General Mechanism for Cross-Coupling Reactions.....	8
Figure 1.8. Proposed Mechanism of Cross-Electrophile Coupling of Aryl Iodides with Alky Iodides.	9
Figure 2.1. Challenges in the Cross-Electrophile Coupling Organic Chlorides.....	13
Figure 2.2. Cross-Selective Coupling with Primary Alkyl Chlorides.	14
Figure 2.3. Reaction Scope for the Nickel-Catalyzed Coupling of Aryl Chlorides with Alkyl Chlorides.	19
Figure 2.4. Evidence for Bromide Co-catalysis.....	21
Figure 2.5. Evidence for Iodide Co-catalysis.....	22
Figure 2.6. Reaction Time Course with Catalytic Amount of Bromide.....	28
Figure 3.1. Challenges for Using Aryl Triflates in Cross-Electrophile Coupling Reactions.....	79
Figure 3.2. Aryl C–O Electrophiles in Cross-Coupling Reactions.....	81
Figure 3.3. A Strategy for Selective Cross-Coupling Between Two Electrophiles.....	82
Figure 3.4. Scope of the Cross-Electrophile Coupling of Aryl Triflates with Alkyl Halides Under Modular Conditions.	86
Figure 3.5. Assessment of the Presence of Organometallic Reagents.	89
Figure 3.6. Effect of LiCl on (phen)NiCl ₂ Catalyzed Reaction.....	90
Figure 3.7. Competition Study Between Phenyl Zinc and Aryl Triflate.	92
Figure 3.8. Competition Study Between Alkyl Zinc and Alkyl Bromide.	92
Figure 3.9. Effect of Li Additives on Product Formation.	93
Figure 3.10. Correlation Between Lithium Iodide Amounts and Alkyl Chloride Consumption.	94
Figure 3.11. Identity of Halide and the Rate of Radical Generation.....	98
Figure 3.12. Proposed Mechanism for the Cross-Electrophile Coupling of Aryl Triflates with Alkyl Halides.....	100

List of Tables

Table 2.1. Effect of Ligands and Additives on the Cross-Electrophile Coupling of Chlorobenzene with Chlorooctane.....	15
Table 2.2. Halide Effect from Nickel Precatalyst.....	16
Table 2.3. Effect of Various Halide Additives.....	16
Table 2.4. Deletion Control Experiments.....	20
Table 2.5. Examination of Alternative Reductants and Additives.....	20
Table 2.6. Optimization of Iodide Concentration.....	22
Table 2.7. Effect of LiCl on the Equilibrium Between Chlorooctane and Bromooctane in the Presence of LiBr.....	24
Table 2.8. Effect of LiCl and ZnCl ₂ on the Equilibrium Between Chlorooctane and Bromooctane.....	25
Table 2.9. Equilibrium Between Chlorooctane and Bromooctane Under Mock Catalytic Conditions at Different Levels of Conversion.....	26
Table 2.10. Effect of LiCl on the Equilibrium Between Chlorooctane and Iodoctane in the Presence of LiI.....	29
Table 2.11. Effect of LiCl on the Equilibrium Between Chlorooctane and Iodoctane in the Presence of ZnI ₂	30
Table 2.12. LiCl Effect on the Equilibrium Between Chlorooctane and Iodoctane in the Presence of LiI.....	31
Table 2.13. LiCl Effect on the Equilibrium Between Chlorooctane and Iodoctane in the Presence of ZnI ₂	32
Table 2.14. Equilibrium Between Chlorooctane and Iodoctane Under Mock Catalytic Conditions at Different Turnover Numbers (TON).....	33
Table 3.1. Ligand Effects on the Cross-Electrophile Coupling of Aryl Triflates with Alkyl Bromides. ^a	83
Table 3.2. Introducing Halide Sources Through Nickel Catalyst and Salt Additives.....	84

List of Symbols and Abbreviations

-	minus, negative, or hyphen
[M]	metal
%	percent
°C	degrees Celsius
+	plus or positive
¹³ C	carbon-13
¹⁹ F	fluorine-19
¹ H	proton
Alk	alkyl
aq	aqueous
Ar	aryl
B	boron
B(OH) ₂	boronic acid
Boc	<i>tert</i> -butoxycarbonyl
Bpin	pinacolato boron
Br	bromide
C	carbon
C(sp ²)	carbon with sp hybridized orbitals
C(sp ³)	carbon with sp ² hybridized orbitals
Cbz	benzyloxycarbonyl
CDCl ₃	chloroform-d
Cl	chloride
cm	centimeter
cod	1,5-cyclooctadiene
d	doublet
D	deuterium
δ	delta
DI	deionized
dme	1,2-dimethoxyethane
ee	enantiomeric excess
equiv	equivalents
Et	ethyl
Et ₂ O	diethyl ether
EtOAc	ethyl acetate
eV	electron volts
Fe	iron
FID	Flame Ionization Detector
FTIR	Fourier transform infrared
g	gram
GC	gas chromatography

GCMS	gas chromatography mass spectrometry
H	hydrogen
h	hour(s)
HRMS	High Resolution Mass Spectrometry
Hz	hertz
I	iodide
<i>I</i> -PrOH	isopropanol
IR	Infrared
<i>J</i>	coupling constant
<i>k</i>	equilibrium constant
m	multiplet
m/z	mass-to-charge ratio
Me	methyl
mg	milligram
Mg	magnesium
MgSO ₄	magnesium sulfate
MHz	megahertz
min	minute(s)
mL	milliliter
mmol	millimole
Mn	manganese
mol	mole
MS	Mass Spectrometry
MW	molecular weight
N	nitrogen atom
N ₂	nitrogen
NaHSO ₄	sodium bisulfate
NaI	sodium iodide
Ni	nickel
NMP	N-methyl-2-pyrolidinone
NMR	Nuclear Magnetic Resonance
o	ortho
OH	alcohol
OMe	methoxy
ONf	nonaflate
OTf	triflate
p	pi
Pd	palladium
ppm	parts per million
psi	pounds per square inch
PTFE	polytetrafluoroethylene, teflon
quart	quartet
R-[M]	organometallic

R–X	alkyl halide
r.t	room temperature
rpm	revolutions per minute
s	singlet or second
Si	silicon
sp	linear hybridized orbitals with 50% s and 50% p character
sp ²	trigonal planar hybridized orbitals with 33% s and 67% p character
sp ³	tetrahedral hybridized orbitals with 25% s and 75% p character
t	triplet
T	temperature
βBu	tert-butyl
TDAE	1,2,2-tetrakis(dimethylamino)ethylene
THF	tetrahydrofuran
TLC	thin-layer chromatography
TMS	trimethylsilyl
TMSCl	chlorotrimethylsilane
V	volt
wt	weight
X	halide
XEC	cross-electrophile coupling
Zn	zinc
ZnBr ₂	zinc bromide
ZnX ₂	zinc halide
β	beta
μ	micro
μL	microliter

Chapter 1: An Introduction to Nickel-Catalyzed Cross-Electrophile Coupling Reactions

1.1. Significance of Developing Methods for the Formation of C(sp²)–C(sp³) Bonds.

Transition metal-catalyzed cross-coupling of carbon nucleophiles and carbon electrophiles has become a powerful synthetic tool to form carbon-carbon bonds, and numerous applications can be found in discovery research and production.^{1,2} With the advances in methodologies for cross-coupling reactions, the coupling of sp-, sp²-, sp³- hybridized carbon nucleophiles with aryl or alkenyl electrophiles is widely studied. This dissertation focuses on the formation of C(sp²)–C(sp³) bonds through cross-electrophile coupling, which is an active area of research interest in the Weix group and others.^{3,4,5,6}

Alkyl electrophiles containing β -hydrogen atoms were initially considered unfavorable substrates for the transition metal-catalyzed cross-coupling reactions.⁶ Often, the oxidative addition of alkyl halides to a metal center is considerably more difficult than the oxidative addition of aryl or alkenyl halides, because C(sp³)–X bonds are more electron-rich than C(sp²)–X bonds. The resulting alkyl metal intermediate is prone to undesirable side reactivities, such as β -hydride elimination or hydrodehalogenation, which can outcompete both intermolecular transmetalation and reductive elimination (Figure 1.1).⁷ Such unwanted reactivity of alkyl electrophiles makes generation and broad applicability of C(sp³)-organometallics challenging.⁷

Figure 1.1. Challenges of Using Alkyl Electrophiles with β -hydrogen atoms for Coupling Partners.

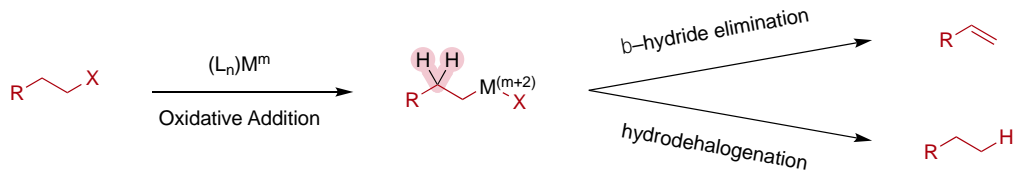
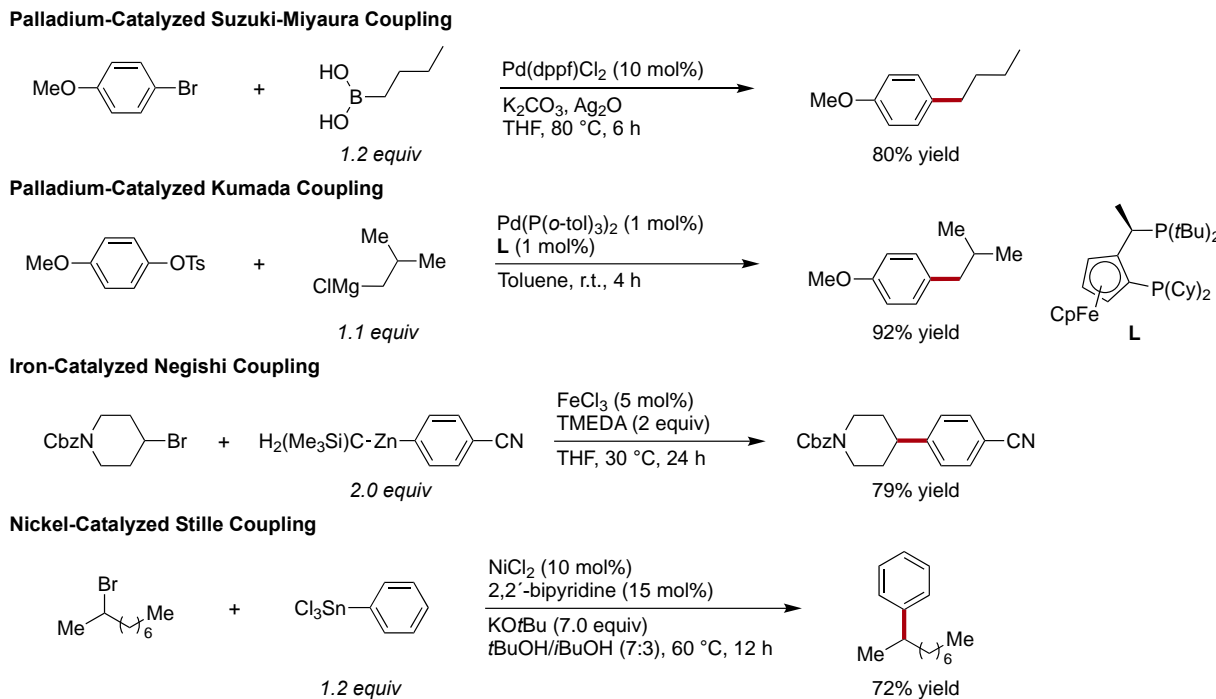


Figure 1.2. Cross-Coupling Reactions Using Nucleophilic Organometallic Reagents to Form C(sp³)–C(sp²) Bonds.



A few examples using transition metal-catalyzed cross-coupling have shown that alkyl nucleophiles derived from the corresponding electrophile can be used in cross-coupling reactions. (Figure 1.2) The reactions use either an aryl nucleophile or an alkyl nucleophile to make C(sp²)–C(sp³) bonds. Examples include carbon nucleophiles such as boronic acids (Suzuki-Miyaura Coupling),⁸ Grignard reagents (Kumada Coupling),⁹ organozinc reagents (Negishi Coupling),¹⁰ and organotin reagents (Stille Coupling).¹¹ These approaches require the use of an organometallic reagent in conjunction with an organohalide.

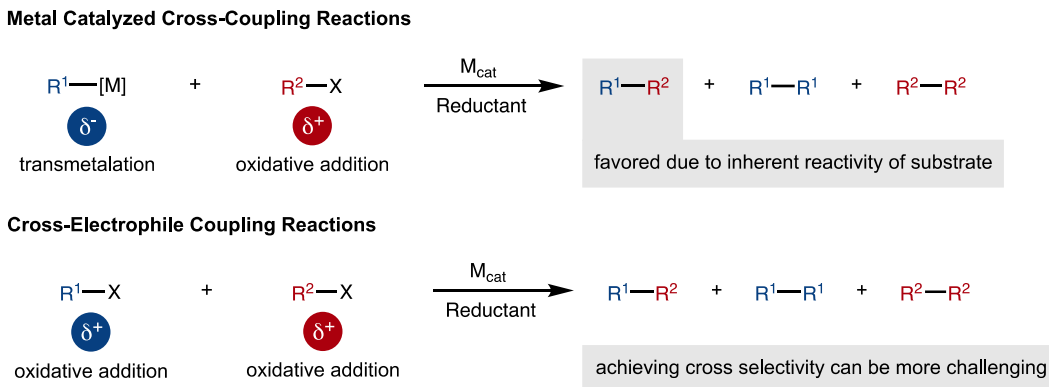
While these conventional cross-coupling reactions are useful in making C–C bonds, the nucleophilic carbon reagents continue to present challenges. For example, the most widely used organoboron nucleophiles have limited commercial availability and some are unstable.¹² As a result, organoboron and other organometallic reagents are synthesized as needed and exclusion of oxygen and moisture is frequently necessary. In some cases, a stoichiometric base additive is required to

facilitate transmetalation between the organometallic reagent and the metal. This can place limitations on the use of functional groups that are electrophilic or that have acidic protons. In addition, organometallic reagents are often prepared from the corresponding organic halides in a separate step. To address the difficulties associated with organometallic reagents, our group has reported methods to directly couple two different carbon electrophiles through nickel catalysis.

1.2. Nickel-Catalyzed Cross-Electrophile Coupling Reactions.

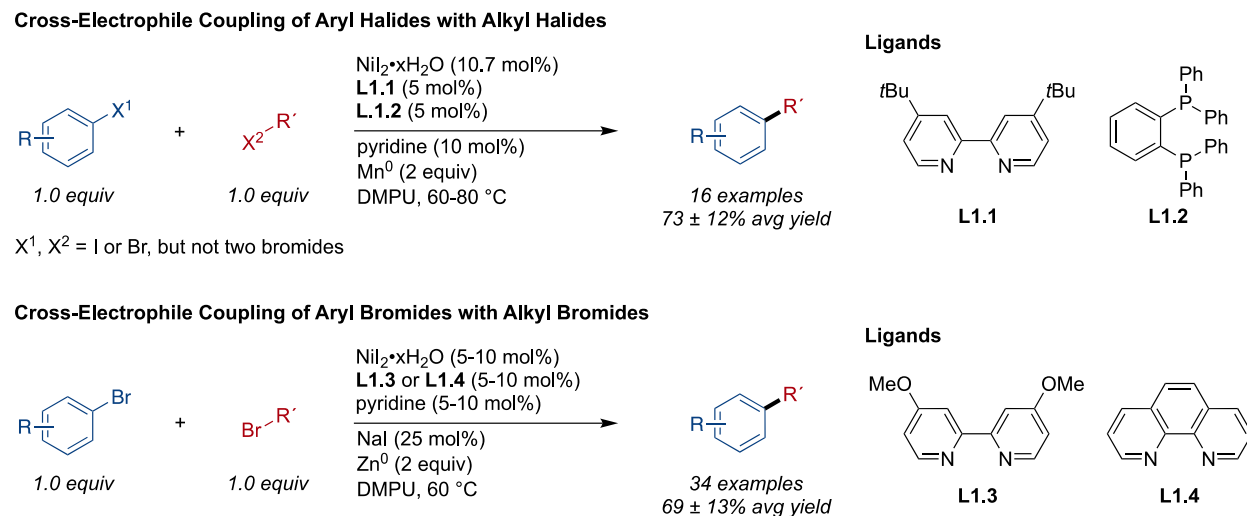
Cross-electrophile coupling reactions provide an opportunity to explore relatively stable, diverse, and readily available carbon electrophiles as coupling partners. This method offers an advantage in that the separate preparation of an organometallic reagent can be avoided and a wide variety of functional groups can be tolerated. One of the challenges, however, is ensuring highly selective cross-coupling of the two electrophiles. Unlike the cross-coupling of a nucleophile with an electrophile, where the selectivity of the two coupling partners comes from the inherent electronic differences in their reactivity, the selectivity in cross-electrophile coupling reactions is not immediately obvious. As a result, reductive homocoupling, hydrodefunctionalization, and catalyst deactivation are potential side reactions.¹³ Therefore, fine tuning of the reaction conditions is important in achieving good selectivity in cross-electrophile coupling.

Figure 1.3. Comparisons of Selectivity Challenges of Cross-Coupling and Cross-Electrophile Coupling.



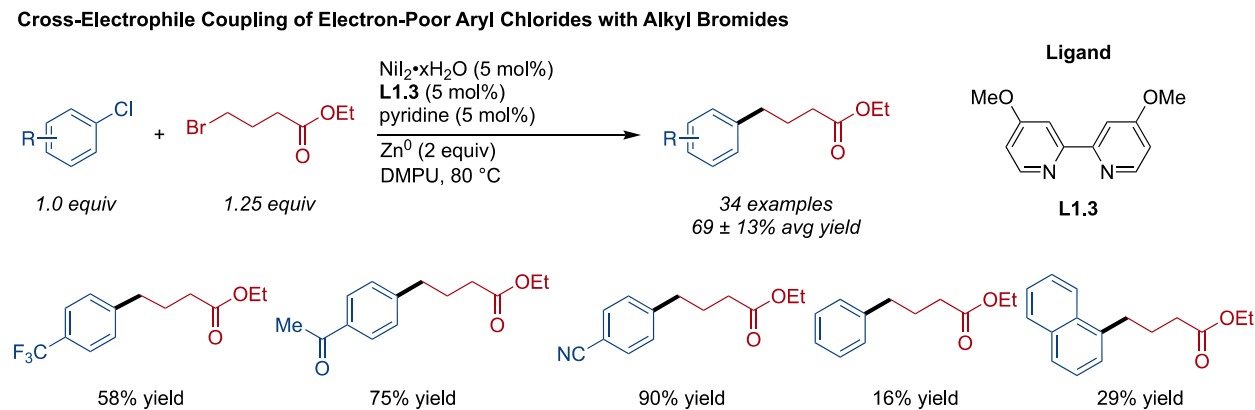
Our group has reported methods for cross-coupling of two unactivated electrophiles, such as an aryl halide and an alkyl halide under reductive conditions (Figure 1.4, top).³ The earth abundant metal nickel has been employed for this catalytic reaction due to its low cost and unique reactivity profile arising from different common oxidation states. Our initial report in 2010 demonstrated that the combination of a bipyridine nickel catalyst and a bisphosphine nickel catalyst afforded the cross-coupled product in high yields. Under these reaction conditions, coupling of primary, secondary, and neopentyl alkyl halides with aryl iodides was achieved. Coupling of aryl bromides with alkyl bromides was demonstrated with adjustments to the previously reported reaction conditions. It required the addition of sodium iodide, bipyridine or phenanthroline ligand, and zinc instead of manganese as a reductant.⁴ A broad range of functional groups were tolerated in this reaction. Notably, high cross-selectivity was achieved using equimolar amounts of each coupling partner.

Figure 1.4. Cross-Electrophile Coupling of Aryl Halides with Alkyl Halides.



In these initial reports, our nickel-catalyzed cross-coupling protocol of aryl bromides/iodides with alkyl bromides/iodides was general and selective (Figure 1.4). However, the coupling of aryl chlorides (e.g., chlorobenzene) was limited to activated substrates. A minor modification of the conditions used for the coupling of electron-rich aryl bromides (Figure 1.4, bottom) improved selectivity for the coupling of electron-poor aryl chlorides with alkyl bromides (Figure 1.5). Omission of sodium iodide, higher reaction temperature, and an excess of alkyl bromide provided the cross-coupled product in high yields.⁴

Figure 1.5. Initial Report on Aryl Chlorides in Cross-Electrophile Coupling.

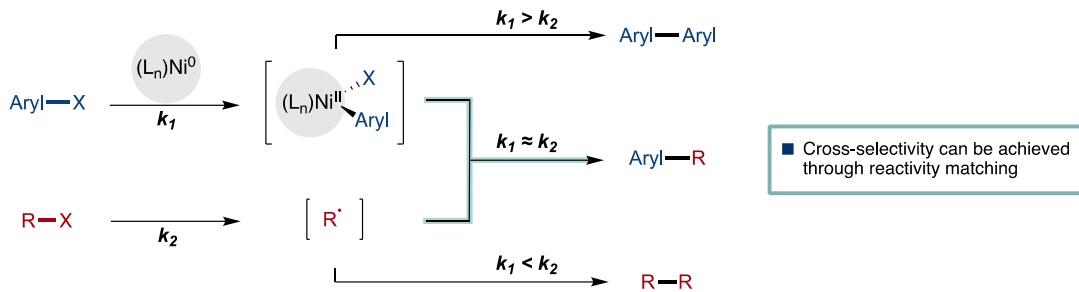


While a good selectivity was achieved for electron poor aryl chlorides, aryl and alkyl bromides and iodides, the coupling of unactivated aryl chlorides remains a challenge. Aryl chlorides are often more readily available and less expensive than aryl bromides or iodides. The ability to couple abundant chloroarenes will contribute in expanding the scope of cross-electrophile coupling.

1.3. General Proposal for Achieving Cross-Selectivity.

The origin of selectivity in a radical chain mechanism occurs due to reactivity differences between $C(sp^2)$ - and $C(sp^3)$ - electrophiles with a nickel catalyst. $C(sp^2)$ electrophiles (aryl and alkenyl) proceed through a two electron oxidative addition. $C(sp^3)$ electrophiles (alkyl) generally react with nickel in a single electron fashion. If the relative rates of each process are matched, then high cross-selectivity should be observed (Figure 1.6).

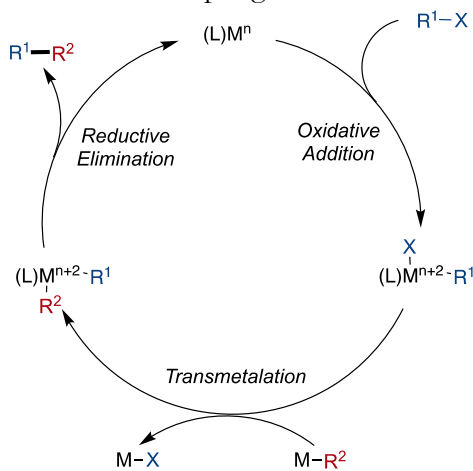
Figure 1.6. Proposed Route for Cross-Selectivity.



The well-established and general mechanism of metal catalyzed cross-coupling reactions consists of three elementary steps: oxidative addition, transmetalation, and reductive elimination (Figure 1.7). On the other hand, the mechanism of cross-electrophile coupling is still developing. In 2013 our group reported a detailed mechanistic study that suggests these reactions proceed through a radical chain mechanism.¹⁴ This type of mechanism, where a radical chain reaction is embedded in the catalytic cycle, was first proposed by Hegedus for the stoichiometric reaction of preformed

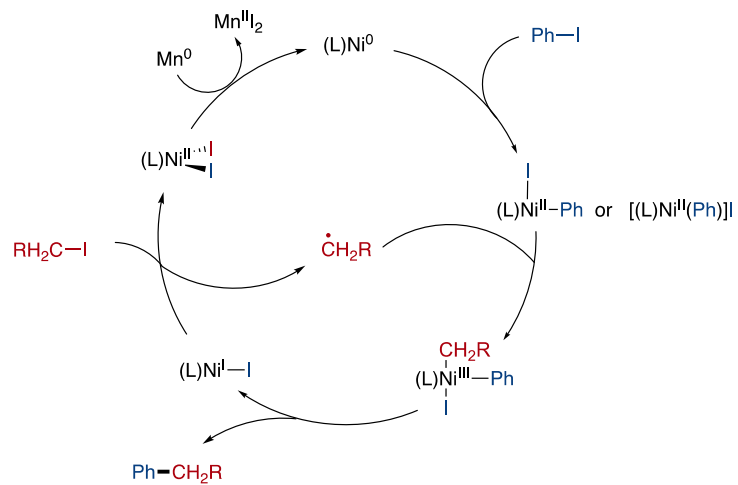
allylnickel(II) reagents with organohalides.¹⁵ However, later studies by Hegedus and Kochi suggested an alternative mechanism wherein transmetalation between a transient alkynickel(III) species and the starting allylnickel(II) complex occurs instead of alkyl radical formation.^{16,17} Durandetti, by an electrochemical analysis, was unable to rule out either hypothesis of having sequential oxidative additions at a single nickel center or the radical chain mechanism.¹⁸

Figure 1.7. General Mechanism for Cross-Coupling Reactions.



Our group proposed the following radical chain mechanism. The reaction begins with selective oxidative addition of an aryl iodide to nickel(0). The resulting arylnickel(II) intermediate reacts with an alkyl radical to form a transient diorganonickel(III) intermediate. Reductive elimination leads to the desired $C(sp^2)-C(sp^3)$ bond formation and generates a nickel(I) species that can react with an alkyl iodide to generate a nickel(II) diiodide and the alkyl radical. Finally, manganese reduces the nickel(II) diiodide to nickel(0), completing the catalytic cycle (Figure 1.8). Our studies suggest that selectivity for cross-coupling is governed by preferential oxidative addition versus radical formation of each coupling partner. This guiding mechanism has been the central hypothesis for the work presented in this dissertation.

Figure 1.8. Proposed Mechanism of Cross-Electrophile Coupling of Aryl Iodides with Alky Iodides.



1.4. References.

(1) Roughley, S. D.; Jordan, A. M. The Medicinal Chemist's Toolbox: An Analysis of Reactions Used in the Pursuit of Drug Candidates. *J. Med. Chem.*, **2011**, *54*, 3451-3479.

(2) Dugger, R. W.; Ragan, J. A.; Ripin, D. H. B. Survey of GMP Bulk Reactions Run in a Research Facility between 1985 and 2002. *Org. Process Res. Dev.*, **2005**, *9*, 253-258.

(3) Everson, D. A.; Shrestha, R.; Weix, D. J. Nickel-Catalyzed Reductive Cross-Coupling of Aryl Halides with Alkyl Halides. *J. Am. Chem. Soc.*, **2010**, *132*, 920-921.

(4) Everson, D. A.; Jones, B. A.; Weix, D. J. Replacing Conventional Carbon Nucleophiles with Electrophiles: Nickel-Catalyzed Reductive Alkylation of Aryl Bromides and Chloride. *J. Am. Chem. Soc.*, **2012**, *132*, 6146-6159

(5) Frisch, A. C.; Beller, M. Catalysts for Cross-Coupling Reactions with Non-activated Alkyl Halides. *Angew. Chem. Int. Ed.*, **2005**, *44*, 674-688.

(6) Rudolph, A.; Lautens, M. Secondary Alkyl Halides in Transition-Metal-Catalyzed Cross-Coupling Reactions. *Angew. Chem. Int. Ed.*, **2009**, *48*, 2656-2670.

(7) Jana, R.; Pathak, T. P.; Sigman, M. S. Advances in Transition Metal (Pd,Ni,Fe)-Catalyzed Cross-Coupling Reactions Using Alkyl-organometallics as Reaction Partners. *Chem. Rev.*, **2011**, *111*, 1417-1492.

(8) Zou, G.; Reddy, Y. K.; Falck, J. R. Ag(I)-promoted Suzuki-Miyaura cross-couplings of *n*-alkylboronic acids. *Tetrahedron Lett.* **2001**, *42*, 7213-7215.

(9) Limmert, M. E.; Roy, A. H.; Hartwig, J. F. Kumada Coupling of Aryl and Vinyl Tosylates under Mild conditions. *J. Org. Chem.* **2005**, *70*, 9364-9370.

(10) Nakamura, M.; Ito, S.; Matsuo, K.; Nakamura, E. Iron-Catalyzed Chemosselective Cross-Coupling of Primary and Secondary Alkyl Halides with Arylzinc Reagents. *Synlett*, **2005**, *11*, 1794-1798.

(11) Powell, D. A.; Maki, T.; Fu, G. C. Stille Cross-Couplings of Unactivated Secondary Alkyl Halides Using Monoorganotin Reagents. *J. Am. Chem. Soc.* **2005**, *127*, 510-511.

(12) Knapp, D. M.; Gillis, E. P.; Burke, M. D. A General Solution for Unstable Boronic Acids: Slow-Release Cross-Coupling from Air-Stable MIDA Boronates. *J. Am. Chem. Soc.*, **2009**, *131*, 6961-6963.

(13) Knappke, C. E. I.; Grupe, S.; Gartner, D.; Corpet, M.; Gosmini, C.; Wangelin, A. J. v. Reductive Cross-Coupling Reactions between Two Electrophiles. *Chem. Eur. J.*, **2014**, *20*, 6828-6842.

(14) Biswas, S.; Weix, D. J. Mechanism and Selectivity in Nickel-Catalyzed Cross-Electrophile Coupling of Aryl Halides with Alkyl Halides. *J. Am. Chem. Soc.*, **2013**, *135*, 16192-16197.

(15) Hegedus, L. S.; Miller, L. L. Reaction of π -allylnickel bromide complexes with organic halides. Stereochemistry and mechanism. *J. Am. Chem. Soc.* **1975**, *97*, 459–460.

(16) Hegedus, L. S.; Thompson, D. H. P. The reactions of organic halides with (π -allyl)nickel halide complexes: a mechanistic study. *J. Am. Chem. Soc.* **1985**, *107*, 5663–5669.

(17) Tsou, T.; Kochi, J. Mechanism of biaryl synthesis with nickel complexes. *J. Am. Chem. Soc.* **1979**, *101*, 7547–7560

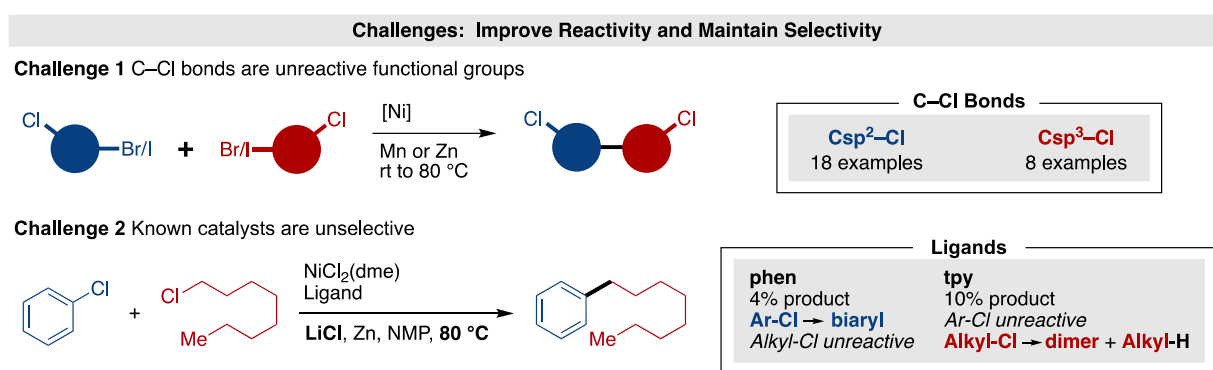
(18) Durandetti, M.; Nedelec, J. -Y.; Perichon, J. Nickel-Catalyzed Direct Electrochemical Cross-Coupling between Aryl Halides and Activated Alkyl Halides. *J. Org. Chem.* **1996**, *61*, 1748–1755.

**Chapter 2: Nickel-Catalyzed Cross-Electrophile Coupling of Aryl Chlorides with Primary
Alkyl Chlorides**

2.1. Introduction.

Cross-electrophile coupling has rapidly become an important approach to the synthesis of Csp^2 – Csp^3 bonds,¹ but engaging less reactive C–Cl bonds, outside of activated systems² or intramolecular reactions,³ has proven challenging. Indeed, unactivated C–Cl bonds are well-tolerated functional groups⁴ in cross-electrophile coupling methods (Figure 2.1).^{5,6} The ability to cross-couple with organic chlorides is valuable for several reasons – first, organic chlorides are more abundant than organic bromides or organic iodides;⁷ second, the low reactivity of the C–Cl bond allows it to be introduced early in a synthesis and later diversified.^{8,9,10}

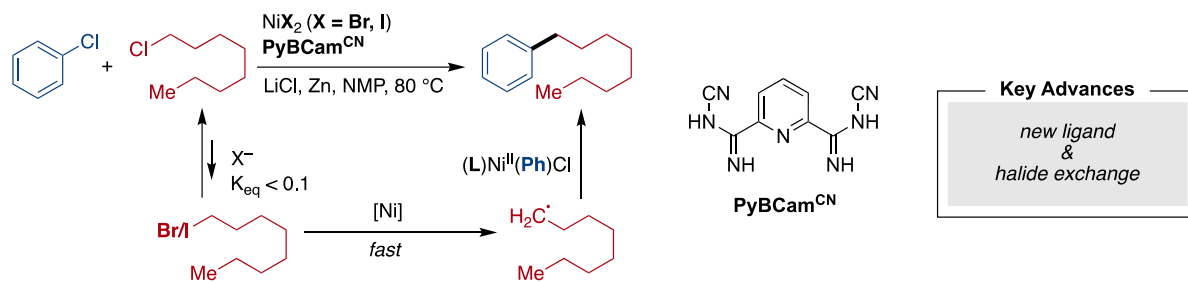
Figure 2.1. Challenges in the Cross-Electrophile Coupling Organic Chlorides.



The central challenge presented by C–Cl bonds in cross-electrophile coupling is the need for higher reactivity without sacrificing selectivity (Figure 2.1). While the homodimerization of alkyl chlorides¹¹ and aryl chlorides^{8c} has been reported, no general cross-selective approach has yet been found.¹² Recently, Zhang reported couplings of a variety of aryl chlorides, but only with an excess of $ClCF_2R$ reagents.¹³ Several groups have reported on the coupling of aryl chlorides with alkyl bromides¹⁴ or tertiary alkyl oxalate esters.¹⁵ However, the coupling of chlorobenzene with a simple alkyl bromide provided less than 25% yield of cross-coupled product.^{14a} Switching to an alkyl chloride further diminishes selectivity and yield using our standard conditions (Figure 2.1).¹⁶

Based upon our proposed mechanism for the coupling of aryl iodides with alkyl iodides,¹⁷⁻¹⁹ overcoming this dual reactivity-selectivity challenge requires a catalyst that selectively reacts with the Ar-Cl over the Alkyl-Cl, yet can slowly generate an alkyl radical from the Alkyl-Cl starting material. We show that this can be accomplished through the use of salt additives to maintain a very low, steady-state concentration of an alkyl bromide/iodide and a uniquely selective pyridine-2,6-bis(*N*-cyanocarboxamidine) (PyBCam^{CN})^{20,21} ligated nickel catalyst (Figure 2.2).

Figure 2.2. Cross-Selective Coupling with Primary Alkyl Chlorides.

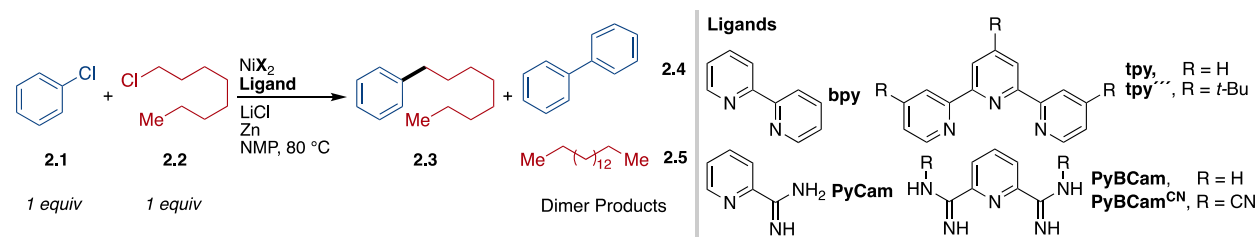


2.2. Reaction Optimization.

During reaction development, we observed a strong synergistic effect between the catalyst and the presence of substoichiometric amounts (10–30 mol%) of bromide or iodide (Table 2.1–2.3). While no catalysts were found that provided high yields of product in the absence of bromide or iodide, high selectivity could be achieved in reactions with PyBCam^{CN} ligand and NiBr_2 or NiI_2 ; and in reactions with PyBCam ligand and NiBr_2 (Table 2.1, bold-faced entries). Reactions with bipyridine (bpy) or pyridine 2-carboxamidine (PyCam) ligands, which are optimal for the coupling of aryl bromides with alkyl bromides,^{20, 22} favored formation of aryl dimer products (bpy) or hydrodehalogenated arene (PyCam) without consuming the alkyl chloride. Reactions with terpyridine (tpy), which is useful for the dimerization of alkyl halides,²³ converted alkyl chloride to dimeric and hydrodehalogenated products without consuming aryl chloride. In contrast to tpy, reactions with 4,4',4''-tri-*tert*-butyl-2,2':6',2''-terpyridine (tpy'''), which is useful in Negishi cross-coupling reactions

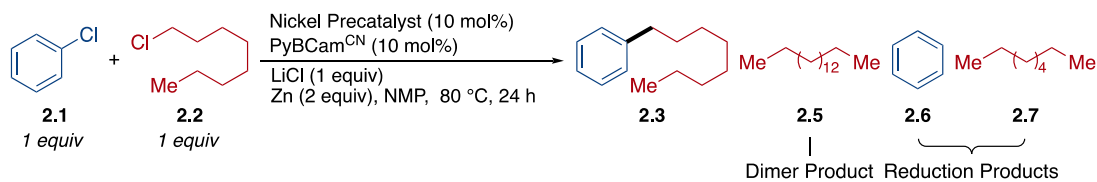
of alkyl halides,²⁴ consumed both substrates but formed approximately 1:1:1 product/alkyl dimer/aryl dimer.

Table 2.1. Effect of Ligands and Additives on the Cross-Electrophile Coupling of Chlorobenzene with Chlorooctane.



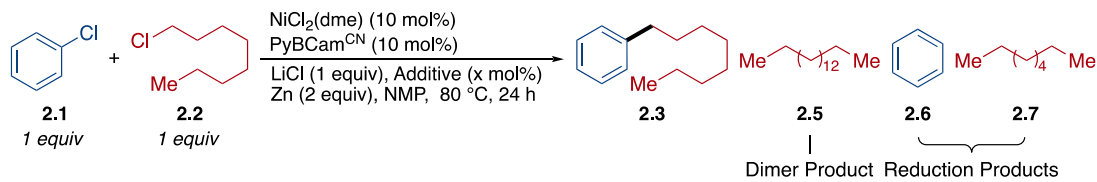
Ligand	X	Yield 2.3 (%) ^b	Yield 2.4 (%) ^b	Yield 2.5 (%) ^b	Ligand	X	Yield 2.3 (%) ^b	Yield 2.4 (%) ^b	Yield 2.5 (%) ^b
bpy	Cl	2	48	1	PyCam	Cl	16	19	6
	Br	9	43	4		Br	43	9	5
	I	17	39	17		I	19	2	3
tpy	Cl	10	0	25	PyBCam	Cl	11	0	0
	Br	4	2	40		Br	53	0	2
	I	1	0	16		I	18	0	23
tpy'''	Cl	38	28	16	PyBCam ^{CN}	Cl	46	1	7
	Br	22	26	19		Br	65	0	9
	I	4	33	8		I	87 (82)^c	0	6

Reaction conditions: chlorobenzene (0.5 mmol), 1-chlorooctane (0.5 mmol), $\text{NiX}_2 = \text{NiI}_2 \cdot 4\text{H}_2\text{O}/\text{NiBr}_2(\text{dme})/\text{NiCl}_2(\text{dme})$ (0.05 mmol), ligand (0.05 mmol), LiCl (0.5 mmol), Zn (1.0 mmol), and NMP (1 mL) were assembled in a N_2 filled glovebox and heated for 24 h. PyCam and PyBCam were added as their HCl salts. ^bYields were determined by GC analysis calibrated against 1,3,5-trimethoxybenzene as an internal standard. ^cIsolated yield after column chromatography.

Table 2.2. Halide Effect from Nickel Precatalyst.

Entry	Ni Precatalyst	2.3 (%)	2.5 (%)	2.6 (%)	2.7 (%)	Returned 2.1 (%)	Returned 2.2 (%)
1	NiCl ₂ (dme)	44	7	30	0	21	40
2	NiBr ₂ (dme)	64	8	15	0	16	12
3	NiBr ₂ •3H ₂ O	68	8	22	0	7	12
4	NiBr ₂ (anhydrous)	68	8	13	4	26	11
5	NiI ₂ •4H ₂ O	89	6	10	2	4	0
6	NiI ₂ (anhydrous)	80	7	5	5	18	0

Yields are determined by GC analysis calibrated against 1,3,5-trimethoxybenzene as an internal standard.

Table 2.3. Effect of Various Halide Additives.

Entry	Additive (x mol%)	2.3 (%)	2.5 (%)	2.6 (%)	2.7 (%)	Returned 2.1 (%)	Returned 2.2 (%)
1	No Additive	43	6	25	1	22	40
2	LiBr (20 mol%)	72	10	18	1	8	7
3	ZnBr ₂ (10 mol%)	64	7	16	2	21	21
4	NBu ₄ Br (20 mol%)	72	10	19	2	11	8
5	LiI (20 mol%)	83	8	10	1	14	0
6	ZnI ₂ (10 mol%)	79	7	4	4	21	1
7	NBu ₄ I (20 mol%)	83	8	10	2	12	0

Yields are determined by GC analysis calibrated against 1,3,5-trimethoxybenzene as an internal standard.

Routine optimization with PyBCam and PyBCam^{CN} demonstrated that PyBCam^{CN} was superior, that reactions were best conducted at 60-80 °C, and that a variety of iodide and bromide additives provide similar results. Reactions with bromide additive provided the highest yields when the alkyl chloride was added slowly, either portionwise via syringe or dropwise through an addition funnel. Reactions with iodide additive did not benefit from slow addition. The primary side products in both cases are the alkyl dimer and aryl hydrodehalogenated product.

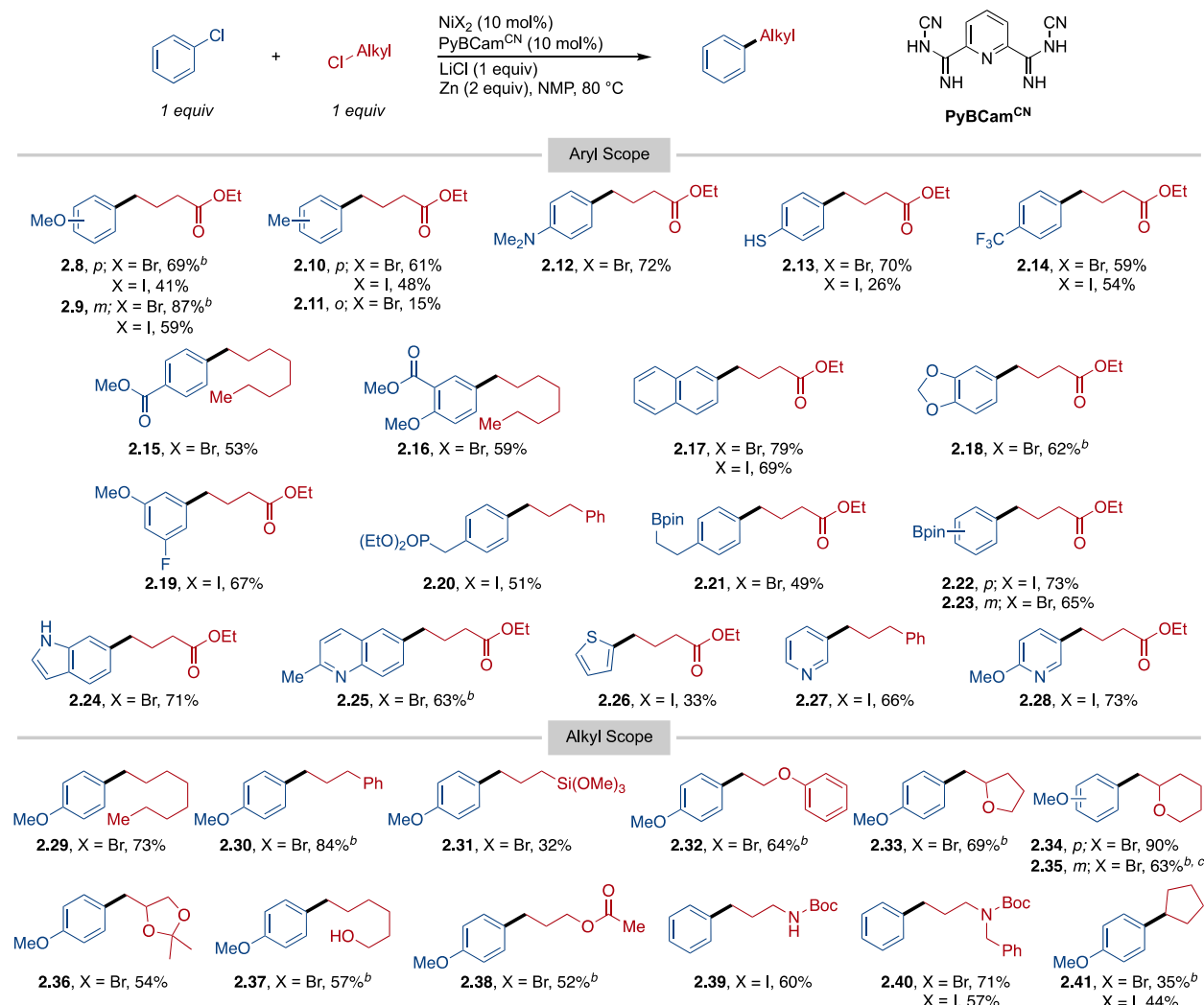
2.3. Reaction Scope.

The optimized conditions were then applied to a variety of primary alkyl chlorides and chloroarenes (Figure 2.3). Electron-rich aryl chlorides, which were unreactive under our previously published conditions, coupled in 69-72% yield (**2.8**, **2.12**, **2.13**, **2.24**). However, a more sterically hindered aryl chloride, 2-chlorotoluene, coupled poorly (**2.11**, 15% yield). While we had coupled electron-poor aryl chlorides with alkyl bromides previously,¹⁴ under these conditions electron-poor aryl chlorides could be coupled with alkyl chlorides for the first time, with yields ranging from 53-73% yield (**2.9**, **2.14**, **2.15**, **2.25**, **2.27**, **2.29**). As expected with PyBCam ligands,²⁰ a variety of heterocycles could be coupled, including both electron-poor quinoline (**2.25**, 63%) and pyridine (**2.27**, 66% and **2.28**, 73%); and electron-rich indole (**2.24**, 71%) and thiophene (**2.26**, 33%). A particular advantage of cross-electrophile coupling is tolerance for alkyl halides with β -leaving groups (**2.32-2.36**). The analogous organometallic reagents would be prone to elimination. Finally, secondary alkyl chlorides do couple under these conditions, but in lower yield (**2.41**, 44%). The remaining mass balance was attributed to unreacted coupling partners.

Despite the higher temperatures, functional group compatibility remained broad. The low basicity of the conditions allowed us to tolerate both aryl and alkyl pinacol boronic acid esters (**2.21-2.23**, 49-73% yield), providing opportunities for further elaboration of the products. Acidic N-H (**2.39**,

60%) and O-H (**2.37**, 57%) groups are tolerated, which would be a challenge for organomagnesium or organozinc reagents.²⁵ As a testament to the low basicity of the conditions, a free thiol was tolerated (**2.13**, 70% yield), avoiding competing S_N2 with the alkyl electrophile and S-arylation (pKa of thiophenol in DMSO is 10.3,²⁶ which makes it more acidic than acetic acid).²⁷ On the other hand, despite the presence of Lewis acids (Zn^{II} salts, Li⁺ salts) at 60-80 °C, Boc groups on nitrogen were still tolerated (**2.39**, 60%; **2.40**, 71%). While esters were tolerated, we did observe scrambling when two different esters were present due to transesterification (for example, methyl and ethyl ester exchange). For this reason, we coupled chloroarenes bearing esters (**2.15**, **2.16**) with 1-chlorooctane. Other functional group highlights include a benzylic diethylphosphonate ester (**2.20**, 51%) and a trimethoxysilane (**2.31**, 32%). Despite the low yield, the cross-coupling to form trimethoxysilane product **2.31** is notable because it is a different approach^{28,29} to forming functionalized silanes that could be useful in attaching molecules to glass or silica.³⁰ As in our previous studies on cross-electrophile coupling reactions with less reactive substrates, this chemistry can be scaled up using standard techniques (**2.35**).³¹

Figure 2.3. Reaction Scope for the Nickel-Catalyzed Coupling of Aryl Chlorides with Alkyl Chlorides.



^aReactions run on 0.5 mmol scale in 1 mL NMP for 18–24 h. NiX_2 was either $\text{NiBr}_2(\text{dme})$ or $\text{NiI}_2 \cdot 4\text{H}_2\text{O}$. For reactions with $X = \text{Br}$, alkyl-Cl was added in portions. ^bReaction was conducted with 1.25 equiv of alkyl chloride (0.75 mmol). ^cReaction was run on a 7.0 mmol scale.

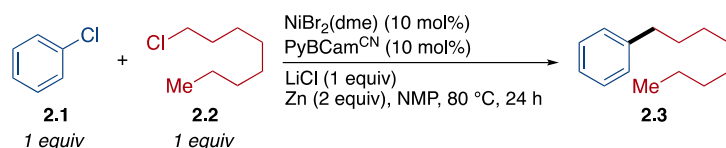
2.4. Mechanistic Studies.

The distinctive feature of this reaction, when compared to other cross-electrophile couplings of aryl halides with alkyl halides, is the ability to engage two relatively unreactive substrates in a selective manner (Figure 2.2). There are three keys to the success of this method.

First, LiCl was essential for efficient reduction of the nickel catalyst by the zinc surface. We have recently noted that ZnCl_2 can have an inhibitory effect on reduction of nickel catalysts and that

lithium chloride is among the best agents for overcoming inhibition,³² consistent with previous reports on reduction of organic molecules.³³ Here too, reactions conducted without LiCl resulted in 3% formation of the cross-coupled product and primarily returned both substrates (Table 2.4). We also verified that neither organic chloride reacts directly with zinc to form an organozinc reagent (Table 2.4).

Table 2.4. Deletion Control Experiments.

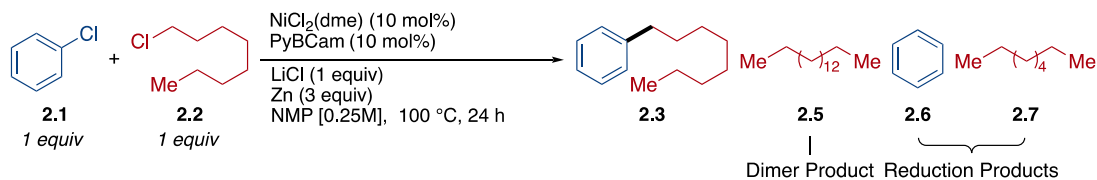


Entry	Deviation	Product 2.3 (%)	Returned 2.1 (%)	Returned 2.2 (%)
1	No NiBr ₂ (dme)	0	99	86 ^a
2	No Zn	0	105	107
3 ^a	No LiCl	3	92	96

^aWe cannot account for the small loss of chlorooctane in this reaction. Neither octane (hydrodehalogenation) or hexadecane (dimerization) could be detected by GC analysis.

^bHydrodehalogenated arene was observed in 7 %. Yields are determined by GC analysis calibrated against 1,3,5-trimethoxybenzene as an internal standard.

Table 2.5. Examination of Alternative Reductants and Additives.

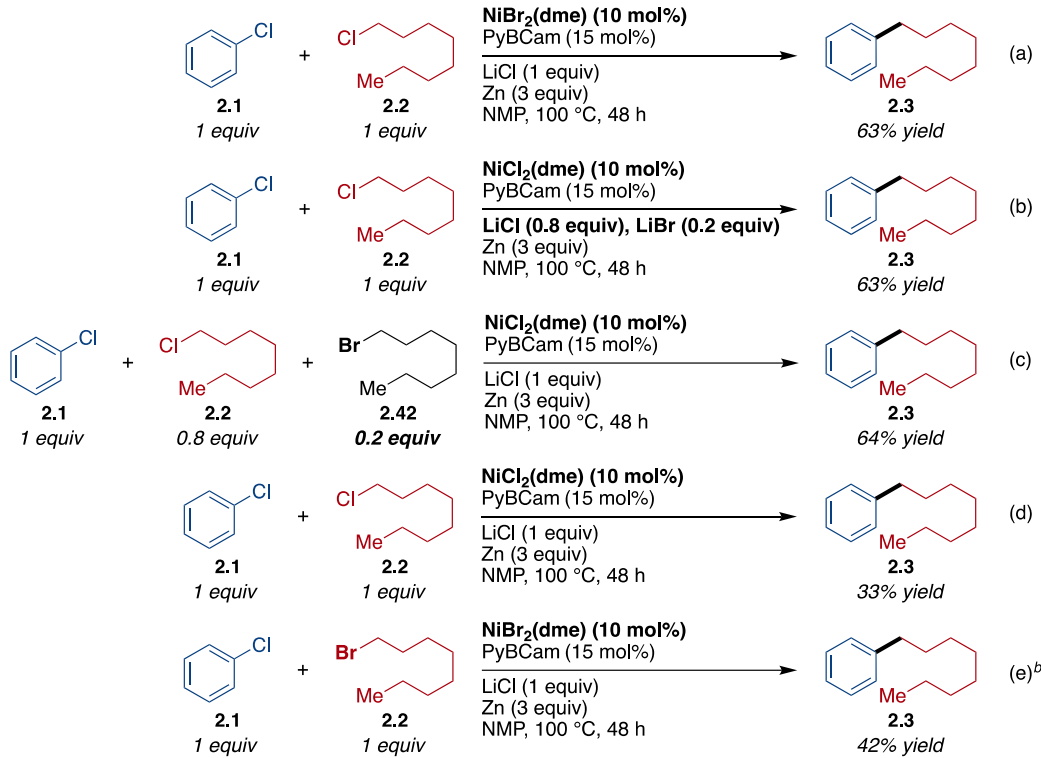


Entry	Deviation from above	2.3 (%)	2.5 (%)	2.6 (%)	2.7 (%)	Returned 2.1 (%) ^a	Returned 2.2 (%)
1	TDAE instead of Zn	0	0	4	0	73	0
2	Mn instead of Zn	14	1	12	33	111	8
3	Mn and LiBr instead of Zn and LiCl ^b	4	13	8	30	80	0
4	LiBr instead of LiCl	42	24	24	8	68	0
5	MgCl ₂ instead of LiCl	41	1	13	20	66	22

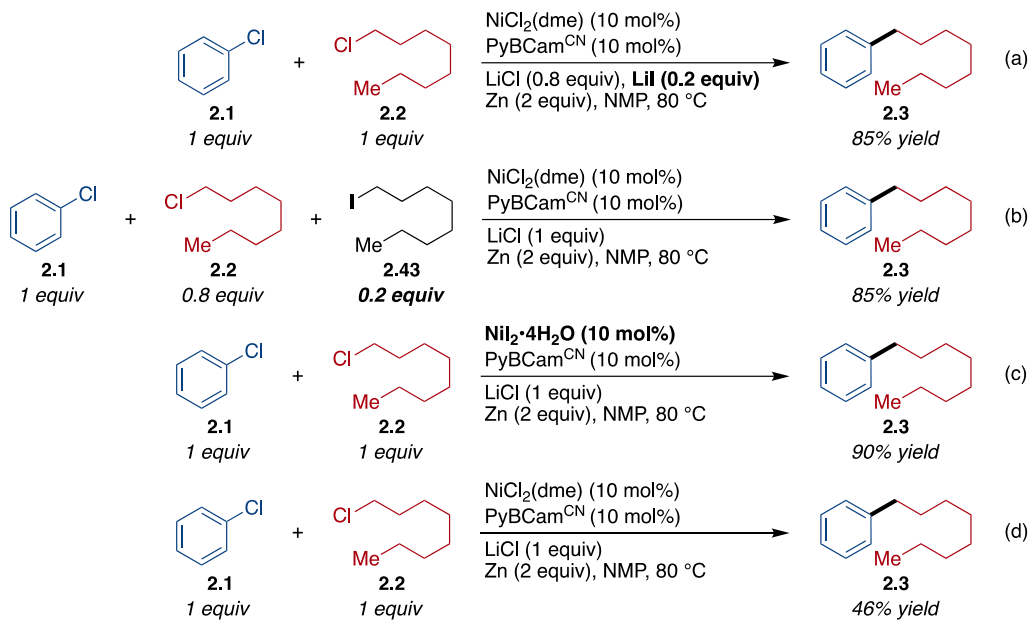
^aCalculated with respect to mmol of alkyl chloride used. ^bChlorobenzene (1 equiv) was used along with DIPEA (20 mol%). DIPEA had no effect on reaction outcome. Yields are determined by GC analysis calibrated against 1,3,5-trimethoxybenzene as an internal standard.

Second, halide exchange plays a key role by increasing the reactivity of the alkyl chloride. We found that 10-30% of bromide or iodide, regardless of how it was introduced, was essential for reasonable reaction rates (Figures 2.4, 2.5 and Tables 2.5, 2.6).

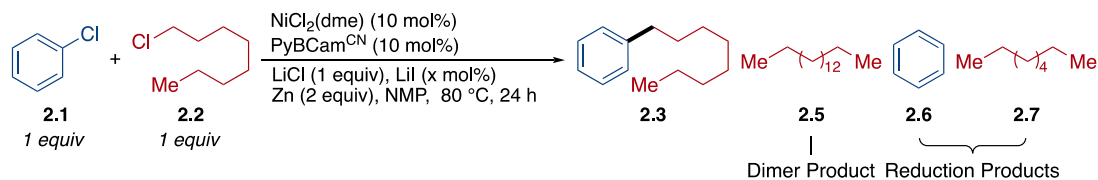
Figure 2.4. Evidence for Bromide Co-catalysis.



^aReactions were run on a 0.5 mmol scale. Yields were determined by GC analysis calibrated against 1,3,5-trimethoxybenzene as an internal standard. ^bReaction run with DIPEA (20 mol%). DIPEA had no effect on reaction outcome.

Figure 2.5. Evidence for Iodide Co-catalysis.

After 24 h of reaction the yields are determined by GC analysis calibrated against 1,3,5-trimethoxybenzene as an internal standard.

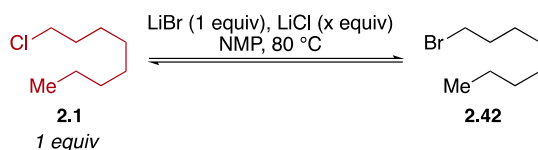
Table 2.6. Optimization of Iodide Concentration.

Entry	LiI (x mol%)	2.3 (%)	2.5 (%)	2.6 (%)	2.7 (%)	Returned 2.1 (%)	Returned 2.2 (%)
1	10	89	6	10	1	3	0
2	20	83	8	11	1	4	0
3	30	85	8	13	2	4	0
4	40	82	10	15	1	3	0
5	50	78	11	18	1	2	0
6	100	59	15	25	2	4	0

Yields are determined by GC analysis calibrated against 1,3,5-trimethoxybenzene as an internal standard.

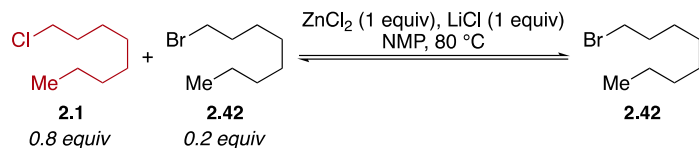
Studies on halide exchange showed that it is fast compared to the rate of reaction (reaching equilibrium in 1-2 h vs 24 h for reaction time) and unfavorable (Table 2.7–2.14, Figure 2.6). Significantly, the presence of zinc and lithium salts altered the equilibrium to more strongly favor alkyl iodide/bromide (Table 2.7–2.14, Figure 2.6). This led to the counterintuitive outcome that increasing total chloride concentration increased alkyl iodide concentration (Table 2.7–2.14, Figure 2.6). Under concentrations of salts chosen to mimic those present catalytic reactions, we found that the amount of alkyl iodide increased as the concentration of $ZnCl_2$ increased, although the ratio of alkyl-Cl/alkyl-I remained large in all cases ($\geq 98:2$, Table 2.14). We tentatively attribute this phenomenon to the favorable formation of $LiZnCl_3$ over $LiZnCl_2Br$ or $LiZnCl_2I$, resulting in sequestration of chloride as the concentration of Zn^{2+} increases at later reaction times.³⁴ The halogen exchange is also somewhat faster than reported for exchanges in amide solvents with only sodium bromide, but this process could be catalyzed by zinc: catalysis of alkyl halogen exchange by titanium, zirconium, rhodium, and iron salts has been reported.³⁵

Table 2.7. Effect of LiCl on the Equilibrium Between Chlorooctane and Bromooctane in the Presence of LiBr.



Entry	LiCl (x equiv)	Time	2.1 (%)	2.42 (%)	2/2.42
1	1	20 min	105	1	143
		40 min	107	1	126
		1 h	106	1	141
		2 h	108	1	136
		5 h	105	1	139
		20 min	100	4	16
2	0	40 min	100	4	15
		1 h	99	4	15
		2 h	100	4	15
		5 h	98	4	15

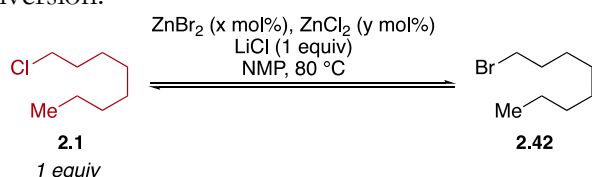
Refer to Section 2.6.3.5: General procedure for equilibrium study was followed with LiBr (43.5 mg, 0.50 mmol, 1.0 equiv), LiCl (21.2 mg, 0.50 mmol, 1.0 equiv), and 1-chlorooctane (85.0 μ L, 0.50 mmol, 1.0 equiv). Yields are determined by GC analysis calibrated against 1,3,5-trimethoxybenzene as an internal standard.

Table 2.8. Effect of LiCl and ZnCl₂ on the Equilibrium Between Chlorooctane and Bromooctane.

Entry	Conditions	Time	2.1 (%)^a	2.42 (%)^a	2.1/2.42
1	Omit LiCl	20 min	86	13	4
		40 min	86	13	4
		1 h	85	12	4
		2 h	86	12	5
		8 h	81	10	5
2	Omit ZnCl ₂	0 min	110	2	45
		5 min	108	0	n/a
		10 min	111	0	n/a
		15 min	107	0	n/a
		20 min	110	0	n/a
3	No deviations	40 min	106	0	n/a
		1 h	107	0	n/a
		2 h	107	0	n/a
		8 h	108	0	n/a
		0 min	94	15	4
		5 min	94	8	7
		10 min	99	5	12
		15 min	99	4	16
		20 min	104	3	22
		40 min	107	1	63
		1 h	105	1	105
		2 h	104	1	128
		8 h	102	<1	132

^aCalculated based on the overall mmol of haloctane (0.5 mmol total). Refer to Section 2.6.3.5: General procedure for equilibrium study was followed with ZnCl₂ (68.2 mg, 0.50 mmol, 1.0 equiv), LiCl (21.2 mg, 0.50 mmol, 1.0 equiv), 1-chlorooctane (68.0 μ L, 0.4 mmol, 0.8 equiv), and 1-bromooctane (17.3 μ L, 0.1 mmol, 0.2 equiv). Yields are determined by GC analysis calibrated against 1,3,5-trimethoxybenzene as an internal standard.

Table 2.9. Equilibrium Between Chlorooctane and Bromooctane Under Mock Catalytic Conditions at Different Levels of Conversion.



TON	Analytical Additive Amounts	Experimental Additive Amounts
0 ^a	100 mol% LiCl	LiCl (21.2 mg, 0.50 mmol)
0 ^b	10 mol% ZnBr ₂ 100 mol% LiCl	ZnBr ₂ (11.3 mg, 0.05 mmol) LiCl (21.2 mg, 0.50 mmol)
1	10 mol% ZnBr ₂ 10 mol% ZnCl ₂ 100 mol% LiCl	ZnBr ₂ (11.3 mg, 0.05 mmol) ZnCl ₂ (6.9 mg, 0.05 mmol) LiCl (21.2 mg, 0.50 mmol)
10	10 mol% ZnBr ₂ 90 mol% ZnCl ₂ 100 mol% LiCl	ZnBr ₂ (11.3 mg, 0.05 mmol) ZnCl ₂ (61.4 mg, 0.45 mmol) LiCl (21.2 mg, 0.50 mmol)

^aPrior to the reduction of $\text{NiBr}_2(\text{dme})$ pre-catalyst to $\text{Ni}(0)$ by Zn . ^bFollowing the $\text{NiBr}_2(\text{dme})$ pre-catalyst reduction by Zn

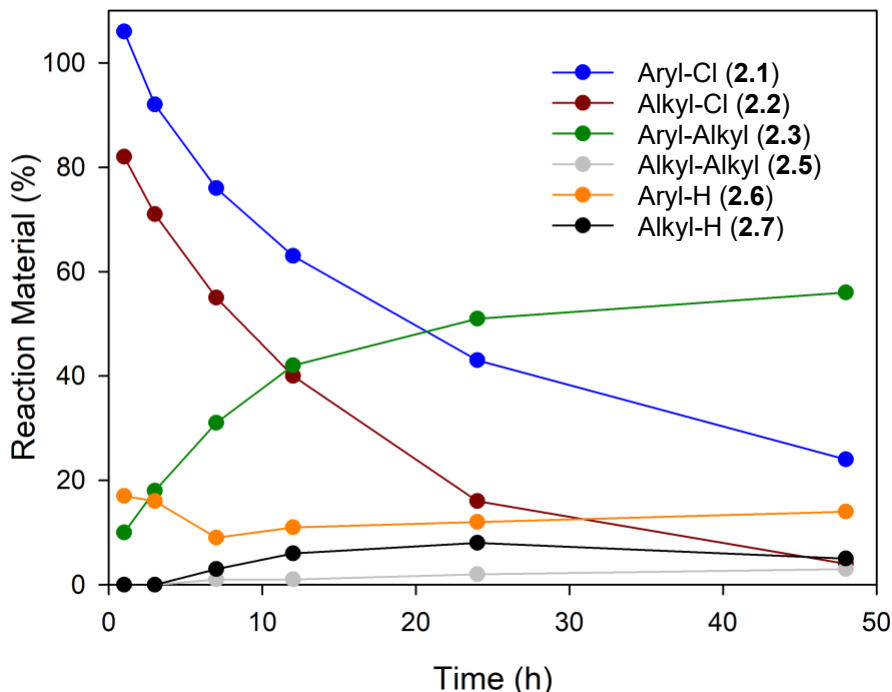
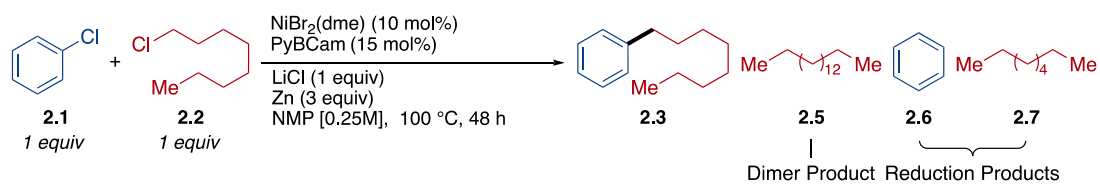
Refer to Section 2.6.3.5: General procedure for equilibrium study was followed with 1-chlorooctane (85.0 μ L, 0.50 mmol, 1.0 equiv) and the experimental additive amounts given in Figure Table 2.9. The amounts of LiCl, ZnBr₂, and ZnCl₂ used in this experiment are based on the proposed catalytic cycle in Figure 1.8. Only LiCl is present before the reduction of NiBr₂(dme) pre-catalyst by Zn. The use of 10 mol% of ZnBr₂ mimics the catalytic conditions after the initial reduction of 10 mol% of NiBr₂(dme) pre-catalyst to Ni(0) by Zn before the first turnover. After the first turn over, 10 mol% of ZnBr₂ and 10 mol% ZnCl₂ would be present following the reduction of (L)NiCl₂. At the usual catalyst loading, complete product formation would be at ten turnovers.

Table 2.9 Continued

Entry	TON		20 min	40 min	1 h	2 h	5 h	7 h
1	0 ^a	2.1 (%)	109	107	101	105	109	105
		2.42 (%)	0	0	0	0	0	0
		2.1/2.42	n/a	n/a	n/a	n/a	n/a	n/a
2	0 ^b	2.1 (%)	102	101	101	102	103	102
		2.42 (%)	0	0	0	0	0	0
		2.1/2.42	n/a	n/a	n/a	n/a	n/a	n/a
3	1	2.1 (%)	104	102	99	101	101	100
		2.42 (%)	0	0	0	0	0	0
		2.1/2.42	n/a	n/a	n/a	n/a	n/a	n/a
4	10	2.1 (%)	104	104	103	103	101	103
		2.42 (%)	1	1	1	1	1	1
		2.1/2.42	177	126	109	96	96	96
5	0 ^b (Omit LiCl)	2.1 (%)	105	105	105	107	106	96 ^c
		2.42 (%)	0	0	0	0	0	0 ^c
		2.1/2.42	n/a	n/a	n/a	n/a	n/a	n/a
6	1 (Omit LiCl)	2.1 (%)	107	106	106	108	105	97 ^c
		2.42 (%)	0	0	0	0	0	0 ^c
		2.1/2.42	n/a	n/a	n/a	n/a	n/a	n/a
7	10 (Omit LiCl)	2.1 (%)	106	107	107	108	105	93 ^c
		2.42 (%)	0	0	0	0	0	0 ^c
		2.1/2.42	n/a	n/a	n/a	n/a	n/a	n/a

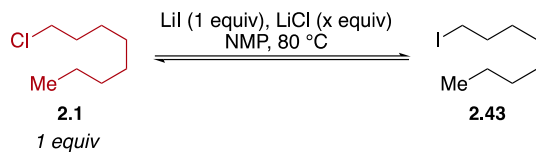
^aPrior to the reduction of NiBr₂(dme) pre-catalyst to Ni(0) by Zn. ^bFollowing the NiBr₂(dme) pre-catalyst reduction by Zn. ^cRecorded at 24 h. Yields are determined by GC analysis calibrated against 1,3,5-trimethoxybenzene as an internal standard.

Figure 2.6. Reaction Time Course with Catalytic Amount of Bromide.



Yields are determined by GC analysis calibrated against 1,3,5-trimethoxybenzene as an internal standard.

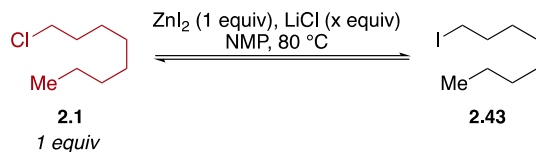
Table 2.10. Effect of LiCl on the Equilibrium Between Chlorooctane and Iodoctane in the Presence of LiI.



Entry	LiCl (x equiv)	Time	2.1 (%)	2.43 (%)	2/2.43
1	1	1 min	100	0	n/a
		20 min	104	0	n/a
		40 min	104	0	n/a
		1 h	104	0	n/a
		2 h	106	0	n/a
		7 h	98	0	n/a
2	0	1 min	95	1	118
		20 min	95	1	100
		40 min	98	1	106
		1 h	98	1	99
		2 h	100	1	95
		7 h	97	1	96

Refer to Section 2.6.3.5: General procedure for equilibrium study was followed with LiI (67.0 mg, 0.50 mmol, 1.0 equiv), LiCl (21.2 mg, 0.50 mmol, 1.0 equiv), and 1-chlorooctane (85.0 μ L, 0.50 mmol, 1.0 equiv). Yields are determined by GC analysis calibrated against 1,3,5-trimethoxybenzene as an internal standard.

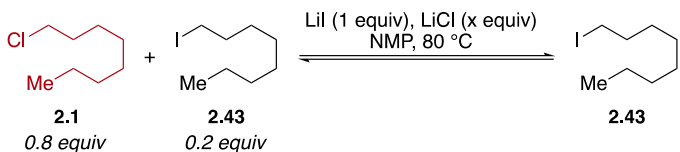
Table 2.11. Effect of LiCl on the Equilibrium Between Chlorooctane and Iodoctane in the Presence of ZnI_2 .



Entry	LiCl (x equiv)	Time	2.1 (%)	2.43 (%)	2.1/2.43
1	1	1 min	97	2	64
		20 min	86	12	7
		40 min	83	22	4
		1 h	75	27	3
		2 h	68	32	2
		7 h	69	33	2
2	0	1 min	100	0	n/a
		20 min	103	0	n/a
		40 min	104	1	195
		1 h	100	1	122
		2 h	102	2	65
		7 h	96	4	22

Refer to Section 2.6.3.5: General procedure for equilibrium study was followed with ZnI_2 (159.6 mg, 0.50 mmol, 1.0 equiv), LiCl (21.2 mg, 0.50 mmol, 1.0 equiv), and 1-chlorooctane (85.0 μ L, 0.50 mmol, 1 equiv). Yields are determined by GC analysis calibrated against 1,3,5-trimethoxybenzene as an internal standard.

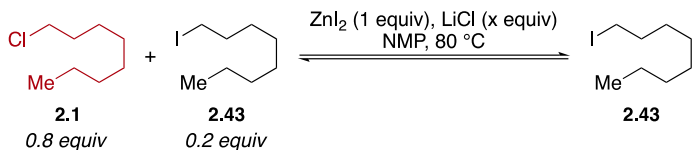
Table 2.12. LiCl Effect on the Equilibrium Between Chlorooctane and Iodoctane in the Presence of LiI.



Entry	LiCl (x equiv)	Time	2.1 (%)^a	2.43 (%)^a	2.1/2.43
1	1.0	1 min	100	0	n/a
		20 min	99	0	n/a
		40 min	102	0	n/a
		1 h	110	0	n/a
		2 h	101	0	n/a
		7 h	92	0	n/a
2	0	1 min	80	20	4
		20 min	78	18	4
		40 min	80	20	4
		1 h	77	17	4
		2 h	78	20	4
		7 h	76	18	4

^aCalculated based on the overall mmol of haloctane (0.5 mmol total). Refer to Section 2.6.3.5: General procedure for equilibrium study was followed with LiI (67.0 mg, 0.50 mmol, 1.0 equiv), LiCl (21.2 mg, 0.50 mmol, 1.0 equiv), 1-chlorooctane (68.0 μL , 0.4 mmol, 0.8 equiv), and 1-iodooctane (18.1 μL , 0.1 mmol, 0.2 equiv). Yields are determined by GC analysis calibrated against 1,3,5-trimethoxybenzene as an internal standard.

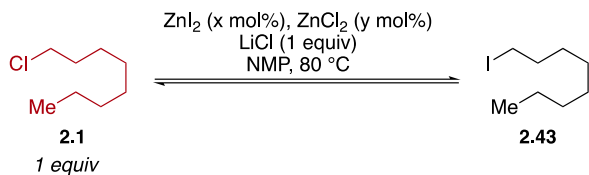
Table 2.13. LiCl Effect on the Equilibrium Between Chlorooctane and Iodoctane in the Presence of ZnI_2 .



Entry	LiCl (x equiv)	Time	2.1 (%) ^a	2.43 (%) ^a	2.1/2.43
1	1.0	1 min	79	19	4
		20 min	71	22	3
		40 min	68	28	2
		1 h	62	27	2
		2 h	61	34	2
		7 h	56	32	2
2	0	1 min	80	20	4
		20 min	80	18	4
		40 min	82	19	4
		1 h	78	16	5
		2 h	79	18	4
		7 h	72	18	4

^aCalculated based on the overall mmol of haloctane (0.5 mmol total). Refer to Section 2.6.3.5: General procedure for equilibrium study was followed with ZnI_2 (159.6 mg, 0.50 mmol, 1.0 equiv), LiCl (21.2 mg, 0.50 mmol, 1.0 equiv), 1-chlorooctane (68.0 μ L, 0.4 mmol, 0.8 equiv), and 1-iodooctane (18.1 μ L, 0.1 mmol, 0.2 equiv). Yields are determined by GC analysis calibrated against 1,3,5-trimethoxybenzene as an internal standard.

Table 2.14. Equilibrium Between Chlorooctane and Iodoctane Under Mock Catalytic Conditions at Different Turnover Numbers (TON).



TON	Analytical Additive Amounts	Experimental Additive Amounts
0 ^a	100 mol% LiCl	LiCl (21.2 mg, 0.50 mmol)
0 ^b	10 mol% ZnI ₂ 100 mol% LiCl	ZnI ₂ (16.0 mg, 0.05 mmol) LiCl (21.2 mg, 0.50 mmol)
1	10 mol% ZnI ₂ 10 mol% ZnCl ₂ 100 mol% LiCl	ZnI ₂ (16.0 mg, 0.05 mmol) ZnCl ₂ (6.9 mg, 0.05 mmol) LiCl (21.2 mg, 0.50 mmol)
10	10 mol% ZnI ₂ 90 mol% ZnCl ₂ 100 mol% LiCl	ZnI ₂ (16.0 mg, 0.05 mmol) ZnCl ₂ (61.4 mg, 0.45 mmol) LiCl (21.2 mg, 0.50 mmol)
20	10 mol% ZnI ₂ 190 mol% ZnCl ₂ 100 mol% LiCl	ZnI ₂ (16.0 mg, 0.05 mmol) ZnCl ₂ (129.5 mg, 0.95 mmol) LiCl (21.2 mg, 0.50 mmol)

^aPrior to the reduction of NiI₂•4H₂O pre-catalyst to Ni(0) by Zn. ^bFollowing the NiI₂•4H₂O pre-catalyst reduction by Zn

Refer to Section 2.6.3.5: General procedure for equilibrium study was followed with 1-chlorooctane (85.0 μ L, 0.50 mmol, 1.0 equiv) and the experimental additive amounts given in Table 2.14. The amounts of LiCl, ZnI₂, and ZnCl₂ used in this experiment are based on the proposed catalytic cycle in Figure 1.8. Only LiCl is present before the reduction of NiI₂•4H₂O pre-catalyst by Zn. The use of 10 mol% of ZnI₂ mimics the catalytic conditions after the initial reduction of 10 mol% of NiI₂•4H₂O pre-catalyst to Ni(0) by Zn before the first turnover. After the first turn over, 10 mol% of ZnI₂ and 10 mol% ZnCl₂ would be present following the reduction of (L)NiCl₂. At the usual catalyst loading, complete product formation would be at ten turnovers. To probe how excess ZnCl₂ affects the equilibrium, 190 mol% of ZnCl₂ was employed.

Table 2.14 Continued

Entry	TON		1 min	20 min	40 min	1 h	2 h	7 h
1	0 ^a	2.1 (%)	102	111	105	104	104	106
		2.43 (%)	0	0	0	0	0	0
		2.1/2.43	n/a	n/a	n/a	n/a	n/a	n/a
2	0 ^b	2.1 (%)	103	102	103	104	103	102
		2.43 (%)	0	0	0	0	0	0
		2.1/2.43	n/a	n/a	n/a	n/a	n/a	n/a
3	1	2.1 (%)	107	106	104	104	105	102
		2.43 (%)	0	0	0	0	0	0
		2.1/2.43	n/a	n/a	n/a	n/a	n/a	n/a
4	10	2.1 (%)	95	97	98	97	99	94
		2.43 (%)	1	1	1	1	1	1
		2.1/2.43	157	70	68	67	67	66
5	20	2.1 (%)	105	102	105	104	104	99
		2.43 (%)	0	1	1	1	2	2
		2.1/2.43	n/a	181	113	85	66	60

^aPrior to the reduction of $\text{NiI}_2 \cdot 4\text{H}_2\text{O}$ pre-catalyst to $\text{Ni}(0)$ by Zn . ^bFollowing the $\text{NiI}_2 \cdot 4\text{H}_2\text{O}$ pre-catalyst reduction by Zn . Yields are determined by GC analysis calibrated against 1,3,5-trimethoxybenzene as an internal standard.

While iodide exchange to enhance the reactivity of alkyl bromides,¹⁴ sulfonic acid esters,³⁶ epoxides,³⁷ and chlorides¹¹ in cross-coupling reactions is now well established, the use of bromide is more rare.³⁸ In cases where iodide co-catalysis isn't practical, the use of bromide co-catalysis should be considered.

Finally, studies with a variety of ligands revealed that PyBCam nickel catalysts are unique in being able to react with both substrates at similar rates, even with activation by halide exchange (Table 2.1). Compared to nickel complexes of tpy³³, which could also react with both substrates but formed both biaryl and bialkyl, nickel PyBCam catalysts avoid biaryl formation entirely and form only small amounts of alkyl dimer. The origin of these differences in reactivity are not yet clear and are the subject of ongoing studies, but it is clear that PyBCam and PyBCam^{CN} are a distinctive, new class of tridentate ligands for nickel catalysis.³⁹

2.5. Conclusions.

In conclusion, the first selective cross-electrophile coupling reaction of aryl chlorides with primary alkyl chlorides has been developed by the synergistic effect of three changes: a new, selective ligand (PyBCam^{CN}), LiCl to enhance catalyst turnover, and bromide/iodide co-catalysis. The mechanism by which PyBCam^{CN} improves yields is under investigation and will be reported in due course. We expect that the generally unreactive nature of alkyl and aryl chlorides should make this new method to functionalize them a useful addition to synthesis.

2.6. Experimental.

2.6.1. Reagents.

Metals

Zinc flake (-325 mesh) was purchased from Alfa Aesar, stored in a nitrogen filled glovebox, and used as received.

Nickel(II) bromide ethylene glycol dimethyl ether (NiBr₂(dme)) was synthesized according to the literature procedure and stored in a nitrogen filled glovebox.⁴⁰ The amount of dme present in the NiBr₂(dme) was determined by elemental analysis and the mass of NiBr₂(dme) was calculated accordingly.

Nickel(II) iodide hydrate was purchased from Strem, stored in a nitrogen filled glovebox, and used as received. The amount of hydrate present in the NiI₂•xH₂O was determined by elemental analysis and the mass of NiI₂•xH₂O was calculated accordingly.

Ligands

Pyridine-2-carboxamidine•HCl (PyCam•HCl, L8•HCl) was synthesized according to the literature procedure.⁴¹

[2,2'-Bipyridine-6-carboximidamide•HCl (BPyCam•HCl, L9)] was synthesized according to the literature procedure.⁴²

Pyridine-2,6-bis(carboximidamide)•2HCl (PyBCam•2HCl) was synthesized according to the literature procedure.⁴³

Pyridine-2,6-bis(N-cyanocarboxamidine) (PyBCam^{CN}) was synthesized according to the literature procedure.⁴⁴

All other ligands tested were purchased from commercial suppliers and used as received.

Solvents

1-Methyl-2-pyrrolidinone (NMP, anhydrous) was purchased from Sigma Aldrich, stored in a nitrogen filled glovebox, and used as received.

Other Reagents

tert-Butyl-3-chloropropylcarbamate was synthesized according to the literature procedure and characterization data matched those reported in the literature.⁴⁵

Boc-3-chloropropylbenzylamine was synthesized according to the literature procedure and characterization data matched those reported in the literature.⁴⁶

All other starting materials were purchased from commercial suppliers and were used as received unless otherwise noted.

2.6.2. Methods.

NMR Spectroscopy

¹H and ¹³C NMR spectra were acquired on 400 and 500 MHz AVANCE spectrometer equipped with a DCH cryoprobe (Bruker), at a sample temperature of 25 °C. NMR spectra were recorded with TopSpin 3.5.6 (Bruker). The Bruker AVANCE 400 NMR spectrometer was supported by NSF grant CHE-1048642. The Bruker AVANCE 500 NMR spectrometer was supported by a generous gift from Paul J. and Margaret M. Bender.

Referencing and absolute referencing to TMS, apodization, Fourier transform, phase and baseline corrections, and spectral analyses were carried out with MestReNova 12.0.4 (Mestrelab Research). NMR chemical shifts are reported in ppm and are referenced to the residual solvent peak for CDCl₃ (δ = 7.26 ppm, ¹H NMR; δ = 77.16 ppm, ¹³C NMR. Coupling constants (J) are reported in Hertz. In the ¹³C NMR spectra of aryl compounds containing boron (**2.21-2.23**) the resonance corresponding to the carbon adjacent to boron was not observed.⁴⁷

Gas Chromatography

GC analyses were performed on an Agilent 7890A GC equipped with dual DB-5 columns (20 m \times 180 μ m \times 0.18 μ m), dual FID detectors, and hydrogen as the carrier gas. A sample volume of 1 μ L was injected at a temperature of 300 °C and a 100:1 split ratio. The initial inlet pressure was 20.3 psi but varied as the column flow was held constant at 1.8 mL/min for the duration of the run. The initial

oven temperature of 50 °C was held for 0.46 min followed by a temperature ramp of 65 °C/min up to 300 °C. The total run time was 5.0 min and the FID temperature was 325 °C.

GC/MS Analysis

GC/MS analyses were performed on a Shimadzu GCMS-QP2010 equipped with an RTX-5MS column (30 m × 0.25 mm × 0.25 μm) with a quadrupole mass analyzer using helium as the carrier gas. The analysis method used in all cases was 1 μL injection of sample, an injection temp of 250 °C, and a 20:1 split ratio. The initial inlet pressure was 8.1 psi, but varied as the column flow was held constant at 1.0 mL/min for the duration of the run. The interface temperature was held at 275 °C, and the ion source (EI⁺, 30 eV) was held at 200 °C. The initial oven temperature was held at 60 °C for 1 min with the detector off, followed by a temperature ramp, with the detector on, to 300 °C at 20 °C/min. Total run time was 13.00 min.

Chromatography

Chromatography was performed on silica gel (EMD, silica gel 60, particle size 0.040-0.063 mm) using standard flash techniques, on a Teledyne Isco CombiFlash instrument using pre-packaged cartridges, on a Teledyne Isco Rf-200 (detection at 210 nm and 280 nm), or on a Biotage Isolera One (detection at 210 nm and 400 nm, on KPsil columns). Products were visualized by UV, KMnO₄ stain, PMA stain, or fractions were analyzed by GC.

Infrared Spectroscopy

Infrared (IR) spectra were recorded on a Bruker Alpha Platinum ATR FT-IR spectrometer and are reported in wavenumbers (cm⁻¹).

Elemental Analysis

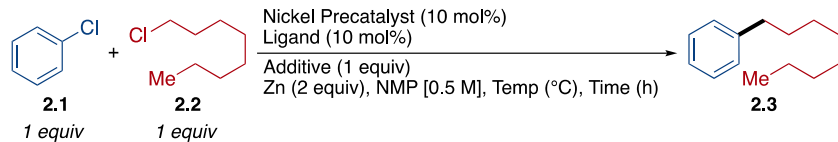
Elemental analyses were performed by CENTC Elemental Analysis Facilities at the University of Rochester, funded by NSF CHE-0650456.

High Resolution Mass Spectrometry

UW-Madison: High resolution mass spectra (HRMS). Mass spectrometry data was collected on a Thermo Q Exactive™ Plus (thermofisher.com) via flow injection with electrospray ionization or via ASAPMS™ (asap-ms.com) by the chemistry mass spectrometry facility at the University of Wisconsin-Madison. The purchase of the Thermo Q Exactive™ Plus in 2015 was funded by NIH Award 1S10 OD020022-1 to the Department of Chemistry.

2.6.3. General Procedures.

2.6.3.1. General Procedure for Reaction Optimization.



Reactions were set up in a N₂ filled glove box. A catalyst solution was prepared by charging an oven dried scintillation vial with a PTFE-coated stirbar, the listed nickel source (0.05 mmol, 10 mol%) and the listed ligand (0.05 mmol, 10 mol%). The solids were dissolved in NMP (1 mL) and allowed to stir for one hour. A second oven-dried 1-dram vial with a PTFE-coated stirbar was charged with the listed additive (0.50 mmol, 1.0 equiv), chlorobenzene (51.0 μ L, 0.50 mmol, 1.0 equiv), 1-chlorooctane (85.0 μ L, 0.50 mmol, 1 equiv), and 1,3,5-trimethoxybenzene (7.4 mg, 0.044 mmol) as an internal standard. This was dissolved in 1 mL of the prepared catalyst solution before the zinc (65.4 mg, 1.0 mmol, 2.0 equiv) was added. The reactions were sealed with a screw cap fitted with a PTFE-faced silicone septum.

The reaction vial was then removed from the glovebox and allowed to stir (1250 RPM) at the listed temperature for the listed reaction time.

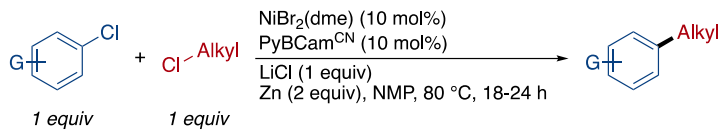
GC Analysis

The reactions were monitored by GC analysis, by taking a 10 μ L aliquot of the crude reaction mixture with a gas-tight syringe. The aliquot was diluted with Et₂O (0.50 mL), quenched with 200 μ L NaHSO₄, filtered through a 2-cm silica plug in a Pasteur pipette, and collected in a GC vial. The resulting solution was analyzed by GC and yields were determined based on the peak area of the analyte compared to 1,3,5-trimethoxybenzene as an internal standard.

Isolation and Purification

Reactions were isolated on a 0.5 mmol scale of chlorobenzene and 1-chlorooctane. The crude reaction mixture was filtered through celite, the celite was washed with acetone (3 \times 4 mL), and the combined filtrate was concentrated by rotary evaporation. The crude mixture was diluted with Et₂O (40 mL) and washed with DI water (40 mL). The aqueous layer was extracted with Et₂O (3 \times 20 mL), the organic layers were combined, dried over MgSO₄, filtered, and the filtrate was concentrated by rotary evaporation. The crude mixture was purified by column chromatography (80:1 pentane/Et₂O) to provide octylbenzene as a clear oil.

2.6.3.2. General Procedure A.



Reactions were set up in a N_2 filled glove box. For a preparative-scale benchtop procedure, see **2.6.3.4.**

Preparative-Scale Benchtop Procedure. A catalyst solution was prepared by charging an oven dried scintillation vial with a PTFE-coated stirbar, $\text{NiBr}_2(\text{dme})$ (15.4 mg, 0.05 mmol, 10 mol%) and $\text{PyBCam}^{\text{CN}}$ (10.7 mg, 0.05 mmol, 10 mol%). The solids were dissolved in NMP (1 mL) and allowed to stir for 30 min-1 h forming a homogenous, forest green solution. However, omitting the $\text{NiBr}_2(\text{dme})$ and ligand pre-stir did not impact productive catalysis. A second oven-dried 1-dram vial with a PTFE-coated stirbar was charged with LiCl (21.2 mg, 0.50 mmol, 1.0 equiv), the appropriate aryl chloride (0.50 mmol, 1.0 equiv), alkyl chloride (0.125 mmol, 0.25 equiv), and 1,3,5-trimethoxybenzene (7.4 mg, 0.044 mmol) as an internal standard. This was dissolved in 1 mL of the prepared catalyst solution before the zinc (65.4 mg, 1.0 mmol, 2.0 equiv) was added. The reactions were sealed with a screw cap fitted with a PTFE-faced silicone septum before being removed from the glovebox. The reaction was allowed to stir at 80°C for 1 h. Using a syringe, N_2 sparged alkyl chloride (0.125 mmol, 0.25 equiv) was added every hour until a total of 0.5 mmol (1.00 equiv) of alkyl chloride was added to the reaction. After these additions the reaction was allowed to stir (1250 RPM) at 80°C for a total of 18-24 h.

GC Analysis

The reactions were monitored by GC analysis, by taking a $10 \mu\text{L}$ aliquot of the crude reaction mixture with a gas-tight syringe. The aliquot was diluted with Et_2O (0.50 mL), quenched with $200 \mu\text{L}$ NaHSO_4 , filtered through a 2-cm silica plug in a Pasteur pipette, and collected in a GC vial. The resulting solution was analyzed by GC and yields were determined based on the peak area of the analyte compared to 1,3,5-trimethoxybenzene as an internal standard.

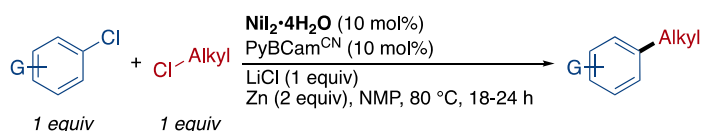
Isolation and Purification

Purification A. Reactions were isolated on a 0.5 mmol scale of aryl chloride and alkyl chloride without the addition of an internal standard to avoid difficulties in separating 1,3,5-trimethoxybenzene from the desired product. The crude reaction mixture was diluted with EtOAc (5 mL) and slurried with 1-3 g of silica gel before the volatile solvents were removed by rotary evaporation. The resulting dry-loaded product was purified by column chromatography on silica to provide the desired products.

Purification B. Reactions were isolated on a 0.5 mmol scale of aryl chloride and alkyl chloride without the addition of an internal standard to avoid difficulties in separating 1,3,5-trimethoxybenzene from the desired product. The crude reaction mixture was filtered through celite, the celite was washed with acetone (3×4 mL), and combined filtrate was concentrated by rotary evaporation. The crude mixture was diluted with Et₂O (40 mL) and washed with DI water (40 mL). The aqueous layer was extracted with Et₂O (3×20 mL), the organic layers were combined, dried over MgSO₄, filtered, and the filtrate was concentrated by rotary evaporation. The crude mixture was purified by column chromatography on silica to provide the desired products.

NOTE: There was no difference in yield when comparing **Purification A** and **Purification B**.

2.6.3.3. General Procedure B.



Reactions were set up in a N₂ filled glove box. A catalyst solution was prepared by charging an oven dried scintillation vial with a PTFE-coated stirbar, NiI₂•4H₂O (19.3 mg, 0.05 mmol, 10 mol%) and PyBCam^{CN} (10.7 mg, 0.05 mmol, 10 mol%). The solids were dissolved in NMP (1 mL) and allowed

to stir for 30 min-1 h forming a homogenous, dark yellow solution. A second oven-dried 1-dram vial with a PTFE-coated stirbar was charged with LiCl (21.2 mg, 0.50 mmol, 1.0 equiv), the appropriate aryl chloride (0.50 mmol, 1.0 equiv), alkyl chloride (0.50 mmol, 1.0 equiv), and 1,3,5-trimethoxybenzene (7.4 mg, 0.044 mmol) as an internal standard. This was dissolved in 1 mL of the prepared catalyst solution before the zinc (65.4 mg, 1.0 mmol, 2.0 equiv) was added. The reactions were sealed with a screw cap fitted with a PTFE-faced silicone septum before being removed from the glovebox. The reaction was allowed to stir (1250 RPM) at 80 °C for 18-24 h.

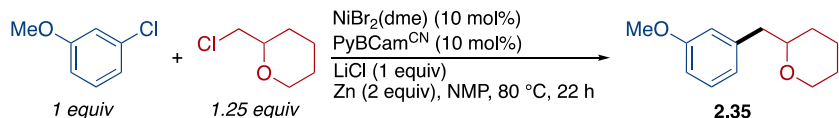
GC Analysis

Same as **Procedure A** as noted above.

Isolation and Purification

Purification B as noted above.

2.6.3.4. Preparative-Scale Benchtop Procedure.



A catalyst solution was prepared on the benchtop by charging a scintillation vial with a PTFE-coated stirbar, NiBr₂(dme) (216 mg, 0.701 mmol, 10 mol%), PyBCam^{CN} (149.4 mg, 0.701 mmol, 10 mol%) with no effort to avoid exposure to air. The scintillation vial was capped with a septa and evacuated before being backfilled with N₂. N₂ sparged NMP (9 mL) was added to the scintillation vial and the solution allowed to stir at rt for 10 min resulting in a clear, homogeneous, forest green solution. A Schlenk flask was fitted with an addition funnel and flame dried under vacuum before being backfilled with N₂. The addition funnel was removed and LiCl (297 mg, 7.01 mmol, 1.0 equiv), 3-chloroanisole

(1.00 g, 7.01 mmol, 1.0 equiv), and zinc (917 mg, 14.0 mmol, 2.0 equiv) were added to the Schlenk flask. The addition funnel was replaced and the reaction evacuated and backfilled with N₂. The catalyst solution was transferred to the reaction via syringe under N₂ and the addition funnel was charged with 2-(chloromethyl)tetrahydropyran (1.18 g, 8.76 mmol, 1.25 equiv), and NMP (5 mL). The reaction vessel was lowered into a pre-heated 80 °C oil bath resulting in a color change from forest green to dark brown and the alkyl chloride solution was added dropwise to the stirring solution over 2 h. After this addition, the reaction was allowed to stir (500 RPM) at 80 °C for an additional 20 h.

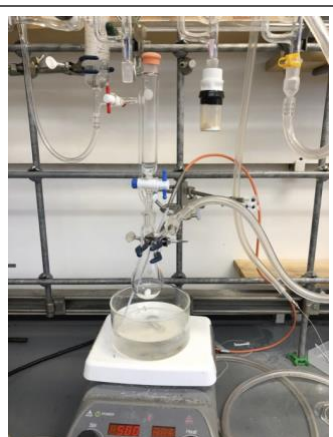


Image 1. Reaction setup with solids weighed into flask to form catalyst solution.



Image 2. Addition of LiCl, aryl chloride, and zinc flake.

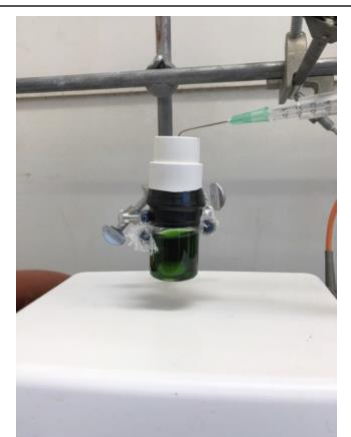


Image 3. Completed catalyst solution.



Image 4. Reaction after addition of the catalyst solution via syringe under N₂.

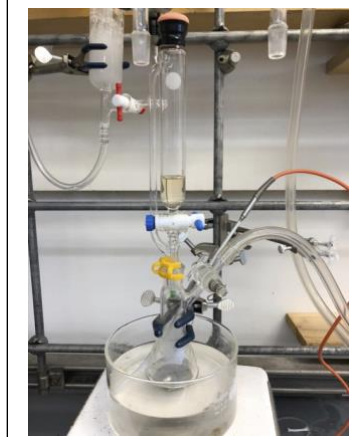


Image 5. Reaction setup prior to dropwise addition (11:30 am).

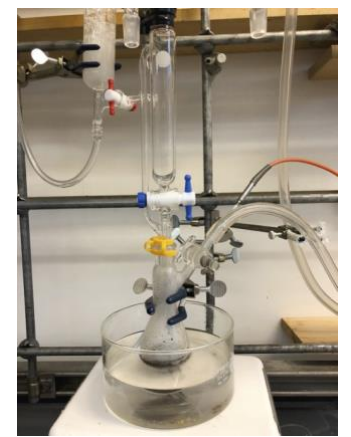


Image 6. Reaction after completion of the dropwise addition (1:35 pm).

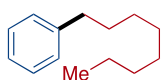
Isolation and Purification

The reaction was cooled to room temperature and diluted with Et₂O (60 mL) before being washed with a solution of saturated brine (60 mL). The Et₂O layer collected and the aqueous layer was extracted with Et₂O (3 × 30 mL). The combined organic layers were dried over MgSO₄, filtered, and the filtrate was concentrated by rotary evaporation. The resulting crude material was diluted with EtOAc and slurried with silica gel before the volatile solvents were removed by rotary evaporation. The resulting dry-loaded product was purified by column chromatography on silica to afford 2-(3-methoxybenzyl)tetrahydropyran (**2.35**) as a clear, colorless oil (915 mg, 63% yield).

2.6.3.5. General procedure for equilibrium study.

Reactions were set up in a N₂ filled glove box. To a 1-dram vial containing a PTFE-coated stir bar was added the listed additives, alkyl halides, and NMP (1 mL). The reaction vials were sealed with a screw cap fitted with a PTFE-faced silicone septum. The reaction vials were then removed from the glovebox and allowed to stir (1250 RPM) in a reaction block at 80 °C. After stirring for the amount of time listed, 10 μ L aliquots of reaction mixture were removed with a 50 μ L gas-tight syringe and quenched with 200 μ L of 1 M aqueous NaHSO₄, diluted with ether (1.5 mL), and filtered through a short silica pad in a pipette packed with glass wool. The filtrate was analyzed by GC.

2.6.4. Specific Procedures and Product Characterization.



Octylbenzene (2.3) [CAS: 2189-60-8]

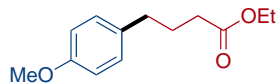
General Procedure A was followed with chlorobenzene (54.8 mg, 0.49 mmol, 1 equiv) and 1-chlorooctane (72.5 mg, 0.49 mmol, 1.0 equiv). After 24 h, the reaction was quenched following Purification B and the crude material was purified by chromatography (hexanes) to afford the product (76.1 mg, 82% yield) as a colorless oil. Characterization data matched those reported in the literature.⁴⁸

¹H NMR (500 MHz, CDCl₃) δ 7.28 (m, 2H), 7.18 (m, 3H), 2.61 (t, *J* = 7.8 Hz, 2H), 1.62 (quint, *J* = 7.4 Hz, 2H), 1.38 – 1.21 (m, 10H), 0.89 (t, *J* = 6.3 Hz, 3H).

¹³C{¹H} NMR (126 MHz, CDCl₃) δ 143.0, 128.4, 128.2, 125.5, 36.0, 31.9, 31.5, 29.5, 29.4, 29.3, 22.7, 14.1.

HRMS (ESI) [M]⁺ m/z calcd for C₁₄H₂₂⁺ 190.1716, ASAP-MS found 190.1715.

IR (cm⁻¹) 3061, 2923, 2853, 1494, 741, 696.



Ethyl 4-(4-anisole)butyrate (2.8) [CAS: 4586-89-4]

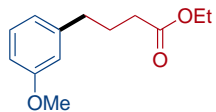
A modified General Procedure A was followed with 4-chloroanisole (71.3 mg, 0.5 mmol, 1 equiv) and ethyl 4-chlorobutyrate (17.5 μL/h (0.125 mmol/h), 0.625 mmol in total, 1.25 equiv). After a total of 19 h, the reaction mixture was filtered through silica gel with 5:1 pentane/Et₂O and the filtrate was concentrated by rotary evaporation. The resulting residue was purified by column chromatography (gradient from 40:1 pentane/Et₂O to 20:1 pent/Et₂O) to afford the product (70.6 mg, 64% yield) as a colorless oil. This procedure was repeated to establish its reproducibility and the second reaction provided the product (76.8 mg, 69% yield) in similar yield. Characterization data matched those reported in the literature.⁴⁹

¹H NMR (500 MHz, CDCl₃) δ 7.10 (d, *J* = 8.6 Hz, 2H), 6.83 (d, *J* = 8.6 Hz, 2H), 4.13 (q, *J* = 7.1 Hz, 2H), 3.78 (s, 3H), 2.60 (t, *J* = 7.6 Hz, 2H), 2.31 (t, *J* = 7.5 Hz, 2H), 1.92 (quint, *J* = 7.5 Hz, 2H), 1.25 (t, *J* = 7.1 Hz, 3H).

¹³C{¹H} NMR (126 MHz, CDCl₃) δ 173.6, 158.0, 133.6, 129.5, 113.9, 60.3, 55.3, 34.3, 33.7, 26.9, 14.3.

HRMS (ESI) [M+Na]⁺ m/z calcd for C₁₃H₁₈O₃Na⁺ 245.1148, found 245.1145.

IR (cm⁻¹) 2937, 2835, 1730, 1612, 1512, 1243, 1176, 1034, 811.



Ethyl 4-(3-anisole)butyrate (2.9) [CAS: 57816-01-0]

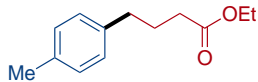
A modified General Procedure A was followed with 3-chloroanisole (71.3 mg, 0.5 mmol, 1 equiv) and ethyl 4-chlorobutyrate (17.5 μL/h (0.125 mmol/h), 0.625 mmol in total, 1.25 equiv). After a total of 24 h, the reaction mixture was filtered through silica gel with 10:1 pentane/EtOAc and the filtrate was concentrated by rotary evaporation. The resulting residue was purified by column chromatography (50:1 pentane/EtOAc) to afford the product (96.8 mg, 87% yield) as a colorless oil. Characterization data matched those reported in the literature.⁴⁹

¹H NMR (500 MHz, CDCl₃) δ 7.20 (td, *J* = 7.3, 1.9 Hz, 1H), 6.83 – 6.68 (m, 3H), 4.13 (q, *J* = 7.2 Hz, 2H), 3.80 (s, 3H), 2.63 (t, *J* = 7.6 Hz, 2H), 2.32 (t, *J* = 7.5 Hz, 2H), 1.96 (quint, *J* = 7.5 Hz, 2H), 1.26 (t, *J* = 7.1 Hz, 3H).

¹³C{¹H} NMR (126 MHz, CDCl₃) δ 173.6, 159.7, 143.2, 129.4, 121.0, 114.3, 111.4, 60.3, 55.2, 35.3, 33.7, 26.5, 14.3.

HRMS (ESI) [M+Na]⁺ m/z calcd for C₁₃H₁₈O₃Na⁺ 245.1148, found 245.1144.

IR (cm⁻¹) 2941, 1730, 1258, 1151, 1038, 776, 695.



Ethyl 4-(4-tolyl)butyrate (2.10) [CAS: 36440-63-8]

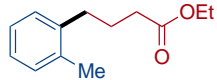
General Procedure A was followed with 4-chlorotoluene (63.3 mg, 0.5 mmol, 1 equiv) and ethyl 4-chlorobutyrate ($4 \times 17.5 \mu\text{L}$, 0.5 mmol, 1 equiv) added portionwise in 4 equal portions over 3 h. After a total of 24 h, the reaction was quenched following Purification A and the crude material was purified by chromatography (50:1 pentane/EtOAc) to afford the product (63.4 mg, 61% yield) as a colorless oil. Characterization data matched those reported in the literature.⁵⁰

$^1\text{H NMR}$ (500 MHz, CDCl_3) δ 7.14 – 7.06 (m, 4H), 4.14 (q, $J = 7.1 \text{ Hz}$, 2H), 2.63 (t, $J = 7.6 \text{ Hz}$, 2H), 2.36 – 2.29 (m, 5H), 1.95 (quint, $J = 7.5 \text{ Hz}$, 2H), 1.27 (t, $J = 7.1 \text{ Hz}$, 3H).

$^{13}\text{C}\{^1\text{H}\} \text{ NMR}$ (126 MHz, CDCl_3) δ 173.6, 138.4, 135.5, 129.1, 128.5, 60.3, 34.8, 33.8, 26.8, 21.1, 14.4.

HRMS (ESI) $[\text{M}+\text{Na}]^+$ m/z calcd for $\text{C}_{13}\text{H}_{18}\text{O}_2\text{Na}^+$ 229.1199, found 229.1196.

IR (cm⁻¹) 2925, 1732, 1515, 1143, 782.



Ethyl 4-(2-tolyl)butyrate (2.11) [CAS: 105986-51-4]

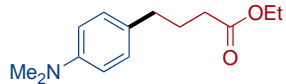
General Procedure A was followed with 2-chlorotoluene (63.3 mg, 0.5 mmol, 1 equiv) and ethyl 4-chlorobutyrate ($4 \times 17.5 \mu\text{L}$, 0.5 mmol, 1 equiv) added portionwise in 4 equal portions over 3 h. After a total 24 h, the reaction was quenched following Purification A and the crude material was purified by chromatography (50:1 pentane/EtOAc) to afford the product (15.6 mg, 15% yield) as a colorless oil. Characterization data matched those reported in the literature.⁴⁹

$^1\text{H NMR}$ (500 MHz, CDCl_3) δ 7.19 – 7.07 (m, 4H), 4.14 (q, $J = 7.1 \text{ Hz}$, 2H), 2.69 – 2.59 (m, 2H), 2.37 (t, $J = 7.4 \text{ Hz}$, 2H), 2.32 (s, 3H), 1.91 (dq, $J = 9.7, 7.5 \text{ Hz}$, 2H), 1.26 (t, $J = 7.1 \text{ Hz}$, 3H).

$^{13}\text{C}\{^1\text{H}\}$ NMR (126 MHz, CDCl_3) δ 173.7, 139.8, 136.1, 130.4, 129.1, 126.2, 126.1, 60.4, 34.1, 32.7, 25.5, 19.4, 14.4.

HRMS (ESI) $[\text{M}+\text{NH}_4]^+$ m/z calcd for $\text{C}_{13}\text{H}_{22}\text{O}_2\text{N}^+$ 224.1645, found 224.1642.

IR (cm^{-1}) 2938, 2868, 1731, 1148, 740.



Ethyl 4-(4-(dimethylamino)phenyl)butanoate (2.12) [CAS: 1365610-67-8]

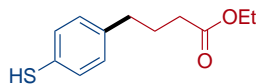
General Procedure A was followed with 4-chloro-*N,N*-dimethylaniline (77.8 mg, 0.5 mmol, 1 equiv) and ethyl 4-chlorobutyrate ($4 \times 17.5 \mu\text{L}$, 0.5 mmol, 1 equiv) added portionwise in 4 equal portions over 3 h. After a total of 24 h, the reaction was quenched following Purification A and the crude material was purified by chromatography (20:1 pentane/EtOAc) to afford the product (85.0 mg, 72% yield) as a colorless oil. Characterization data matched those reported in the literature.⁴⁹

^1H NMR (500 MHz, CDCl_3) δ 7.07 (d, $J = 8.6 \text{ Hz}$, 2H), 6.71 (d, $J = 8.6 \text{ Hz}$, 2H), 4.13 (q, $J = 7.1 \text{ Hz}$, 2H), 2.92 (s, 6H), 2.57 (t, $J = 7.6 \text{ Hz}$, 2H), 2.32 (t, $J = 7.6 \text{ Hz}$, 2H), 1.92 (quint, $J = 7.7 \text{ Hz}$, 2H), 1.26 (t, $J = 7.1 \text{ Hz}$, 3H).

$^{13}\text{C}\{^1\text{H}\}$ NMR (126 MHz, CDCl_3) δ 173.8, 149.2, 129.7, 129.2, 113.1, 60.3, 41.0, 34.2, 33.8, 27.0, 14.4.

HRMS (ESI) $[\text{M}+\text{H}]^+$ m/z calcd for $\text{C}_{14}\text{H}_{22}\text{NO}_2^+$ 236.1645, found 236.1641.

IR (cm^{-1}) 2979, 2936, 2800, 1730, 1615, 1520, 1143, 824.



Ethyl 4-(4-mercaptophenyl)butanoate (2.13)

General Procedure A was followed with 4-chlorothiophenol (72.3 mg, 0.5 mmol, 1 equiv) and ethyl 4-chlorobutyrate ($4 \times 17.5 \mu\text{L}$, 0.5 mmol, 1 equiv) added portionwise in 4 equal portions over 3 h.

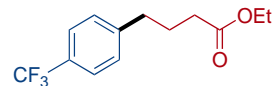
After a total of 24 h, the reaction was quenched following Purification A and the crude material was purified by chromatography (gradient from 20:1 pentane/EtOAc to 10:1 pentane/EtOAc) to afford the product (78.7 mg, 70% yield) as a clear oil.

¹H NMR (500 MHz, CDCl₃) δ 7.28 – 7.20 (m, 4H), 4.11 (q, *J* = 7.1 Hz, 2H), 2.92 (t, *J* = 7.2 Hz, 2H), 2.43 (t, *J* = 7.2 Hz, 2H), 1.92 (quint, *J* = 7.2 Hz, 2H), 1.23 (t, *J* = 7.2 Hz, 3H).

¹³C{¹H} NMR (126 MHz, CDCl₃) δ 172.9, 134.7, 132.0, 130.7, 129.1, 60.5, 33.2, 32.9, 24.3, 14.3.

HRMS (ESI) [M+Na]⁺ m/z calcd for C₁₂H₁₆O₂SnNa⁺ 247.0763, found 247.0760.

IR (cm⁻¹) 2980, 1728, 1477, 1204, 1095, 811.



Ethyl 4-(4-(trifluoromethyl)phenyl)butanoate (2.14) [CAS: 1235271-20-1]

General Procedure A was followed with 4-chlorobenzotrifluoride (90.3 mg, 0.5 mmol, 1 equiv) and ethyl 4-chlorobutyrate (4 × 17.5 μL, 0.5 mmol, 1 equiv) added portionwise in 4 equal portions over 3 h. After a total of 24 h, the reaction was quenched following Purification B and the crude material was purified by chromatography (50:1 pentane/EtOAc) to afford the product (76.8 mg, 59% yield) as a colorless oil. Characterization data matched those reported in the literature.⁴⁹

¹H NMR (500 MHz, CDCl₃) δ 7.53 (d, *J* = 7.9 Hz, 2H), 7.29 (d, *J* = 7.9 Hz, 2H), 4.13 (q, *J* = 7.1 Hz, 2H), 2.71 (t, *J* = 7.7 Hz, 2H), 2.32 (t, *J* = 7.4 Hz, 2H), 1.97 (quint, *J* = 7.5 Hz, 2H), 1.25 (t, *J* = 7.1 Hz, 3H).

¹³C{¹H} NMR (126 MHz, CDCl₃) δ 173.3, 145.7 (q, *J* = 1.5 Hz), 128.9, 128.4 (q, *J* = 32.1 Hz), 125.4 (q, *J* = 3.8 Hz), 124.4 (q, *J* = 271.8 Hz), 60.4, 35.0, 33.6, 26.3, 14.3.

HRMS (ESI) [M+Na]⁺ m/z calcd for C₁₃H₁₅F₃O₂Na⁺ 283.0916, found 283.0914.

IR (cm⁻¹) 2939, 1731, 1322, 1115, 843.



Methyl 4-octylbenzoate (2.15) [CAS: 54256-51-8]

General Procedure A was followed with methyl 4-chlorobenzoate (85.3 mg, 0.5 mmol, 1 equiv) and 1-chlorooctane ($4 \times 21.2 \mu\text{L}$, 0.5 mmol, 1 equiv) added portionwise in 4 equal portions over 3 h. After a total of 24 h, the reaction was quenched following Purification A and the crude material was purified by chromatography (40:1 pentane/EtOAc) to afford the product (65.2 mg, 53% yield) as a colorless oil. Characterization data matched those reported in the literature.⁵¹

$^1\text{H NMR}$ (500 MHz, CDCl_3) δ 7.95 (d, $J = 8.3$ Hz, 2H), 7.24 (d, $J = 8.1$ Hz, 2H), 3.90 (s, 3H), 2.68 – 2.62 (m, 2H), 1.62 – 1.59 (m, 2H), 1.33 – 1.24 (m, 10H), 0.88 (t, $J = 6.9$ Hz, 3H).

$^{13}\text{C}\{^1\text{H}\} \text{ NMR}$ (126 MHz, CDCl_3) δ 167.3, 148.7, 129.7, 128.6, 127.7, 52.1, 36.2, 32.0, 31.3, 29.6, 29.4, 29.4, 22.8, 14.2.

HRMS (ESI) $[\text{M}+\text{H}]^+$ m/z calcd for $\text{C}_{16}\text{H}_{25}\text{O}_2^+$ 249.1849, found 249.1845.

IR (cm^{-1}) 2925, 2855, 1721, 1610, 1274, 1107, 762.



Methyl 2-methoxy-5-octylbenzoate (2.16)

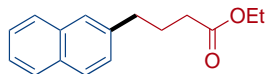
General Procedure A was followed with methyl 5-chloro-2-methoxybenzoate (100.3 mg, 0.5 mmol, 1 equiv) and 1-chlorooctane ($4 \times 21.2 \mu\text{L}$, 0.5 mmol, 1 equiv) added portionwise in 4 equal portions over 3 h. After a total of 23 h, the reaction was quenched following Purification A and the crude material was purified by chromatography (gradient from 20:1 pentane/EtOAc to 10:1 pentane/EtOAc) to afford the product (81.9 mg, 59% yield) as a colorless oil.

¹H NMR (500 MHz, CDCl₃) δ 7.60 (d, *J* = 2.3 Hz, 1H), 7.26 (dd, *J* = 8.5, 2.4 Hz, 1H), 6.88 (d, *J* = 8.5 Hz, 1H), 3.88 (s, 3H), 3.87 (s, 3H), 2.55 (t, *J* = 7.7 Hz, 2H), 1.57 (quint, *J* = 7.3 Hz, 2H), 1.32 – 1.22 (m, 10H), 0.87 (t, *J* = 7.0 Hz, 3H).

¹³C{¹H} NMR (126 MHz, CDCl₃) δ 167.0, 157.3, 134.7, 133.5, 131.5, 119.7, 112.1, 56.2, 52.1, 34.9, 32.0, 31.6, 29.6, 29.4, 29.3, 22.8, 14.2.

HRMS (ESI) [M+H]⁺ m/z calcd for C₁₇H₂₇O₃⁺ 279.1955, found 279.1951.

IR (cm⁻¹) 2925, 2854, 1729, 1254, 1082, 731.



Ethyl 4-(3-naphthyl)butyrate (2.17) [CAS: 6326-90-5]

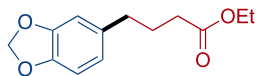
General Procedure A was followed with 3-chloronaphthalene (81.3 mg, 0.5 mmol, 1 equiv) and ethyl 4-chlorobutyrate (4 × 17.5 μL, 0.5 mmol, 1 equiv) added portionwise in 4 equal portions over 3 h. After a total of 22 h, the reaction was quenched following Purification A and the crude material was purified by chromatography (gradient from 40:1 pentane/EtOAc to 20:1 pentane/EtOAc) to afford the product (95.8 mg, 79% yield) as a colorless oil. Characterization data matched those reported in the literature.⁵⁰

¹H NMR (500 MHz, CDCl₃) δ 7.84 – 7.77 (m, 3H), 7.63 (s, 1H), 7.45 (dqd, *J* = 8.1, 6.8, 1.4 Hz, 2H), 7.35 (dd, *J* = 8.3, 1.8 Hz, 1H), 4.14 (q, *J* = 7.1 Hz, 2H), 2.84 (t, *J* = 7.6 Hz, 2H), 2.37 (t, *J* = 7.5 Hz, 2H), 2.12 – 2.02 (m, 2H), 1.27 (dt, *J* = 7.1, 4.1 Hz, 3H).

¹³C{¹H} NMR (126 MHz, CDCl₃) δ 173.6, 139.0, 133.7, 132.1, 128.1, 127.7, 127.5, 127.3, 126.7, 126.0, 125.3, 60.4, 35.4, 33.7, 26.5, 14.3.

HRMS (ESI) [M+Na]⁺ m/z calcd for C₁₆H₁₈O₂Na⁺ 265.1199, found 265.1194.

IR (cm⁻¹) 2935, 1729, 1600, 1179, 817, 746.



Ethyl 4-(3,4-benzodioxole)butyrate (2.18) [CAS: 99557-75-2]

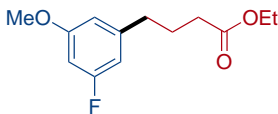
A modified General Procedure A was followed with 5-chloro-1,3-benzodioxole (78.3 mg, 0.5 mmol, 1 equiv) and ethyl 4-chlorobutyrate (17.5 μ L/h (0.125 mmol/h), 0.625 mmol in total, 1.25 equiv). After a total of 24 h, the reaction mixture was filtered through silica gel with 10:1 pentane/EtOAc and the filtrate was concentrated by rotary evaporation. The resulting residue was purified by column chromatography (gradient from 50:1 pentane/EtOAc to 10:1 pentane/EtOAc) to afford the product (73.1 mg, 62% yield) as a colorless oil. 1 H NMR matches literature,⁵² but no 13 C NMR has been reported to date.

1 H NMR (500 MHz, CDCl₃) δ 6.71 (d, *J* = 7.9 Hz, 1H), 6.66 (d, *J* = 1.7 Hz, 1H), 6.61 (dd, *J* = 7.8, 1.7 Hz, 1H), 5.90 (s, 2H), 4.12 (q, *J* = 7.1 Hz, 2H), 2.56 (t, *J* = 7.6 Hz, 2H), 2.29 (t, *J* = 7.5 Hz, 2H), 1.90 (quint, *J* = 7.5 Hz, 2H), 1.24 (t, *J* = 7.2 Hz, 3H).

13 C{ 1 H} NMR (126 MHz, CDCl₃) δ 173.6, 147.7, 145.8, 135.3, 121.3, 109.0, 108.2, 100.9, 60.3, 34.9, 33.6, 26.9, 14.3.

HRMS (ESI) [M+Na]⁺ m/z calcd for C₁₃H₁₆O₄Na⁺ 259.0941, found 259.0936.

IR (cm⁻¹) 2936, 1729, 1489, 1243, 1035, 808.



Ethyl 4-(3-fluoro-5-methoxyphenyl)butanoate (2.19)

General Procedure B was followed with 1-chloro-3-fluoro-5-methoxybenzene (80.3 mg, 0.5 mmol, 1 equiv) and ethyl 4-chlorobutyrate (75.3 mg, 0.5 mmol, 1 equiv). After 18 h, the reaction was quenched

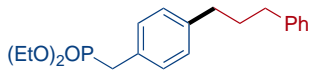
following Purification B and the crude material was purified by chromatography (gradient from hexanes to 2:23 EtOAc/hexanes) to afford the product (81.0 mg, 67% yield) as a colorless oil.

¹H NMR (500 MHz, CDCl₃) δ 6.53 – 6.47 (m, 2H), 6.45 (dt, *J* = 10.7, 2.3 Hz, 1H), 4.13 (q, *J* = 7.1 Hz, 2H), 3.78 (s, 3H), 2.61 (t, *J* = 7.5 Hz, 2H), 2.31 (t, *J* = 7.4 Hz, 2H), 1.94 (quint, *J* = 7.6 Hz, 2H), 1.26 (t, *J* = 7.1 Hz, 3H).

¹³C{¹H} NMR (126 MHz, CDCl₃) δ 173.3, 163.6 (d, *J* = 245.7 Hz), 160.9 (d, *J* = 11.3 Hz), 144.5 (d, *J* = 8.8 Hz), 110.1 (d, *J* = 2.5 Hz), 107.6 (d, *J* = 21.4 Hz), 99.1 (d, *J* = 25.2 Hz), 60.3, 55.4, 35.1 (d, *J* = 2.5 Hz), 33.5, 26.1, 14.24.

HRMS (ESI) [M+H]⁺ m/z calcd for C₁₃H₁₈FO₃⁺ 241.1235, ASAP-MS found 241.1231.

IR (cm⁻¹) 2939, 1729, 1590, 1461, 1134, 1034, 838.



Diethyl (4-(3-phenylpropyl)benzyl)phosphonate (2.20)

General Procedure B was followed with diethyl 4-chlorobenzylphosphonate (131.4 mg, 0.5 mmol, 1 equiv) and 1-chloro-3-phenylpropane (77.4 mg, 0.5 mmol, 1 equiv). After 18 h, the reaction was quenched following Purification B and the crude material was purified by chromatography (gradient from 3:7 EtOAc/hexanes to 4:1 EtOAc/hexanes) to afford the product (88.3 mg, 51% yield) as a colorless oil.

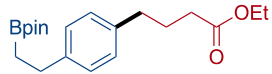
¹H NMR (500 MHz, CDCl₃) δ 7.32 – 7.25 (m, 3H), 7.21 (dd, *J* = 8.1, 2.5 Hz, 2H), 7.18 (d, *J* = 8.0 Hz, 2H), 7.13 (d, *J* = 7.8 Hz, 2H), 4.05 – 3.96 (m, 4H), 3.12 (d, *J* = 21.5 Hz, 2H), 2.66 – 2.60 (m, 4H), 1.98 – 1.90 (m, 2H), 1.24 (t, *J* = 7.1 Hz, 6H).

¹³C{¹H} NMR (126 MHz, CDCl₃) δ 142.3, 140.3 (d, *J* = 3.8 Hz), 129.7 (d, *J* = 7.6 Hz), 128.8 (d, *J* = 8.8 Hz), 128.6 (d, *J* = 2.5 Hz), 128.4, 128.3, 125.7, 60.0 (d, *J* = 7.6 Hz), 35.4, 35.0, 33.4 (d, *J* = 138.6 Hz), 32.9 (d, *J* = 1.3 Hz), 16.4 (d, *J* = 5.0 Hz).

³¹P NMR (162 MHz, CDCl₃) δ 26.7.

HRMS (ESI) [M+H]⁺ m/z calcd for C₂₀H₂₈O₃P⁺ 347.1771, ASAP-MS found 347.1766.

IR (cm⁻¹) 3024, 2981, 1507, 1245, 1022, 956, 847.



Ethyl 4-(4-(2-(4,4,5,5-tetramethyl-1,3,2-dioxaborolan-2-yl)ethyl)phenyl)butanoate (2.21)

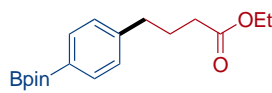
General Procedure A was followed with 2-(4-chlorophenethyl)-4,4,5,5-tetramethyl-1,3,2-dioxaborolane (133.3 mg, 0.5 mmol, 1 equiv) and ethyl 4-chlorobutyrate (4 × 17.5 μL, 0.5 mmol, 1 equiv) added portionwise in 4 equal portions over 3 h. After a total of 22 h, the reaction was quenched following Purification A and the crude material was purified by chromatography (gradient from 50:1 pentane/EtOAc to 20:1 pentane/EtOAc) to afford the product (85.1 mg, 49% yield) as a colorless oil. ¹³C NMR spectrum of **2.21** is missing the resonance corresponding to the carbon adjacent to boron, consistent with other reports.⁵³

¹H NMR (500 MHz, CDCl₃) δ 7.13 (d, *J* = 7.7 Hz, 2H), 7.06 (d, *J* = 7.7 Hz, 2H), 4.11 (q, *J* = 7.1 Hz, 2H), 2.71 (t, *J* = 8.2 Hz, 2H), 2.60 (t, *J* = 7.6 Hz, 2H), 2.30 (t, *J* = 7.7 Hz, 2H), 1.92 (quint, *J* = 7.6 Hz, 2H), 1.29 – 1.19 (m, 15H), 1.12 (t, *J* = 7.8 Hz, 2H).

¹³C{¹H} NMR (126 MHz, CDCl₃) δ 173.7, 142.1, 138.6, 128.4, 128.1, 83.2, 60.3, 34.8, 33.8, 29.6, 26.7, 24.9, 14.4.

HRMS (ESI) [M+NH₄]⁺ m/z calcd for C₂₀H₃₅BNO₄⁺ 363.2690, found 363.2691.

IR (cm⁻¹) 2979, 2936, 1733, 1371, 1143, 733.



Ethyl 4-(4-(4,4,5,5-tetramethyl-1,3,2-dioxaborolan-2-yl)phenyl)butanoate (2.22) [CAS: 1365610-75-8]

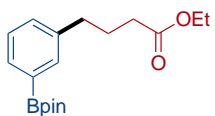
General Procedure B was followed with 4-chlorophenylboronic acid pinacol ester (119.3 mg, 0.5 mmol, 1 equiv) and ethyl 4-chlorobutyrate (75.3 mg, 0.5 mmol, 1 equiv). After 18 h, the reaction was quenched following Purification B and the crude material was purified by chromatography (gradient from hexanes to 2:23 EtOAc/hexanes) to afford the product (116.2 mg, 73% yield) as a colorless oil. Characterization data matched those reported in the literature.⁴⁹ ¹³C NMR spectrum of **2.22** is missing the resonance corresponding to the carbon adjacent to boron, consistent with other reports.⁵³

¹H NMR (500 MHz, CDCl₃) δ 7.73 (d, *J* = 7.9 Hz, 2H), 7.19 (d, *J* = 7.9 Hz, 2H), 4.12 (q, *J* = 7.1 Hz, 2H), 2.66 (t, *J* = 7.6 Hz, 2H), 2.30 (t, *J* = 7.5 Hz, 2H), 1.95 (quint, *J* = 7.7 Hz, 2H), 1.34 (s, 12H), 1.25 (t, *J* = 7.1 Hz, 3H).

¹³C{¹H} NMR (126 MHz, CDCl₃) δ 173.4, 144.8, 134.9, 127.9, 83.7, 60.2, 35.3, 33.6, 26.4, 24.9, 14.2.

HRMS (ESI) [M+Na]⁺ *m/z* calcd for C₁₈H₂₇BO₄Na⁺ 341.1895, found 341.1893.

IR (cm⁻¹) 2978, 2933, 1731, 1610, 1357, 1141, 1088, 856.



Ethyl 4-(3-(4,4,5,5-tetramethyl-1,3,2-dioxaborolan-2-yl)phenyl)butanoate (2.23)

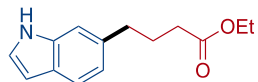
General Procedure A was followed with 2-(3-chlorophenyl)-4,4,5,5-tetramethyl-1,3,2-dioxaborolane (119.3 mg, 0.5 mmol, 1 equiv) and ethyl 4-chlorobutyrate (4 × 17.5 μL, 0.5 mmol, 1 equiv) added portionwise in 4 equal portions over 3 h. After a total of 24 h, the reaction was quenched following Purification A and the crude material was purified by chromatography (20:1 pentane/EtOAc) to afford the product (104.0 mg, 65% yield) as a clear oil. ¹³C NMR spectrum of **2.23** is missing the resonance corresponding to the carbon adjacent to boron, consistent with other reports.⁵³

¹H NMR (500 MHz, CDCl₃) δ 7.65 – 7.63 (m, 2H), 7.33 – 7.26 (m, 2H), 4.12 (q, *J* = 7.1 Hz, 2H), 2.65 (t, *J* = 7.6 Hz, 2H), 2.31 (t, *J* = 7.5 Hz, 2H), 1.96 (quint, *J* = 7.6 Hz, 2H), 1.35 (s, 12H), 1.25 (t, *J* = 7.1 Hz, 3H).

¹³C{¹H} NMR (126 MHz, CDCl₃) δ 173.7, 140.9, 135.0, 132.6, 131.6, 128.0, 83.9, 60.4, 35.2, 33.9, 26.8, 25.0, 14.4.

HRMS (ESI) [M+Na]⁺ m/z calcd for C₁₈H₂₇BO₄Na⁺ 340.1931, found 340.1926.

IR (cm⁻¹) 2979, 2934, 1733, 1355, 1143, 709.



Ethyl 4-(1H-indol-6-yl)butanoate (2.24)

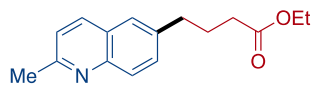
General Procedure A was followed with 6-chloro-1H-indole (75.8 mg, 0.5 mmol, 1 equiv) and ethyl 4-chlorobutyrate (4 × 17.5 μL, 0.5 mmol, 1 equiv) added portionwise in 4 equal portions over 3 h. After a total of 23 h, the reaction was quenched following Purification A and the crude material was purified by chromatography (gradient from 10:1 pentane/EtOAc to 8:1 pentane/EtOAc) to afford the product (81.6 mg, 71% yield) as a pale yellow oil.

¹H NMR (500 MHz, CDCl₃) δ 8.10 (s, 1H), 7.56 (d, *J* = 8.1 Hz, 1H), 7.19 (s, 1H), 7.15 (dd, *J* = 3.2, 2.4 Hz, 1H), 6.97 (dd, *J* = 8.0, 1.5 Hz, 1H), 6.52 (ddd, *J* = 3.1, 2.0, 1.0 Hz, 1H), 4.13 (q, *J* = 7.1 Hz, 2H), 2.77 (t, *J* = 7.5 Hz, 2H), 2.35 (t, *J* = 7.5 Hz, 2H), 2.02 (quint, *J* = 7.6 Hz, 2H), 1.26 (t, *J* = 7.1 Hz, 3H).

¹³C{¹H} NMR (126 MHz, CDCl₃) δ 173.9, 136.3, 135.6, 126.2, 123.9, 121.1, 120.6, 110.7, 102.5, 60.4, 35.5, 33.9, 27.2, 14.4.

HRMS (ESI) [M+H]⁺ m/z calcd for C₁₄H₁₈NO₂⁺ 232.1332, found 232.1328.

IR (cm⁻¹) 3400, 2932, 2858, 1712, 1250, 721.



Ethyl 4-(2-methylquinolin-6-yl)butyrate (2.25)

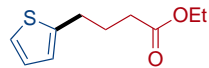
A modified General Procedure A was followed with 6-chloro-2-methylquinoline (88.8 mg, 0.5 mmol, 1 equiv) and ethyl 4-chlorobutyrate (17.5 μ L/h (0.125 mmol/h), 0.625 mmol in total, 1.25 equiv). After a total of 24 h, the reaction was quenched following Purification A and the crude material was purified by chromatography (gradient from 50:1 pentane/EtOAc to 10:1 pentane/EtOAc) to afford the product (81.7 mg, 63% yield) as a slightly yellow oil.

$^1\text{H NMR}$ (500 MHz, CDCl_3) δ 7.94 (dd, J = 13.5, 8.4 Hz, 2H), 7.50 (d, J = 8.9 Hz, 2H), 7.23 (d, J = 8.4 Hz, 1H), 4.10 (q, J = 7.1 Hz, 2H), 2.80 (t, J = 7.6 Hz, 2H), 2.71 (s, 3H), 2.33 (t, J = 7.4 Hz, 2H), 2.07 – 1.98 (m, 2H), 1.23 (t, J = 7.2 Hz, 3H).

$^{13}\text{C}\{^1\text{H}\} \text{ NMR}$ (126 MHz, CDCl_3) δ 173.5, 158.4, 146.8, 138.9, 135.8, 130.8, 128.7, 126.5, 126.2, 122.1, 60.4, 35.1, 33.7, 26.4, 25.4, 14.3.

HRMS (ESI) $[\text{M}+\text{H}]^+$ m/z calcd for $\text{C}_{16}\text{H}_{20}\text{NO}_2^+$ 258.1489, found 258.1485.

IR (cm^{-1}) 2939, 1728, 1601, 1374, 1179, 1026, 827.



Ethyl 4-(thiophen-2-yl)butanoate (2.26) [CAS: 91950-17-3]

General Procedure B was followed with 2-chlorothiophene (59.3 mg, 0.5 mmol, 1 equiv) and ethyl 4-chlorobutyrate (75.3 mg, 0.5 mmol, 1 equiv). After 18 h, the reaction was quenched following Purification B with 5% aq NH_4OH instead of brine and the crude material was purified by chromatography (gradient from hexanes to 2:23 EtOAc/hexanes) to afford the product (32.7 mg, 33% yield) as a colorless oil. A $^1\text{H NMR}$ for **2.26** was reported in CDCl_3 (example 17),⁵⁴ but it appears to

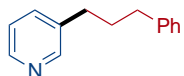
actually be of the methyl ester according to the experimental (esterification in methanol) and the reported spectrum: it is missing the expected ethyl CH_3 at 1.26 ppm and the 2H signal at 4.13 ppm and has an unexpected 3H singlet at 3.67 ppm.

$^1\text{H NMR}$ (500 MHz, CDCl_3) δ 7.12 (dd, $J = 5.1, 1.2$ Hz, 1H), 6.92 (dd, $J = 5.1, 3.4$ Hz, 1H), 6.80 (dd, $J = 3.5, 1.1$ Hz, 1H), 4.13 (q, $J = 7.1$ Hz, 2H), 2.88 (t, $J = 7.5$ Hz, 2H), 2.36 (t, $J = 7.4$ Hz, 2H), 2.01 (quint, $J = 7.5$ Hz, 2H), 1.26 (t, $J = 7.1$ Hz, 3H).

$^{13}\text{C}\{^1\text{H}\} \text{ NMR}$ (126 MHz, CDCl_3) δ 173.2, 144.1, 126.8, 124.5, 123.2, 60.3, 33.4, 29.1, 26.9, 14.2.

HRMS (ESI) $[\text{M}+\text{H}]^+$ m/z calcd for $\text{C}_{10}\text{H}_{15}\text{O}_2\text{S}^+$ 199.0787, ASAP-MS found 199.0785.

IR (cm^{-1}) 2934, 1729, 1163, 1026, 847, 823, 694.



3-(3-phenylpropyl)pyridine (2.27) [CAS: 1802-34-2]

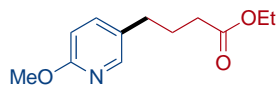
General Procedure B was followed with diethyl 3-chloropyridine (56.8 mg, 0.5 mmol, 1 equiv) and 1-chloro-3-phenylpropane (77.4 mg, 0.5 mmol, 1 equiv). After 16 h, the reaction was quenched following Purification B with 5% aq NH_4OH instead of brine and the crude material was purified by chromatography (2:3 EtOAc/cyclohexane) to afford the product (65.0 mg, 66% yield) as a pale yellow oil. Characterization data matched those reported in the literature.⁴⁴

$^1\text{H NMR}$ (500 MHz, CDCl_3) δ 8.47 – 8.42 (m, 2H), 7.49 (dt, $J = 7.8, 2.0$ Hz, 1H), 7.29 (dd, $J = 8.2, 6.8$ Hz, 2H), 7.22 – 7.16 (m, 4H), 2.66 (q, $J = 8.1$ Hz, 4H), 2.01 – 1.92 (m, 2H).

$^{13}\text{C}\{^1\text{H}\} \text{ NMR}$ (126 MHz, CDCl_3) δ 150.0, 147.4, 141.7, 137.4, 135.7, 128.4, 125.9, 123.2, 35.3, 32.6, 32.4.

HRMS (ESI) $[\text{M}+\text{H}]^+$ m/z calcd for $\text{C}_{14}\text{H}_{16}\text{N}^+$ 198.1277, found 198.1276.

IR (cm^{-1}) 3025, 2930, 2855, 1598, 1485, 1075, 744, 703.



Ethyl 4-(6-methoxypyridin-3-yl)butanoate (2.28)

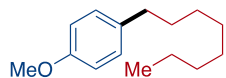
General Procedure B was followed with 5-chloro-2-methoxypyridine (71.8 mg, 0.5 mmol, 1 equiv) and ethyl 4-chlorobutyrate (75.3 mg, 0.5 mmol, 1 equiv). After 16 h, the reaction was quenched following Purification B with 5% aq NH₄OH instead of brine and the crude material was purified by chromatography (10:1 DCM/MeOH) to afford the product (81.5 mg, 73% yield) as a yellow oil. Characterization data matched those reported in the literature.⁴⁴

¹H NMR (500 MHz, CDCl₃) δ 7.96 (d, *J* = 2.4 Hz, 1H), 7.40 (dd, *J* = 8.5, 2.5 Hz, 1H), 6.68 (d, *J* = 8.5 Hz, 1H), 4.12 (q, *J* = 7.2 Hz, 2H), 3.91 (s, 3H), 2.57 (t, *J* = 7.6 Hz, 2H), 2.31 (t, *J* = 7.4 Hz, 2H), 1.91 (quint, *J* = 7.5 Hz, 2H), 1.25 (t, *J* = 7.1 Hz, 3H).

¹³C{¹H} NMR (126 MHz, CDCl₃) δ 173.3, 162.8, 146.1, 138.9, 129.2, 110.5, 60.3, 53.3, 33.4, 31.3, 26.5, 14.2.

HRMS (ESI) [M+H]⁺ m/z calcd for C₁₂H₁₈NO₃⁺ 224.1281, found 224.1279.

IR (cm⁻¹) 2940, 1729, 1606, 1489, 1387, 1283, 1252, 1176, 1142, 1023, 828.



4-octylanisole (2.29) [CAS: 3307-19-5]

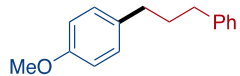
General Procedure A was followed with 4-chloroanisole (71.3 mg, 0.5 mmol, 1 equiv) and 1-chlorooctane (74.3 mg, 0.5 mmol, 1.0 equiv) added in one portion. After 24 h, the reaction mixture was loaded directly onto a silica gel column and purified by column chromatography (40:1 pentane/Et₂O) to afford the product (72.2 mg, 66% yield) as a colorless oil. Characterization data matched those reported in the literature.⁴⁸

¹H NMR (500 MHz, CDCl₃) δ 7.10 (d, *J* = 8.5 Hz, 2H), 6.83 (d, *J* = 8.6 Hz, 2H), 3.79 (s, 3H), 2.54 (t, *J* = 7.2 Hz, 2H), 1.68 – 1.49 (m, 2H), 1.37 – 1.09 (m, 10H), 0.88 (t, *J* = 6.8 Hz, 3H).

¹³C{¹H} NMR (126 MHz, CDCl₃) δ 157.7, 135.2, 129.4, 113.8, 55.4, 35.2, 32.0, 31.9, 29.6, 29.5, 29.4, 22.8, 14.3.

HRMS (ESI) [M+H]⁺ m/z calcd for C₁₅H₂₅O⁺ 221.1900, ASAP-MS found 221.1900.

IR (cm⁻¹) 2922, 2852, 1611, 1510, 1459, 1242, 1038, 818.



1-methoxy-4-(3-phenylpropyl)benzene (2.30)

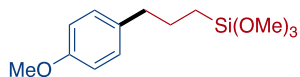
A modified General Procedure A was followed with 4-chloroanisole (71.3 mg, 0.5 mmol, 1 equiv) and 1-chloro-3-phenylpropane (17.9 μL/h (0.125 mmol/h), 0.625 mmol in total, 1.25 equiv). After a total of 19 h, the reaction mixture was filtered through silica gel with 5:1 pentane/Et₂O and the filtrate was concentrated by rotary evaporation. The resulting residue was purified by column chromatography (50:1 pentane/Et₂O) to afford the product (94.6 mg, 84% yield) as a colorless oil. Characterization data matched those reported in the literature.⁵⁵

¹H NMR (500 MHz, CDCl₃) δ 7.36 – 7.29 (m, 2H), 7.26 – 7.19 (m, 3H), 7.17 – 7.12 (d, *J* = 8.6 Hz, 2H), 6.90 – 6.85 (d, *J* = 8.6 Hz, 2H), 3.82 (s, 3H), 2.68 (t, *J* = 7.7 Hz, 2H), 2.64 (t, *J* = 7.7 Hz, 2H), 1.97 (tt, *J* = 9.3, 6.8 Hz, 2H).

¹³C{¹H} NMR (126 MHz, CDCl₃) δ 157.8, 142.5, 134.5, 129.4, 128.6, 128.4, 125.8, 113.8, 55.4, 35.5, 34.6, 33.3.

HRMS (ESI) [M+H]⁺ m/z calcd for C₁₆H₁₉O⁺ 227.1430, ASAP-MS found 227.1428.

IR (cm⁻¹) 3027, 2933, 2856, 1611, 1511, 1243, 1036, 731.



Trimethoxy-[3-(4-methoxyphenyl)propyl]silane (2.31) [CAS: 40715-68-2]

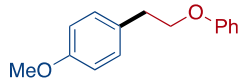
General Procedure A was followed with 4-chloroanisole (71.3 mg, 0.5 mmol, 1 equiv) and (3-chloropropyl)trimethoxysilane ($4 \times 22.8 \mu\text{L}$, 0.5 mmol, 1 equiv) added portionwise in 4 equal portions over 3 h. After a total of 24 h, the reaction was quenched following Purification B and the crude material was purified by chromatography (9:1 hexanes/EtOAc) to afford the product (43.3 mg, 32% yield) as a colorless oil.

$^1\text{H NMR}$ (400 MHz, CDCl_3) δ 7.09 (d, $J = 8.6 \text{ Hz}$, 2H), 6.82 (d, $J = 8.6 \text{ Hz}$, 2H), 3.78 (s, 3H), 3.55 (s, 9H), 2.58 (t, $J = 7.6 \text{ Hz}$, 2H), 1.76 – 1.64 (m, 2H), 0.72 – 0.63 (m, 2H).

$^{13}\text{C}\{^1\text{H}\} \text{ NMR}$ (126 MHz, CDCl_3) δ 157.8, 134.5, 129.5, 113.8, 55.4, 50.7, 38.4, 24.9, 8.9.

HRMS (ESI) $[\text{M}+\text{Na}]^+$ m/z calcd for $\text{C}_{13}\text{H}_{22}\text{O}_4\text{SiNa}^+$ 293.1180, found 293.1176.

IR (cm^{-1}) 2934, 2838, 1510, 1460, 1243, 1183, 1077, 1037, 806.



1-methoxy-4-(2-phenoxyethyl)benzene (2.32) [CAS: 127294-20-6]

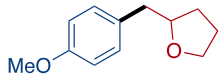
A modified General Procedure A was followed with 4-chloroanisole (71.3 mg, 0.5 mmol, 1 equiv) and (2-chloroethoxy)benzene ($17.3 \mu\text{L}/\text{h}$ (0.125 mmol/h), 0.625 mmol in total, 1.25 equiv). After a total of 19 h, the reaction mixture was filtered through silica gel with 5:1 pentane/Et₂O and the filtrate was concentrated by rotary evaporation. The resulting residue was purified by column chromatography (gradient from 40:1 pentane/Et₂O to 30:1 pentane/Et₂O) to afford the product (73.3 mg, 64% yield) as a colorless oil. Characterization data matched those reported in the literature.⁵⁶

$^1\text{H NMR}$ (500 MHz, CDCl_3) δ 7.34 (t, $J = 7.9 \text{ Hz}$, 2H), 7.28 (d, $J = 8.9 \text{ Hz}$, 2H), 7.04 – 6.90 (m, 5H), 4.20 (t, $J = 7.1 \text{ Hz}$, 2H), 3.86 (s, 3H), 3.11 (t, $J = 7.1 \text{ Hz}$, 2H).

$^{13}\text{C}\{\text{H}\}$ NMR (126 MHz, CDCl_3) δ 158.9, 158.4, 130.4, 130.1, 129.5, 120.8, 114.6, 114.0, 68.9, 55.3, 35.0.

HRMS (ESI) $[\text{M}-\text{OPh}]^+$ m/z calcd for $\text{C}_9\text{H}_{11}\text{O}^+$ 135.0804, found 135.0803.

IR (cm^{-1}) 2937, 2836, 1513, 1241, 1033, 906, 727.



2-(4-methoxybenzyl)tetrahydrofuran (2.33) [CAS: 859999-32-9]

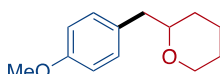
A modified General Procedure A was followed with 4-chloroanisole (71.3 mg, 0.5 mmol, 1 equiv) and 2-(chloromethyl)tetrahydrofuran (13.6 $\mu\text{L}/\text{h}$ (0.125 mmol/h), 0.625 mmol in total, 1.25 equiv). After a total of 22 h, the reaction was quenched following Purification A and the crude material was purified by chromatography (gradient from 50:1 pentane/EtOAc to 20:1 pentane/EtOAc) to afford the product (66.3 mg, 69% yield) as a colorless oil. Characterization data matched those reported in the literature.⁵⁷

^1H NMR (500 MHz, CDCl_3) δ 7.15 (d, $J = 8.4$ Hz, 2H), 6.84 (d, $J = 8.6$ Hz, 2H), 4.03 (quint, $J = 6.6$ Hz, 1H), 3.89 (q, $J = 7.2$ Hz, 1H), 3.78 (s, 3H), 3.74 (td, $J = 7.9, 6.3$ Hz, 1H), 2.86 (dd, $J = 13.7, 6.5$ Hz, 1H), 2.70 (dd, $J = 13.7, 6.4$ Hz, 1H), 1.96 – 1.79 (m, 3H), 1.55 (dq, $J = 11.5, 8.0$ Hz, 1H).

$^{13}\text{C}\{\text{H}\}$ NMR (126 MHz, CDCl_3) δ 158.1, 131.1, 130.2, 113.8, 80.3, 68.0, 55.3, 41.1, 31.0, 25.7.

HRMS (ESI) $[\text{M}+\text{H}]^+$ m/z calcd for $\text{C}_{12}\text{H}_{17}\text{O}_2^+$ 193.1223, ASAP-MS found 193.1221.

IR (cm^{-1}) 2935, 2835, 1612, 1512, 1244, 1177, 1034.



2-(4-methoxybenzyl)tetrahydropyran (2.34) [CAS: 1408141-63-8]

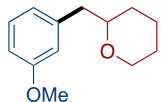
General Procedure A was followed with 4-chloroanisole (71.3 mg, 0.5 mmol, 1 equiv) and 2-(chloromethyl)tetrahydropyran ($4 \times 15.7 \mu\text{L}$, 0.5 mmol, 1.0 equiv) added portionwise in 4 equal portions over 3 h. After a total of 24 h, the reaction was quenched following Purification A and the crude material was purified by chromatography (gradient from 20:1 pentane/EtOAc to 15:1 pentane/EtOAc) to afford the product (93.0 mg, 90% yield) as a colorless oil. Characterization data matched those reported in the literature.⁵⁶

¹H NMR (500 MHz, CDCl₃) δ 7.13 (d, *J* = 8.6 Hz, 2H), 6.83 (d, *J* = 8.7 Hz, 2H), 3.98 (ddt, *J* = 11.5, 4.1, 1.8 Hz, 1H), 3.79 (s, 3H), 3.48 – 3.36 (m, 2H), 2.82 (dd, *J* = 13.8, 6.6 Hz, 1H), 2.59 (dd, *J* = 13.8, 6.5 Hz, 1H), 1.80 (dq, *J* = 12.4, 2.7 Hz, 1H), 1.56 (tt, *J* = 12.1, 4.1 Hz, 2H), 1.52 – 1.36 (m, 2H), 1.27 (tdd, *J* = 12.9, 10.9, 4.0 Hz, 1H).

¹³C{¹H} NMR (126 MHz, CDCl₃) δ 158.1, 131.0, 130.4, 113.7, 79.1, 68.7, 55.3, 42.4, 31.5, 26.2, 23.6.

HRMS (ESI) [M+H]⁺ m/z calcd for C₁₃H₁₉O₂⁺ 207.1380, ASAP-MS found 207.1377.

IR (cm⁻¹) 2934, 2835, 1612, 1511, 1243, 1036.



2-(3-methoxybenzyl)tetrahydropyran (2.35) [CAS: 1258063-60-3]

The preparative-scale benchtop procedure was followed with 3-chloroanisole (1.0 g, 7.01 mmol, 1 equiv) and 2-(chloromethyl)tetrahydropyran (1.18 g, 8.76 mmol, 1.25 equiv) added dropwise via addition funnel over 2 h. After stirring at 80 °C for a total of 24 h, the reaction was cooled to room temperature and diluted with Et₂O (20 mL). The reaction was washed with a solution of saturated brine (4 \times 50 mL). The combined aqueous layer was extracted with Et₂O (20 mL) and the organic layers were combined, dried over MgSO₄, and concentrated by rotary evaporation to provide a yellow oil. The resulting crude was dry-loaded and purified by column chromatography (gradient from 20:1

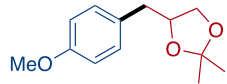
pentane/EtOAc to 10:1 pentane/EtOAc) to provide the product (915 mg, 63% yield) as a clear, colorless oil. Characterization data matched those reported in the literature.⁵⁸

¹H NMR (500 MHz, CDCl₃) δ 7.20 (t, *J* = 7.8 Hz, 1H), 6.83 – 6.73 (m, 3H), 4.01 – 3.95 (m, 1H), 3.80 (s, 3H), 3.49 (dtd, *J* = 10.8, 6.6, 2.0 Hz, 1H), 3.42 (td, *J* = 11.8, 2.4 Hz, 1H), 2.86 (dd, *J* = 13.6, 6.6 Hz, 1H), 2.62 (dd, *J* = 13.6, 6.5 Hz, 1H), 1.85 – 1.77 (m, 1H), 1.65 – 1.53 (m, 2H), 1.52 – 1.38 (m, 2H), 1.34 – 1.24 (m, 1H).

¹³C{¹H} NMR (126 MHz, CDCl₃) δ 159.6, 140.6, 129.3, 121.9, 115.3, 111.5, 78.8, 68.8, 55.3, 43.4, 31.6, 26.2, 23.6.

HRMS (ESI) [M+H]⁺ m/z calcd for C₁₃H₁₉O⁺ 207.1380, ASAP-MS found 207.1378.

IR (cm⁻¹) 2935, 2836, 1256, 1087, 1041, 696.



4-(4-methoxybenzyl)-2,2-dimethyl-1,3-dioxolane (2.36)

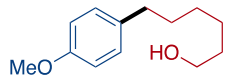
General Procedure A was followed with 4-chloroanisole (71.3 mg, 0.5 mmol, 1 equiv) and 4-(chloromethyl)-2,2-dimethyl-1,3-dioxolane (4 × 17.7 μL, 0.5 mmol, 1.0 equiv) added portionwise in 4 equal portions over 3 h. After a total of 24 h, the reaction was quenched following Purification A and the crude material was purified by chromatography (gradient from 20:1 pentane/EtOAc to 10:1 pentane/EtOAc) to afford the product (59.7 mg, 54% yield) as a colorless oil. Characterization data matched those reported in the literature.⁵⁹

¹H NMR (500 MHz, CDCl₃) δ 7.13 (d, *J* = 8.6 Hz, 2H), 6.84 (d, *J* = 8.6 Hz, 2H), 4.33 – 4.24 (m, 1H), 3.95 (dd, *J* = 8.1, 5.9 Hz, 1H), 3.79 (s, 3H), 3.63 (dd, *J* = 8.1, 6.9 Hz, 1H), 2.96 (dd, *J* = 13.8, 6.1 Hz, 1H), 2.72 (dd, *J* = 13.8, 7.2 Hz, 1H), 1.43 (s, 3H), 1.35 (s, 3H).

¹³C{¹H} NMR (126 MHz, CDCl₃) δ 158.4, 130.2, 129.7, 114.0, 109.2, 77.0, 69.1, 55.3, 39.3, 27.1, 25.8.

HRMS (ESI) $[M+H]^+$ m/z calcd for $C_{13}H_{19}O_3^+$ 223.1329, ASAP-MS found 223.1327.

IR (cm^{-1}) 2986, 2936, 2836, 1613, 1513, 1245, 1035.



6-(4-methoxyphenyl)hexan-1-ol (2.37) [CAS: 102831-36-7]

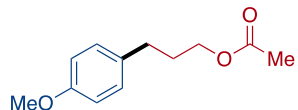
A modified General Procedure A was followed with 4-chloroanisole (71.3 mg, 0.5 mmol, 1 equiv) and 6-chlorohexan-1-ol (16.7 $\mu\text{L}/\text{h}$ (0.125 mmol/h), 0.625 mmol in total, 1.25 equiv). After a total of 22 h, the reaction was quenched following Purification A and the crude material was purified by chromatography (gradient from 20:1 pentane/EtOAc to 5:1 pentane/EtOAc) to afford the product (69.6 mg, 67% yield) as a colorless oil. Characterization data matched those reported in the literature.⁶⁰

$^1\text{H NMR}$ (500 MHz, CDCl_3) δ 7.09 (d, $J = 8.8$ Hz, 2H), 6.82 (d, $J = 8.1$ Hz, 2H), 3.79 (s, 3H), 3.63 (t, $J = 6.6$ Hz, 2H), 2.55 (t, $J = 7.7$ Hz, 2H), 1.61 (s, 1H), 1.57 (tq, $J = 12.8, 7.2$ Hz, 4H), 1.36 (tq, $J = 11.0, 5.8, 5.0$ Hz, 4H).

$^{13}\text{C}\{^1\text{H}\} \text{ NMR}$ (126 MHz, CDCl_3) δ 157.7, 135.0, 129.4, 113.8, 63.1, 55.4, 35.1, 32.9, 31.8, 29.1, 25.7.

HRMS (ESI) $[M+H]^+$ m/z calcd for $C_{13}H_{21}O_2^+$ 209.1536, $[M-\text{OH}]^+$ m/z calcd for $C_{13}H_{19}O^+$ 191.1430, ASAP-MS found 209.1534, 191.1428.

IR (cm^{-1}) 3338, 2929, 2855, 1612, 1511, 1243, 1035, 731.



3-(4-methoxyphenyl)propyl acetate (2.38)

A modified General Procedure A was followed with 4-chloroanisole (71.3 mg, 0.5 mmol, 1 equiv) and 3-chloropropyl acetate (15.4 $\mu\text{L}/\text{h}$ (0.125 mmol/h), 0.625 mmol in total, 1.25 equiv). After a total of

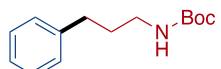
22 h, the reaction was quenched following Purification A and the crude material was purified by chromatography (gradient from 40:1 pentane/EtOAc to 15:1 pentane/EtOAc) to afford the product (54.4 mg, 52% yield) as a colorless oil. Characterization data matched those reported in the literature.⁶¹

¹H NMR (500 MHz, CDCl₃) δ 7.10 (d, *J* = 8.5 Hz, 2H), 6.83 (d, *J* = 8.3 Hz, 2H), 4.07 (t, *J* = 6.6 Hz, 2H), 3.79 (s, 3H), 2.63 (t, *J* = 7.7 Hz, 2H), 2.05 (s, 3H), 1.97 – 1.88 (m, 2H).

¹³C{¹H} NMR (126 MHz, CDCl₃) δ 171.3, 158.0, 133.3, 129.4, 113.9, 63.9, 55.4, 31.3, 30.5, 21.1.

HRMS (ESI) [M+NH₄]⁺ m/z calcd for C₁₂H₂₀NO₃⁺ 226.1438, found 226.1434.

IR (cm⁻¹) 2953, 2836, 1735, 1612, 1512, 1236, 1034, 810.



Tert-butyl (3-phenylpropyl)carbamate (2.39) [CAS: 147410-39-7]

General Procedure B was followed with chlorobenzene (56.3 mg, 0.5 mmol, 1 equiv) and *tert*-butyl (3-chloropropyl)carbamate (92.3 μ L, 0.5 mmol, 1 equiv) added in one portion. After 42 h, the reaction was quenched following Purification B and the crude material was purified by chromatography (gradient from hexanes to 4:1 hexanes/EtOAc) to afford the product (72.9 mg, 62% yield) as a colorless oil. Characterization data matched those reported in the literature.⁴⁹

¹H NMR (500 MHz, CDCl₃) δ 7.34 (t, *J* = 7.6 Hz, 2H), 7.25 (t, *J* = 7.2 Hz, 3H), 4.70 (s, 1H), 3.26 – 3.10 (m, 2H), 2.70 (t, *J* = 7.8 Hz, 2H), 1.87 (quint, *J* = 7.3 Hz, 2H), 1.52 (s, 9H).

¹³C{¹H} NMR (126 MHz, CDCl₃) δ 156.1, 141.6, 128.5, 128.4, 126.0, 79.1, 40.3, 33.2, 31.8, 28.5.

HRMS (ESI) [M+Na]⁺ m/z calcd for C₁₄H₂₁NO₂Na⁺ 258.1465, found 258.1463.

IR (cm⁻¹) 3345, 2972, 2928, 2861, 1689, 1505, 1451, 1363, 1246, 1165, 740, 697.



tert-butyl benzyl(3-phenylpropyl)carbamate (2.40)

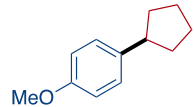
General Procedure A was followed with chlorobenzene (56.3 mg, 0.5 mmol, 1 equiv) and tert-butyl benzyl(3-chloropropyl)carbamate ($4 \times 36.1 \mu\text{L}$, 0.5 mmol, 1 equiv) added portionwise in 4 equal portions over 3 h. After a total of 24 h, the reaction was quenched following Purification B procedure and the crude material was purified by chromatography (gradient from hexanes to 9:1 hexanes/EtOAc) to afford the product (100.7 mg, 62% yield) as a colorless oil.

$^1\text{H NMR}$ (500 MHz, CDCl_3) δ 7.38 – 7.13 (m, 10H), 4.46 (d, $J = 24.8$ Hz, 2H), 3.26 (d, $J = 62.4$ Hz, 2H), 2.60 (s, 2H), 1.84 (s, 2H), 1.50 (s, 9H).

$^{13}\text{C}\{^1\text{H}\} \text{NMR}$ (126 MHz, CDCl_3) δ 156.1, 155.7, 141.9, 141.7, 138.8, 138.6, 128.6, 128.5, 128.4, 128.4, 127.8, 127.2, 125.9, 79.7, 50.7, 50.1, 46.6, 46.3, 33.3, 29.8, 28.5.

HRMS (ESI) $[\text{M}+\text{Na}]^+$ m/z calcd for $\text{C}_{21}\text{H}_{27}\text{NO}_2\text{Na}^+$ 348.1934, found 348.1931.

IR (cm^{-1}) 3061, 3027, 2972, 2928, 1688, 1455, 1412, 1363, 1156, 882, 735, 697.



1-cyclopentyl-4-methoxybenzene (2.41) [CAS: 1507-97-7]

A modified General Procedure A was followed with 4-chloroanisole (71.3 mg, 0.5 mmol, 1 equiv) and chlorocyclopentane ($15.1 \mu\text{L}/\text{h}$ (0.125 mmol/h), 0.625 mmol in total, 1.25 equiv). After a total of 22 h, the reaction was quenched following Purification A procedure and the crude material was purified by chromatography (100:1 pentane/EtOAc) to afford the product (31.0 mg, 35% yield) as a colorless oil. Characterization data matched those reported in the literature.⁶²

$^1\text{H NMR}$ (500 MHz, CDCl_3) δ 7.17 (d, $J = 8.6$ Hz, 2H), 6.84 (d, $J = 8.5$ Hz, 2H), 3.80 (s, 3H), 2.95 (tt, $J = 9.9, 7.4$ Hz, 1H), 2.10 – 2.00 (m, 2H), 1.80 (ddd, $J = 9.9, 7.1, 4.9$ Hz, 2H), 1.74 – 1.63 (m, 2H), 1.61 – 1.50 (m, 2H).

$^{13}\text{C}\{\text{H}\}$ NMR (126 MHz, CDCl_3) δ 157.6, 138.5, 127.9, 113.6, 55.3, 45.1, 34.7, 25.4.

HRMS (ESI) $[\text{M}+\text{H}]^+$ m/z calcd for $\text{C}_{12}\text{H}_{17}\text{O}^+$ 177.1274, ASAP-MS found 177.1272.

IR (cm^{-1}) 2951, 2866, 2834, 1612, 1512, 1242, 1038, 824.

2.7. References.

- (1) (a) Goldfogel, M. J.; Huang, L.; Weix, D. J.: Cross-Electrophile Coupling. In *Nickel Catalysis in Organic Synthesis*; Ogoshi, S., Ed.; Wiley-VCH: Weinheim, 2020; pp 183–222. (b) Wang, X.; Dai, Y.; Gong, H. Nickel-Catalyzed Reductive Couplings. *Top. Curr. Chem.* **2016**, *374*, 43. (c) Everson, D. A.; Weix, D. J. Cross-Electrophile Coupling: Principles of Reactivity and Selectivity. *J. Org. Chem.* **2014**, *79*, 4793–4798. (d) Knappke, C. E. I.; Grupe, S.; Gärtner, D.; Corpet, M.; Gosmini, C.; Jacobi von Wangelin, A. Reductive Cross-Coupling Reactions between Two Electrophiles. *Chem.–Eur. J.* **2014**, *20*, 6828–6842.
- (2) For example, benzylic chlorides, allylic chlorides, and α -chloroesters react rapidly under conditions that were effective with unactivated alkyl bromides. See the following examples: (a) Ackerman, L. K. G.; Anka-Lufford, L. L.; Naodovic, M.; Weix, D. J. Cobalt co-catalysis for cross-electrophile coupling: diarylmethanes from benzyl mesylates and aryl halides. *Chem. Sci.* **2015**, *6*, 1115–1119. (b) Durandetti, M.; Nédélec, J.-Y.; Périchon, J. Nickel-Catalyzed Direct Electrochemical Cross-Coupling between Aryl Halides and Activated Alkyl Halides. *J. Org. Chem.* **1996**, *61*, 1748–1755.
- (3) Erickson, L. W.; Lucas, E. L.; Tollefson, E. J.; Jarvo, E. R. Nickel-Catalyzed Cross-Electrophile Coupling of Alkyl Fluorides: Stereospecific Synthesis of Vinylcyclopropanes. *J. Am. Chem. Soc.* **2016**, *138*, 14006–14011.
- (4) A survey of the literature discussed in reference 1a had 18 examples of C_{sp^2} –Cl and 8 examples of C_{sp^3} –Cl bonds being tolerated as functional groups in reactions to form C_{sp^2} – C_{sp^3} bonds.
- (5) The coupling of aryl C–Cl bonds and alkyl C–Cl bonds with CO_2 and related π -electrophiles has been reported. See the following lead references: (a) Fujihara, T.; Nogi, K.; Xu, T.; Terao, J.; Tsuji, Y. Nickel-Catalyzed Carboxylation of Aryl and Vinyl Chlorides Employing Carbon Dioxide. *J. Am. Chem. Soc.* **2012**, *134*, 9106–9109; (b) Börjesson, M.; Moragas, T.; Martin, R. Ni-Catalyzed Carboxylation of Unactivated Alkyl Chlorides with CO_2 . *J. Am. Chem. Soc.* **2016**, *138*, 7504–7507.
- (6) See also a recent report on the coupling of Ar–Cl with C–H bonds via arylnickel(II) intermediates: Shields, B. J.; Doyle, A. G. Direct $C(sp^3)$ –H Cross Coupling Enabled by Catalytic Generation of Chlorine Radicals. *J. Am. Chem. Soc.* **2016**, *138*, 12719–12722.
- (7) About 1.8 million organic chlorides are commercially available compared to about 841,000 organic bromides. Organic iodides and organometal reagents each have <100,000 examples. Notably, aryl chlorides represent about $\frac{1}{2}$ of all commercially available aryl-X ($X \neq H$).
- (8) Aryl chlorides are relatively unreactive under conditions used for aryl bromides and usually require specialized conditions. See: (a) Grushin, V. V.; Alper, H. Transformations of Chloroarenes, Catalyzed by Transition-Metal Complexes. *Chem. Rev.* **1994**, *94*, 1047–1062. (b) Littke, A. F.; Fu, G. C. Palladium-Catalyzed Coupling Reactions of Aryl Chlorides. *Angew. Chem., Int. Ed.* **2002**, *41*, 4176–4211. (c) Hassan, J.; Sévignon, M.; Gozzi, C.; Schulz, E.; Lemaire, M. Aryl-Aryl Bond Formation One Century after the Discovery of the Ullmann Reaction. *Chem. Rev.* **2002**, *102*, 1359–1470.

(9) Alkyl chlorides often require different conditions than alkyl bromides for success. See: (a) Frisch, A. C.; Beller, M. Catalysts for Cross-Coupling Reactions with Non-activated Alkyl Halides. *Angew. Chem., Int. Ed.* **2005**, *44*, 674–688. (b) Zhou, J.; Fu, G. C. Palladium-Catalyzed Negishi Cross-Coupling Reactions of Unactivated Alkyl Iodides, Bromides, Chlorides, and Tosylates. *J. Am. Chem. Soc.* **2003**, *125*, 12527–12530.

(10) Substitution reactions of alkyl bromides vs alkyl chlorides have k_{rel} of about 20. For oxidative addition, k_{rel} can be as high as 10^3 . See: (a) Richard, J. P.; Jencks, W. P. Concerted bimolecular substitution reactions of 1-phenylethyl derivatives. *J. Am. Chem. Soc.* **1984**, *106*, 1383–1396. (b) Labinger, J. A. Tutorial on Oxidative Addition. *Organometallics* **2015**, *34*, 4784–4795. (c) Labinger, J. A.; Osborn, J. A.; Coville, N. J. Mechanistic studies of oxidative addition to low-valent metal complexes. Mechanisms for addition of alkyl halides to iridium(I). *Inorg. Chem.* **1980**, *19*, 3236–3243.

(11) Prinsell, M. R.; Everson, D. A.; Weix, D. J. Nickel-Catalyzed, Sodium Iodide-Promoted Reductive Dimerization of Alkyl Halides, Alkyl Pseudohalides, and Allylic Acetates. *Chem. Commun.* **2010**, *46*, 5743–5745.

(12) Martin has reported on the coupling of unactivated alkyl chlorides with CO_2 , see reference 5b. In collaboration with Pfizer and Asymchem, we had noted a selective coupling with an alkyl chloride for the first time, but it was not general, see reference 20b. Finally, couplings with activated alkyl chlorides are well known, see reference 2.

(13) Xu, C.; Guo, W.-H.; He, X.; Guo, Y.-L.; Zhang, X.-Y.; Zhang, X. Difluoromethylation of (hetero)aryl chlorides with chlorodifluoromethane catalyzed by nickel. *Nat. Commun.* **2018**, *9*, 1170. (b) Liu, J.; Zhang, J.; Li, X.; Wu, C.; Liu, H.; Liu, H.; Sun, F.; Li, Y.; Liu, Y.; Li, X. Nickel-Catalyzed 1,1-Difluoroethylation of (Hetero)aryl Halides with 1,1-Difluoroethyl Chloride ($\text{CH}_3\text{CF}_2\text{Cl}$). *Asian Journal of Organic Chemistry, Online Ahead of Print*. <https://doi.org/10.1002/ajoc.202000004> [Accessed 2/25/2020].

(14) (a) Czaplik, W. M.; Mayer, M.; Jacobi von Wangelin, A. Domino Iron Catalysis: Direct Aryl-Alkyl Cross-Coupling. *Angew. Chem., Int. Ed.* **2009**, *48*, 607–610. (b) Everson, D. A.; Jones, B. A.; Weix, D. J. Replacing Conventional Carbon Nucleophiles with Electrophiles: Nickel-Catalyzed Reductive Alkylation of Aryl Bromides and Chlorides. *J. Am. Chem. Soc.* **2012**, *134*, 6146–6159. (b) Yang, Y.; Luo, G.; Li, Y.; Tong, X.; He, M.; Zeng, H.; Jiang, Y.; Liu, Y.; Zheng, Y. Nickel-Catalyzed Reductive Coupling for Transforming Unactivated Aryl Electrophiles into β -Fluoroethylarenes. *Chem. – Asian J.* **2020**, *15*, 156–162.

(15) Ye, Y.; Chen, H.; Sessler, J. L.; Gong, H. Zn-Mediated Fragmentation of Tertiary Alkyl Oxalates Enabling Formation of Alkylated and Arylated Quaternary Carbon Centers. *J. Am. Chem. Soc.* **2019**, *141*, 820–824.

(16) In reference 14a Jacobi von Wangelin reported the coupling of chlorocyclohexane with 2-bromoanisole (63% yield) and bromobenzene (25% yield) using iron catalysis and Mg as the terminal reductant.

(17) Biswas, S.; Weix, D. J. Mechanism and Selectivity in Nickel-Catalyzed Cross-Electrophile Coupling of Aryl Halides with Alkyl Halides. *J. Am. Chem. Soc.* **2013**, *135*, 16192–16197.

(18) For related studies, see: (a) Breitenfeld, J.; Ruiz, J.; Wodrich, M. D.; Hu, X. Bimetallic Oxidative Addition Involving Radical Intermediates in Nickel-Catalyzed Alkyl-Alkyl Kumada Coupling Reactions. *J. Am. Chem. Soc.* **2013**, *135*, 12004–12012; (b) Schley, N. D.; Fu, G. C. Nickel-Catalyzed Negishi Arylations of Propargylic Bromides: A Mechanistic Investigation. *J. Am. Chem. Soc.* **2014**, *136*, 16588–16593; (c) Zhao, C.; Jia, X.; Wang, X.; Gong, H. Ni-Catalyzed Reductive Coupling of Alkyl Acids with Unactivated Tertiary Alkyl and Glycosyl Halides. *J. Am. Chem. Soc.* **2014**, *136*, 17645–17651.

(19) For alternative mechanistic hypotheses for related reactions, see: (a) Lin, Q.; Diao, T. Mechanism of Ni-Catalyzed Reductive 1,2-Dicarbofunctionalization of Alkenes. *J. Am. Chem. Soc.* **2019**, *141*, 17937–17948. (b) Gutierrez, O.; Tellis, J. C.; Primer, D. N.; Molander, G. A.; Kozlowski, M. C. Nickel-Catalyzed Cross-Coupling of Photoredox-Generated Radicals: Uncovering a General Manifold for Stereoconvergence in Nickel-Catalyzed Cross-Couplings. *J. Am. Chem. Soc.* **2015**, *137*, 4896–4899. (c) Mohadjer Beromi, M.; Brudvig, G. W.; Hazari, N.; Lant, H. M. C.; Mercado, B. Q. Synthesis and Reactivity of Paramagnetic Nickel Polypyridyl Complexes Relevant to C(sp²)–C(sp³) Coupling Reactions. *Angew. Chem., Int. Ed.* **2019**, *58*, 6094–6098.

(20) (a) Hansen, E. C.; Pedro, D. J.; Wotal, A. C.; Gower, N. J.; Nelson, J. D.; Caron, S.; Weix, D. J. New ligands for nickel catalysis from diverse pharmaceutical heterocycle libraries. *Nat. Chem.* **2016**, *8*, 1126–1130; (b) Hansen, E. C.; Li, C.; Yang, S.; Pedro, D.; Weix, D. J. Coupling of Challenging Heteroaryl Halides with Alkyl Halides via Nickel-Catalyzed Cross-Electrophile Coupling. *J. Org. Chem.* **2017**, *82*, 7085–7092.

(21) PyBCam (Order No. 902047) and PyBCam^{CN} (Order No. 902063) are commercially available from Sigma-Aldrich.

(22) Johnson, K. A.; Biswas, S.; Weix, D. J. Cross-Electrophile Coupling of Vinyl Halides with Alkyl Halides. *Chem.–Eur. J.* **2016**, *22*, 7399–7402.

(23) Goldup, S. M.; Leigh, D. A.; McBurney, R. T.; McGonigal, P. R.; Plant, A. Ligand-assisted nickel-catalysed sp³–sp³ homocoupling of unactivated alkyl bromides and its application to the active template synthesis of rotaxanes. *Chem. Sci.* **2010**, 383–386.

(24) (a) Anderson, T. J.; Jones, G. D.; Vicić, D. A. Evidence for a NiI Active Species in the Catalytic Cross-Coupling of Alkyl Electrophiles. *J. Am. Chem. Soc.* **2004**, *126*, 8100–8101. (b) Jones, G. D.; Martin, J.; McFarland, C.; Allen, O.; Hall, R.; Haley, A.; Brandon, R.; Konovalova, T.; Desrochers, P.; Pulay, P.; Vicić, D. Ligand Redox Effects in the Synthesis, Electronic Structure, and Reactivity of an Alkyl–Alkyl Cross-Coupling Catalyst. *J. Am. Chem. Soc.* **2006**, *128*, 13175–13183.

(25) While Csp³–Csp² bond-forming Negishi reactions with aryl iodides and bromides have been shown to tolerate O–H and N–H bonds in many cases, fewer examples exist for couplings with C–Cl bonds. (a) Leroux, M.; Vorherr, T.; Lewis, I.; Schaefer, M.; Koch, G.; Karaghiosoff, K.; Knochel, P. Late-Stage Functionalization of Peptides and Cyclopeptides Using Organozinc Reagents. *Angew. Chem. Int. Ed.* **2014**, *53*, 1000–1004.

Chem., Int. Ed. **2019**, *58*, 8231–8234. (b) Pompeo, M.; Froese, R. D. J.; Hadei, N.; Organ, M. G. Pd-PEPPSI-IPentCl: A Highly Effective Catalyst for the Selective Cross-Coupling of Secondary Organozinc Reagents. *Angew. Chem., Int. Ed.* **2012**, *51*, 11354–11357.

(26) Bordwell, F. G.; Hughes, D. L. Thiol acidities and thiolate ion reactivities toward butyl chloride in dimethyl sulfoxide solution. The question of curvature in Brønsted plots. *J. Org. Chem.* **1982**, *47*, 3224–3232.

(27) Nickel is known to catalyze C–S bond formation of aryl thiols with aryl chlorides. Arylzinc reagents and zinc powder have been used as promoters. See: (a) Jones, K. D.; Power, D. J.; Bierer, D.; Gericke, K. M.; Stewart, S. G. Nickel Phosphite/Phosphine-Catalyzed C–S Cross-Coupling of Aryl Chlorides and Thiols. *Org. Lett.* **2018**, *20*, 208–211. (b) Gehrtz, P. H.; Geiger, V.; Schmidt, T.; Sršan, L.; Fleischer, I. Cross-Coupling of Chloro(hetero)arenes with Thiolates Employing a Ni(0)-Precatalyst. *Org. Lett.* **2019**, *21*, 50–55. (c) Gogoi, P.; Hazarika, S.; Sarma, M. J.; Sarma, K.; Barman, P. Nickel–Schiff base complex catalyzed C–S cross-coupling of thiols with organic chlorides. *Tetrahedron* **2014**, *70*, 7484–7489.

(28) Generally, these compounds are made by hydrosilylation of olefins (with HSiCl_3 or $\text{HSi}(\text{OMe})_3$) or Grignard reactions (with tetrachlorosilane). Hydrosilylation to form trimethoxysilanes requires $(\text{MeO})_3\text{SiH}$, which can form pyrophoric SiH_4 . A workaround is to use HSiCl_3 , but this is also prone to rapid decomposition. (a) Buslov, I.; Song, F.; Hu, X. An Easily Accessed Nickel Nanoparticle Catalyst for Alkene Hydrosilylation with Tertiary Silanes. *Angew. Chem., Int. Ed.* **2016**, *55*, 12295–12299. (b) Katoh, K.; Ito, S.; Wada, Y.; Higashi, E.; Suzuki, Y.; Kubota, K.; Nakano, K.; Wada, Y. Investigation of thermal hazard during the hydrosilylation of 1,6-divinyl(perfluorohexane) with trichlorosilane. *J. Chem. Thermodyn.* **2011**, *43*, 1229–1234.

(29) The Kumada coupling of trimethoxysilanes is reported to be impractical, but triethoxysilanes can be cross-coupled. See: Brondani, D. J.; Corriu, R. J. P.; El Ayoubi, S.; Moreau, J. J. E.; Wong Chi Man, M. Polyfunctional carbosilanes and organosilicon compounds. Synthesis via grignard reactions. *Tetrahedron Lett.* **1993**, *34*, 2111–2114.

(30) (a) Sagiv, J. Organized monolayers by adsorption. 1. Formation and structure of oleophobic mixed monolayers on solid surfaces. *J. Am. Chem. Soc.* **1980**, *102*, 92–98. (b) Wasserman, S. R.; Tao, Y. T.; Whitesides, G. M. Structure and reactivity of alkylsiloxane monolayers formed by reaction of alkyltrichlorosilanes on silicon substrates. *Langmuir* **1989**, *5*, 1074–1087. (c) Ulman, A. Formation and Structure of Self-Assembled Monolayers. *Chem. Rev.* **1996**, *96*, 1533–1554. (d) Haensch, C.; Hoeppener, S.; Schubert, U. S. Chemical modification of self-assembled silane based monolayers by surface reactions. *Chem. Soc. Rev.* **2010**, *39*, 2323–2334.

(31) See Supporting Information for a detailed procedure. For additional details on the scale-up, see: Everson, D. A.; George, D. T.; Weix, D. J.; Buergler, J. F.; Wood, J. L. Nickel-Catalyzed Cross-Coupling of Aryl Halides with Alkyl Halides: Ethyl 4-(4-(4-methylphenylsulfonamido)-phenyl)butanoate. *Org. Synth.* **2013**, *90*, 200–214.

(32) Huang, L.; Ackerman, L. K. G.; Kang, K.; Parsons, A. M.; Weix, D. J. LiCl-Accelerated Multimetallic Cross-Coupling of Aryl Chlorides with Aryl Triflates. *J. Am. Chem. Soc.* **2019**, *141*, 10978–10983.

(33) (a) Krasovskiy, A.; Malakhov, V.; Gavryushin, A.; Knochel, P. Efficient Synthesis of Functionalized Organozinc Compounds by the Direct Insertion of Zinc into Organic Iodides and Bromides. *Angew. Chem., Int. Ed.* **2006**, *45*, 6040–6044. (b) Koszinowski, K.; Böhrer, P. Formation of Organozincate Anions in LiCl-Mediated Zinc Insertion Reactions. *Organometallics* **2009**, *28*, 771–779. (c) Feng, C.; Cunningham, D. W.; Easter, Q. T.; Blum, S. A. Role of LiCl in Generating Soluble Organozinc Reagents. *J. Am. Chem. Soc.* **2016**, *138*, 11156–11159. (d) Jess, K.; Kitagawa, K.; Tagawa, T. K. S.; Blum, S. A. Microscopy Reveals: Impact of Lithium Salts on Elementary Steps Predicts Organozinc Reagent Synthesis and Structure. *J. Am. Chem. Soc.* **2019**, *141*, 9879–9884.

(34) (a) Anderson, T. J.; Vicić, D. A. Direct Observation of Noninnocent Reactivity of ZnBr₂ with Alkyl Halide Complexes of Nickel. *Organometallics* **2004**, *23*, 623–625. (b) Koszinowski, K.; Böhrer, P. Formation of Organozincate Anions in LiCl-Mediated Zinc Insertion Reactions. *Organometallics* **2009**, *28*, 771–779. (c) Achonduh, G. T.; Hadei, N.; Valente, C.; Avola, S.; O'Brien, C. J.; Organ, M. G. On the role of additives in alkyl-alkyl Negishi cross-couplings. *Chem. Commun.* **2010**, *46*, 4109–4111. (d) Hunter, H. N.; Hadei, N.; Blagojević, V.; Patschinski, P.; Achonduh, G. T.; Avola, S.; Bohme, D. K.; Organ, M. G. Identification of a Higher-Order Organozincate Intermediate Involved in Negishi Cross-Coupling Reactions by Mass Spectrometry and NMR Spectroscopy. *Chem.–Eur. J.* **2011**, *17*, 7845–7851. (e) McCann, L. C.; Hunter, H. N.; Clyburne, J. A. C.; Organ, M. G. Higher-Order Zincates as Transmetalators in Alkyl–Alkyl Negishi Cross-Coupling. *Angew. Chem., Int. Ed.* **2012**, *51*, 7024–7027.

(35) (a) Yoon, K. B.; Kochi, J. K. Catalytic bromide and iodide exchange of alkyl chlorides with hydrogen bromide and hydrogen iodide. *J. Org. Chem.* **1989**, *54*, 3028–3036. (b) Willy, W. E.; McKean, D. R.; Garcia, B. A. Conversion of Alkyl Chlorides to Bromides, Selective Reactions of Mixed Bromochloroalkanes, and Halogen Exchange. *Bull. Chem. Soc. Jpn.* **1976**, *49*, 1989–1995. (c) Wang, J.; Tong, X.; Xie, X.; Zhang, Z. Rhodium-Catalyzed Activation of C(sp³)–X (X = Cl, Br) Bond: An Intermolecular Halogen Exchange Case. *Org. Lett.* **2010**, *12*, 5370–5373. (d) Mizukami, Y.; Song, Z.; Takahashi, T. Halogen Exchange Reaction of Aliphatic Fluorine Compounds with Organic Halides as Halogen Source. *Org. Lett.* **2015**, *17*, 5942–5945. (e) Petrone, D. A.; Ye, J.; Lautens, M. Modern Transition-Metal-Catalyzed Carbon–Halogen Bond Formation. *Chem. Rev.* **2016**, *116*, 8003–8104.

(36) (a) Molander, G. A.; Traister, K. M.; O'Neill, B. T. Engaging Nonaromatic, Heterocyclic Tosylates in Reductive Cross-Coupling with Aryl and Heteroaryl Bromides. *J. Org. Chem.* **2015**, *80*, 2907–2911. (b) Do, H.-Q.; Chandrashekhar, E. R. R.; Fu, G. C. Nickel/Bis(oxazoline)-Catalyzed Asymmetric Negishi Arylations of Racemic Secondary Benzylic Electrophiles to Generate Enantioenriched 1,1-Diarylalkanes. *J. Am. Chem. Soc.* **2013**, *135*, 16288–16291.

(37) Zhao, Y.; Weix, D. J. Nickel-Catalyzed Regiodivergent Opening of Epoxides with Aryl Halides: Co-Catalysis Controls Regioselectivity. *J. Am. Chem. Soc.* **2014**, *136*, 48–51.

(38) While several reports on the conversion of alkyl chlorides to bromides are known (reference 35), we could not find explicit examples of this strategy for transition-metal catalysis. Given the frequent use of metal bromide salts as catalyst precursors, we suspect this phenomenon is common.

(39) Hughes, J. M. E.; Fier, P. S. Desulfonylative Arylation of Redox-Active Alkyl Sulfones with Aryl Bromides. *Org. Lett.* **2019**, *21*, 5650–5654.

(40) Ward, L. G. L.; Pipal, J. R. *Inorg. Synth.* **1972**, *13*, 154–164.

(41) Slee, D. H.; Chen, Y.; Zhang, X.; Moorjani, M.; Lanier, M. C.; Lin, E.; Rueter, J. K.; Williams, J. P.; Lechner, S. M.; Markison, S.; et al. 2-Amino-N-Pyrimidin-4-Ylacetamides as A2A Receptor Antagonists: 1. Structure-Activity Relationships and Optimization of Heterocyclic Substituents. *J. Med. Chem.* **2008**, *51*, 1719–1729.

(42) Bejan, E.; Ait-Haddou, H.; Daran, J.-C.; Balavoine, G. G. A. Enaminones in the Synthesis of New Polyaza Heterocycles. *Eur. J. Org. Chem.* **1998**, *12*, 2907–2912.

(43) Mauro, M.; Aliprandi, A.; Cebrián, C.; Wang, D.; Kübel, C.; De Cola, L. Self-Assembly of a Neutral Platinum(II) Complex into Highly Emitting Microcrystalline Fibers through Metallophilic Interactions. *Chem. Commun.* **2014**, *50*, 7269–7272.

(44) Hansen, E. C.; Li, C.; Yang, S.; Pedro, D.; Weix, D. J. Coupling of Challenging Heteroaryl Halides with Alkyl Halides via Nickel-Catalyzed Cross-Electrophile Coupling. *J. Org. Chem.* **2017**, *82*, 7085–7092.

(45) Albers, A. E.; Rawls, K. A.; Chang, C. J. Activity-Based Fluorescent Reporters for Monoamine Oxidases in Living Cells. *Chem. Commun.* **2007**, 4647–4649.

(46) Wu, S.; Lee, S.; Beak, P. Asymmetric Deprotonation by BuLi/(-)-Sparteine: Convenient and Highly Enantioselective Syntheses of (S)-2-Aryl-Boc-Pyrrolidines. *J. Am. Chem. Soc.* **1996**, *118*, 715–721.

(47) Wrackmeyer, B. Carbon-13 NMR Spectroscopy of Boron Compounds. *Prog. Nucl. Magn. Reson. Spectrosc.* **1979**, *12*, 227–259.

(48) Everson, D. A.; Shrestha, R.; Weix, D. J. Nickel-Catalyzed Reductive Cross-Coupling of Aryl Halides with Alkyl Halides. *J. Am. Chem. Soc.* **2010**, *132*, 920–921.

(49) Everson, D. A.; Jones, B. A.; Weix, D. J. Replacing Conventional Carbon Nucleophiles with Electrophiles: Nickel-Catalyzed Reductive Alkylation of Aryl Bromides and Chlorides. *J. Am. Chem. Soc.* **2012**, *134*, 6146–6159.

(50) Nani, R. R.; Reisman, S. E. α -Diazo- β -Ketonitriles: Uniquely Reactive Substrates for Arene and Alkene Cyclopropanation. *J. Am. Chem. Soc.* **2013**, *135*, 7304–7311.

(51) Sheng, J.; Ni, H. Q.; Zhang, H. R.; Zhang, K. F.; Wang, Y. N.; Wang, X. S. Nickel-Catalyzed Reductive Cross-Coupling of Aryl Halides with Monofluoroalkyl Halides for Late-Stage Monofluoroalkylation. *Angew. Chem. Int. Ed.* **2018**, *57*, 7634–7639.

(52) Kurono, N.; Sugita, K.; Takasugi, S.; Tokuda, M. One-Step Cross-Coupling Reaction of Functionalized Alkyl Iodides with Aryl Halides by the Use of an Electrochemical Method. *Tetrahedron* **1999**, *55*, 6097–6108.

(53) Boebel, T. A.; Hartwig, J. F. Silyl-Directed, Iridium-Catalyzed Ortho-Borylation of Arenes. A One-Pot Ortho-Borylation of Phenols, Arylamines, and Alkylarenes. *J. Am. Chem. Soc.* **2008**, *130*, 7534–7535.

(54) Tomoji, A.; Kentarou, K.; Nagatoshi, W.; Kouki, I. 1,8-Naphthyridin-2(1H)-One Derivatives. U.S. Patent 6,642,250 B2, November 4, 2003.

(55) Hofmayer, M. S.; Hammann, J. M.; Cahiez, G.; Knochel, P. Iron-Catalyzed C(Sp₂)-C(Sp₃) Cross-Coupling Reactions of Di(Hetero)Arylmanganese Reagents and Primary and Secondary Alkyl Halides. *Synlett* **2018**, *29*, 65–70.

(56) Fleury-Brégeot, N.; Presset, M.; Beaumard, F.; Colombel, V.; Oehlrich, D.; Rombouts, F.; Molander, G. A. Suzuki-Miyaura Cross-Coupling of Potassium Alkoxyethyltrifluoroborates: Access to Aryl/Heteroarylethoxy Motifs. *J. Org. Chem.* **2012**, *77*, 10399–10408.

(57) Hamilton, D. S.; Nicewicz, D. A. Direct Catalytic Anti-Markovnikov Hydroetherification of Alkenols. *J. Am. Chem. Soc.* **2012**, *134*, 18577–18580.

(58) Molander, G. A.; Argintaru, O. A.; Aron, I.; Dreher, S. D. Nickel-Catalyzed Cross-Coupling of Potassium Aryl- and Heteroaryltrifluoroborates with Unactivated Alkyl Halides. *Org. Lett.* **2010**, *12*, 5783–5785.

(59) Lingamurthy, M.; Nalliboina, G. R.; Rao, M. V.; Rao, B. V.; Reddy, B. S.; Sampath Kumar, H. M. DDQ Mediated Stereoselective Intermolecular Benzylic CN Bond Formation: Synthesis of (–)-Cytoxazole, (–)-4-Epi-Cytoxazole and Their Analogues and Immunological Evaluation of Their Cytokine Modulating Activity. *Tetrahedron* **2017**, *73*, 1473–1481.

(60) Pandey, G.; Laha, R.; Mondal, P. K. Heterocyclization Involving Benzylic C(sp³)-H Functionalization Enabled by Visible Light Photoredox Catalysis. *Chem. Commun.* **2019**, *55*, 9689–9692.

(61) Jouffroy, M.; Primer, D. N.; Molander, G. A. Base-Free Photoredox/Nickel Dual-Catalytic Cross-Coupling of Ammonium Alkylsilicates. *J. Am. Chem. Soc.* **2016**, *138*, 475–478.

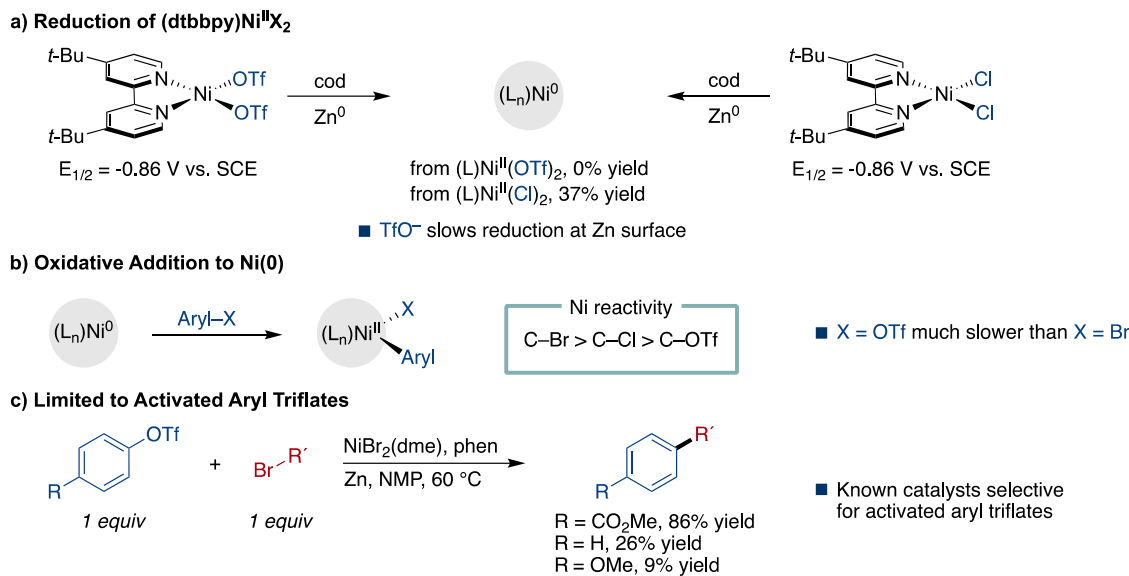
(62) Primer, D. N.; Karakaya, I.; Tellis, J. C.; Molander, G. A. Single-Electron Transmetalation: An Enabling Technology for Secondary Alkylboron Cross-Coupling. *J. Am. Chem. Soc.* **2015**, *137*, 2195–2198.

Chapter 3: Nickel-Catalyzed Cross-Electrophile Coupling of Aryl Triflates with Alkyl Halides

3.1. Introduction.

In the past decade, $C(sp^2)$ – $C(sp^3)$ cross-electrophile coupling (XEC) has emerged as a powerful tool for exploring chemical space with abundant, readily available starting materials from a variety of substrate pools.^{1,2,3} The scope of this approach has improved dramatically with better understanding of reaction mechanisms allowing for the development of new catalytic systems that can promote couplings with previously inaccessible classes of substrates such as aryl chlorides,⁴ aliphatic alcohols,^{5,6,7} and carboxylic acid derivatives.^{8,9,10} However, one useful, distinct class of substrates that has remained notably absent from XEC reaction development is phenol-derived aryl sulfonate esters. Despite the wealth of literature showing aryl C–O electrophiles are competent reactants in nickel-catalyzed cross-coupling reactions,^{11,12,13} there are only a few reports employing them in $C(sp^2)$ – $C(sp^3)$ XEC reactions,^{14,15} perhaps due to challenges associated with aryl triflates under reductive conditions. This underrepresentation arises from three main issues (Figure 3.1): 1) triflate anions have been shown to inhibit the rate of reduction of Ni(II) species at the surface of zinc;¹⁶ 2) oxidative addition of aryl triflates is more challenging than the analogous aryl bromide¹⁷ and chloride,⁴ and 3) while electron-poor aryl triflates work in some cases, electron-neutral and electron-rich aryl triflates provide very low yields. We show here how the challenges associated with aryl triflates can be overcome by individually addressing three issues: substrate activation selectivity, inhibition of catalyst turnover by triflate anions, and competing side reactions.

Figure 3.1. Challenges for Using Aryl Triflates in Cross-Electrophile Coupling Reactions.



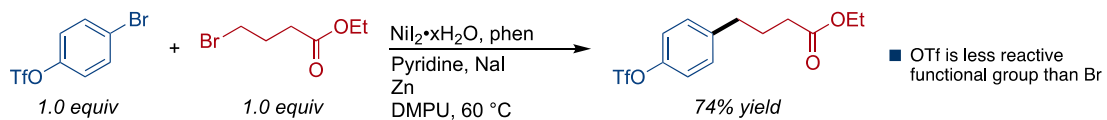
Aryl triflates have posed a long-standing challenge for nickel XEC.¹⁸ In redox neutral C–C couplings, conditions have been developed that can not only engage aryl triflates in productive cross-couplings, but also considerably less reactive aryl methyl ethers. However, our work in cross-Ullman chemistry has shown that nickel bipyridine (and related catalysts) are unreactive towards aryl triflates,¹⁷ and select reductive XEC methodologies have demonstrated preferential oxidative addition into aryl halides in the presence of aryl triflates.¹⁸ This challenge is, in part, due to inhibition of reduction of nickel by triflate anions (Figure 3.1a). Despite having similar reduction potentials, the reduction of $(dtbbpy)NiCl_2$ occurs more readily than the reduction of $(dtbbpy)Ni(OTf)_2$ at the surface of zinc.¹⁶ This inhibitory effect can be overturned with the addition of sufficient quantities of alkali chloride salts, increasing the yield of Ni^0 from 0% to 44%. $ZnCl_2$, which is inevitably generated under the reaction conditions, did not counteract this inhibitory effect, suggesting cation identity can significantly influence reduction kinetics. Additionally, some reports have shown that the addition of lithium bromide can promote oxidative addition of aryl triflates by nickel catalysts. Consequently,

lithium halide salts present in sufficient quantities should both aid in the consumption of aryl triflates and effective turnover of the nickel catalyst.

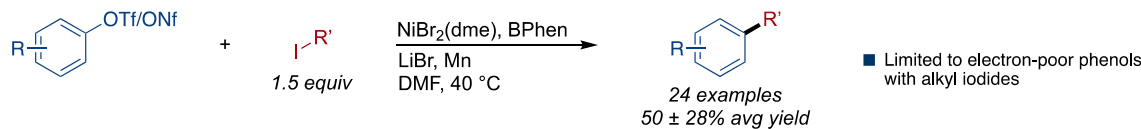
Despite these insights, the challenge of achieving a general, selective XEC reaction with aryl triflates has been elusive for a decade. In 2017 Hosoya and coworkers reported the cross-coupling of electron-deficient/electron-neutral aryl triflates and nonaflates with alkyl iodides (24 examples $50 \pm 28\%$, Figure 3.2b).¹⁴ Electron-rich aryl triflates afforded no cross-coupled product and employing alkyl bromides instead of alkyl iodides under these conditions led to a 68% decrease in yield, presumably due to slower formation of the requisite alkyl radical (and suggesting that there is a reactivity difference between electron-rich and electron-poor aryl triflate). In 2019 Shu reported the alkylation of tyrosine on peptide through conversion of the side-chain phenol to the corresponding aryl triflate followed by subsequent cross-coupling with primary alkyl bromides generated *in situ* via treatment of alkyl tosylates with alkali bromide salts.¹⁵ Though reaction yields were typically high (21 examples, $69 \pm 14\%$, Figure 3.2c), the effects of deviations on the steric and electronic profile of the aryl triflate were not studied. To date, no report has demonstrated a general XEC reaction for both electron-rich and electron-deficient aryl triflates (Figure 3.2). The methods presented by both Hosoya and Shu employ a nickel bathophenanthroline catalyst, suggesting that evaluating other catalysts could be key to addressing the limitations in applying aryl triflates in nickel XEC. In 2020, our group published a method for the cross-electrophile coupling of aryl chlorides with alkyl chlorides, two functional groups that are commonly unreactive under conventional XEC conditions, that was enabled by the use of PyBCam^{CN} as the ancillary ligand.⁴ Accordingly, we hypothesized that this ligand could be used to promote the oxidative addition of electron-rich aryl triflates, which should have analogous reactivity to aryl chlorides.

Figure 3.2. Aryl C–O Electrophiles in Cross-Coupling Reactions.

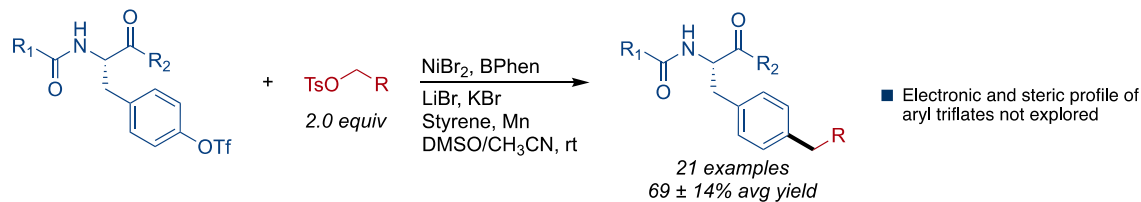
a) Cross-Electrophile Coupling of Aryl Bromides with Alkyl Bromides (Weix 2012)



b) Cross-electrophile Coupling of Aryl Triflates and Nonaflates with Alkyl Iodides (Hosoya 2017)

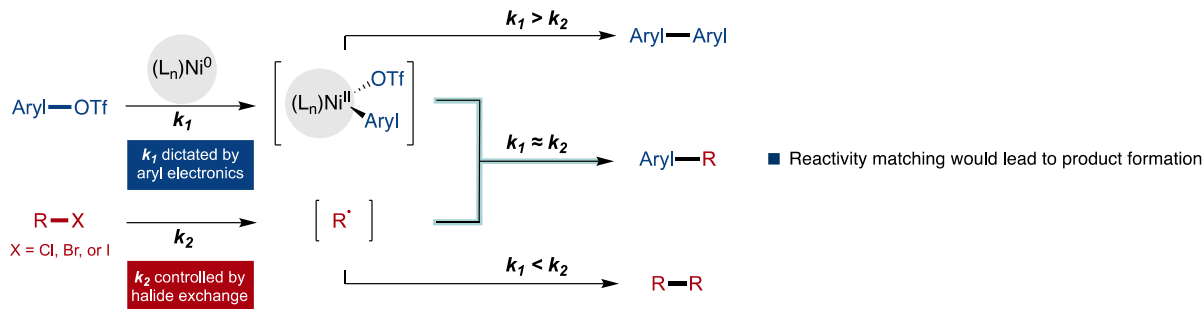


c) Cross-electrophile Coupling of Aryl Triflates with Alkyl Sulfonates (Shu 2019)



Another critical parameter to ensure a selective XEC reaction is controlling alkyl radical generation. The rate of radical generation must be closely matched with the rate of oxidative addition, otherwise formation of undesired homodimer species will dominate. In situ conversion of unreactive alkyl electrophiles into reactive species has been used in a variety of $\text{C}(\text{sp}^2)\text{--C}(\text{sp}^3)$ XEC methodologies. Most notably, alkali iodide salts are used to generate alkyl iodides from alkyl sulfonate esters,⁷ alkyl bromides,¹⁸ and alkyl chlorides⁴ effectively “turning on” reactivity with diverse electrophiles and enabling cross-selective reactions. We envision halide exchange can be a useful tool to not only upregulate alkyl electrophile reactivity, but to fine-tune and even downregulate alkyl reactivity by modulating both the identity and stoichiometry of the employed halide additive (Figure 3.3).

Figure 3.3. A Strategy for Selective Cross-Coupling Between Two Electrophiles.



3.2. Reaction Optimization.

3.2.1. Aryl Triflates and Alkyl Bromides

Early into our studies, we observed significant ligand effects depending on the electronics of the aryl triflate. Initial evaluation of the reaction with electron-poor 4-carbomethoxyphenyl triflate (**3.1**) and 1-bromoocetane (**3.2**) afforded methyl 4-octylbenzoate (**3.3**) in 90% yield using phenanthroline (phen) as the ligand (Table 3.1, entry 1). Reactions employing other bidentate amine ligands, such as bathophenanthroline (**L2**) and bipyridines (**L3–L5**), provided **3.3** in 8–74% yields (Table 3.1, entries 2–5). Changing from NMP as solvent reduced yields, as did decreasing the reaction temperature from 60 °C. The primary side reactions observed were reductive dimerization of 1-bromoocetane, reduction of the aryl triflate to generate methyl benzoate, and homocoupling of the arene.

Table 3.1. Ligand Effects on the Cross-Electrophile Coupling of Aryl Triflates with Alkyl Bromides.^a

phen (L1), R = H
BPhen (L2), R = Ph

bpy (L3), R = H
dtbbpy (L4), R = iBu
dmbypy (L5), R = OMe

terpy (L6)

BpyCam (L7)

PyBCam·2HCl (L8)

PyBCam^{CN} (L9)

Entry	Ar-OTf	Alk-Br	Ligand	Additive	Product ^b (%)	Prod/Dimer
1	3.1	3.2	phen	—	90	9.4
2	3.1	3.2	BPhen	—	74	4.6
3	3.1	3.2	Bpy	—	57	1.6
4	3.1	3.2	dtbbpy	—	15	0.3
5	3.1	3.2	dmbypy	—	8	0.2
6	3.5	3.6	phen	—	18	0.4
7	3.5	3.6	phen	LiCl	25	2.1
8	3.5	3.6	Terpy	LiCl	9	0.3
9	3.5	3.6	BpyCam	LiCl	7	0.2
10	3.5	3.6	PyBCam	LiCl	41	1.8
11	3.5	3.6	PyBCam ^{CN}	LiCl	52	2.5

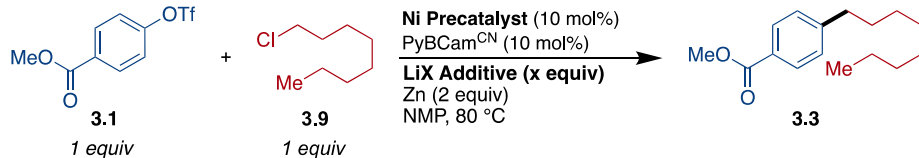
^aReactions run on a 0.2 mmol scale in 250 μ L of NMP. ^bYields were determined by GC analysis calibrated against dodecane as an internal standard.

Under the same reaction conditions that provided high yield of **3.3**, cross-electrophile coupling of electron-rich 4-methoxyphenyl triflate (**3.5**) with ethyl 4-bromobutyrate (**3.6**) afforded the cross-coupled product **3.7** in 18% yield due to competitive alkyl dimerization (Table 3.1, entry 6). The addition of LiCl reduced alkyl dimer formation and improved yields of **3.3** to 25%. Different lithium salt additives decreased selectivity and yield. The use of tridentate amine ligand pyridine 2-carboxamidine (PyBCam) further improved the cross-selectivity towards the product, while terpyridine and bipyridine 6-carboxamidine (BpyCam) ligands gave low yield. An improvement to 52% yield was achieved by using PyBCam^{CN} (**L9**) as a ligand (Table 3.1, entry 11).

3.2.2. Aryl Triflates and Alkyl Chlorides.

The ability to couple both alkyl bromides and chlorides would be versatile in multistep synthesis, but alkyl chlorides are much less reactive. Cross-coupling between 4-methoxyphenyl triflate **3.5** with ethyl 4-chlorobutyrate afforded product in 55% yield using PyBCam^{CN} and LiCl. However, under the same conditions, coupling between an electron-deficient 4-carbomethoxyphenyl triflate **3.1** with 1-chlorooctane **3.9** resulted in 5% yield of cross-coupled product and unconsumed alkyl chloride. Under the hypothesis that halide exchange may help achieve cross-selectivity, various halide sources were introduced through the nickel precatalysts and exogenous salt additives (Table 3.2). Elevating temperature to 80 °C and introducing a catalytic amount of iodide increased the product yield but did not lead to full consumption of the alkyl chloride. PyBCam^{CN} was again the optimal ligand as it allowed activation of aryl triflate and resulted in minimal aryl dimerization.

Table 3.2. Introducing Halide Sources Through Nickel Catalyst and Salt Additives.



Entry	Ni Precatalysts	LiX Additives	Total Amount of I ⁻	3.3 (%)
1	NiBr ₂ (dme) ^a	LiCl (1 equiv)	10 mol% ^b	5
2	NiI ₂ •4H ₂ O	LiCl (1 equiv)	20 mol%	44
3	NiCl ₂ (dme)	LiCl (1 equiv), LiI (20 mol%)	20 mol%	41
4	NiCl ₂ (dme)	LiCl (1 equiv), LiI (1 equiv)	100 mol%	88
5	NiCl ₂ (dme)	LiI (1 equiv)	100 mol%	60
6	NiCl ₂ (dme)	LiI (2 equiv)	200 mol%	>99

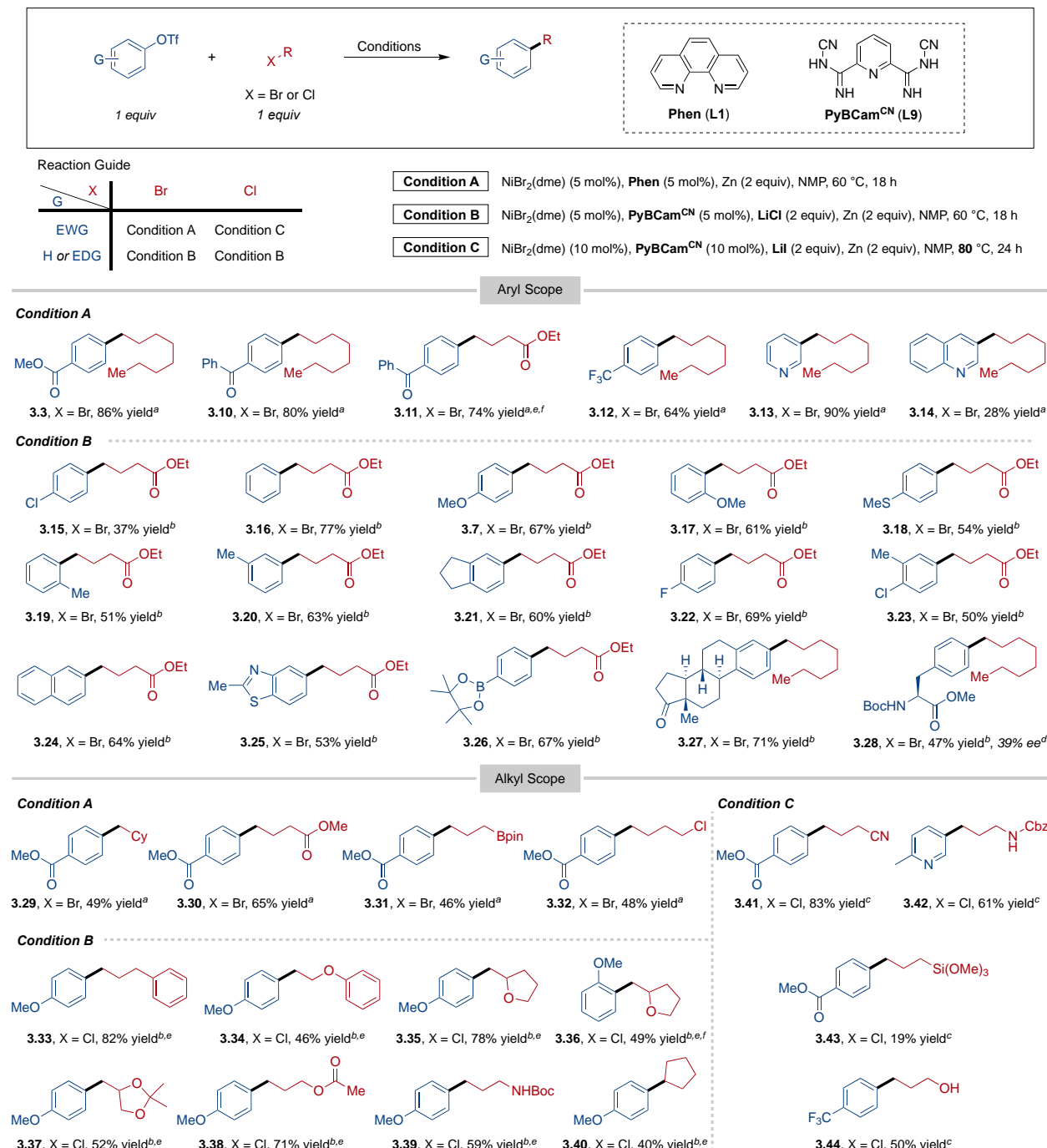
^a5 mol% of catalyst loading was used. ^bTotal amount of bromide is noted. Yields reported are calibrated against 1,3,5-trimethoxybenzene as an internal standard.

3.3. Reaction Scope.

Electron-deficient aryl triflates such as those bearing ketone and trifluoromethyl substituents coupled in high yields (**3.2**, **3.10–3.12**). While electron-deficient heteroaryl triflate pyridine coupled in high yield (**3.13**), quinoline coupled in low yield (**3.14**). When 4-chlorophenyl triflate was employed as a substrate lower yield was observed, presumably due to selectivity problems associated with oxidative addition to the chloride rather than the triflate. Electron-rich aryl triflates (**3.7** and **3.18**) coupled well and steric encumberment ortho- to the triflate are well tolerated (**3.17** and **3.19**).

Electron-rich aryl triflates bearing thioether and aliphatic substituents were coupled in good yields (**3.7**, **3.17**, and **3.18**). The reaction tolerates halogenated arenes with fluorine or chlorine substituted compounds **3.22** and **3.23** being formed in 69% and 50% yields, respectively. The improved yield of **3.20** compared to **3.19** is attributed to the additional steric bias for triflate coupling provided by the methyl group. Reactions with aryl triflates bearing more reactive halogen substituents, such as bromine, iodine, or activated chlorines (i.e.: 2-chloropyridine) were unsuccessful, presumably due to competitive oxidative addition. Naphthalene (**3.24**) and benzothiazole (**3.25**) derived aryl triflates coupled in 64% and 53% yields. Orthogonality to conventional cross-coupling was demonstrated by the synthesis of the pinacol boronic ester **3.26** in 67% yield. We also explored the application of this coupling to more complex substrates and observed couplings with estrone (**3.27**) and tyrosine (**3.28**) derivatives in 71% and 47% yields, although the stereocenter in **3.28** was partially racemized from >95% to 39% ee.

Figure 3.4. Scope of the Cross-Electrophile Coupling of Aryl Triflates with Alkyl Halides Under Modular Conditions.



^aReaction run using Condition A. ^bReaction run using Condition B. ^cReaction run using Condition C.

^dEnantiomeric excess determined by SFC equipped with a chiral column. ^eThe reaction was stirred for 48 h. ^fReaction was run at 4 mmol scale.

Alkyl bromides with β -branching were effective coupling partners and that both esters and boranes were tolerated; alkyl branched product **3.29** was formed in 49% yield and functionalized products **3.30** and **3.31** were generated in 67% and 46% yields, respectively. The selectivity of the reaction for alkyl bromides was excellent, as 1-bromo-4-chlorobutane coupled exclusively with the alkyl bromide to provide **3.32** in 48% yield (rest were returned aryl triflate). The decrease in yield observed with variation to the alkyl bromide are due to increased alkyl dimerization and protodetriflation.

Couplings with alkyl chlorides tolerate aryl and alkyl ethers, including substrates with a β -leaving group susceptible to elimination, as shown by the formation of compounds **3.34** and **3.35** in 46% and 78% yields. A variety of functional groups can be included, such as acetonides (**3.37**), acylated alcohols (**3.38**), and carbamate protected amines (**3.39**), formed in 52%, 71%, and 59% yields, respectively. Secondary alkyl chlorides are challenging, but compound **3.40** formed in 40% yield. Both reaction conditions were tested on gram-scale on the benchtop to show the synthetic utility of this transformation.

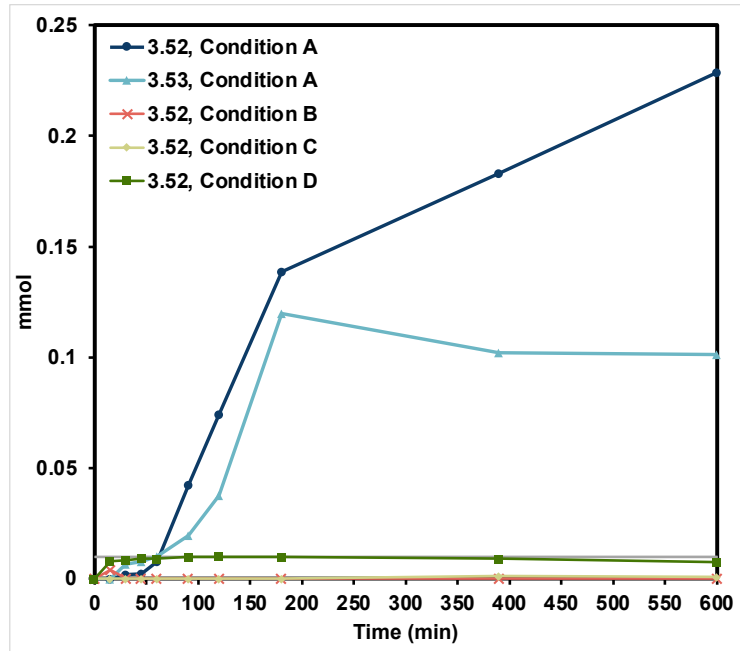
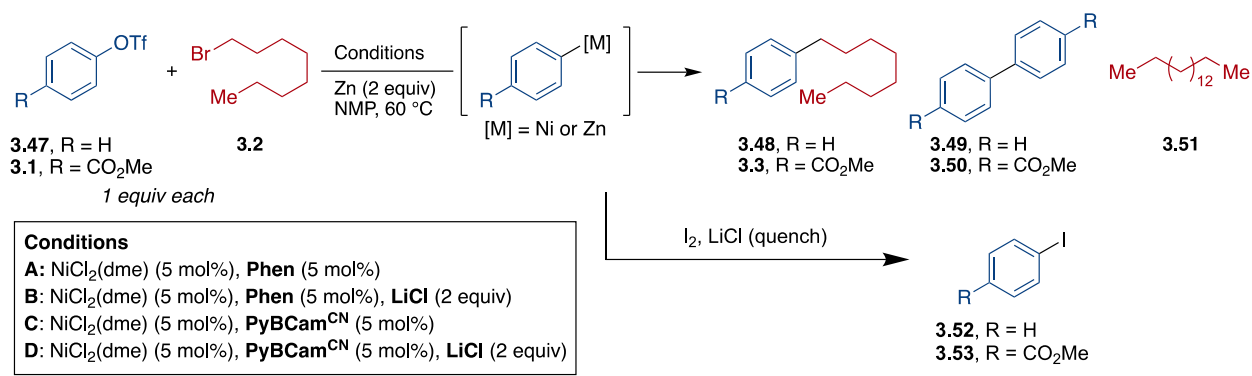
3.4. Mechanistic Studies.

The need to employ different ligands depending on the arene electronics and changes in byproduct profiles suggested that there may be subtle mechanistic differences between these couplings. General substrate trends showed reactions with PyBCam^{CN} were more selective for product formation over aryl dimerization but required longer reaction times. Additionally, reactions with PyBCam^{CN} worked well to couple both alkyl bromides and chlorides, whereas phen was only successful in coupling of activated aryl triflates with alkyl bromides. A series of mechanistic studies were run to gain a better understanding of the origins of these reactivity differences.

3.4.1. Comparisons of Reactions with Phen and PyBCam^{CN}.

The cross-coupling reaction between phenyl triflate (**3.47**) with 1-bromoocetane (**3.2**) was followed over time and compared with the two conditions using either phen or PyBCam^{CN}. The reaction aliquots were quenched with I₂/LiCl to quantify the formation of organometallic reagents in the reaction mixture (Figure 3.5).¹⁹ XEC reactions with phenyl triflate (**3.47**) using phen as the ligand for nickel resulted in 62% yield of Ph–I compared to 2% using PyBCam^{CN} as the ligand. Concentrations of Ph–I above the 5 mol% Ni loading were attributed to an arylzinc reagent (PhZnCl) generated *in situ* by transmetalation from nickel to zinc. When 4-carbomethoxyphenyl triflate (**3.1**) was used in place of phenyl triflate (**3.47**) under phen/nickel catalysis, the corresponding aryl iodide was observed in 28% yield.

Figure 3.5. Assessment of the Presence of Organometallic Reagents.

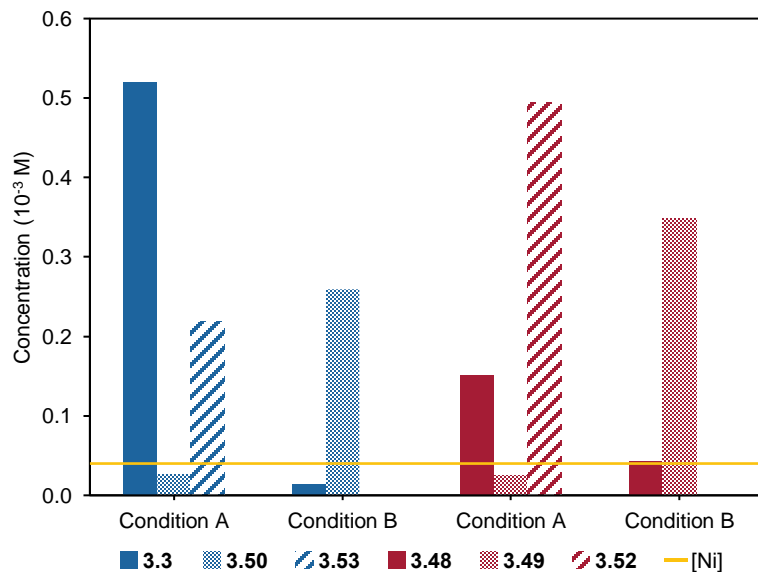
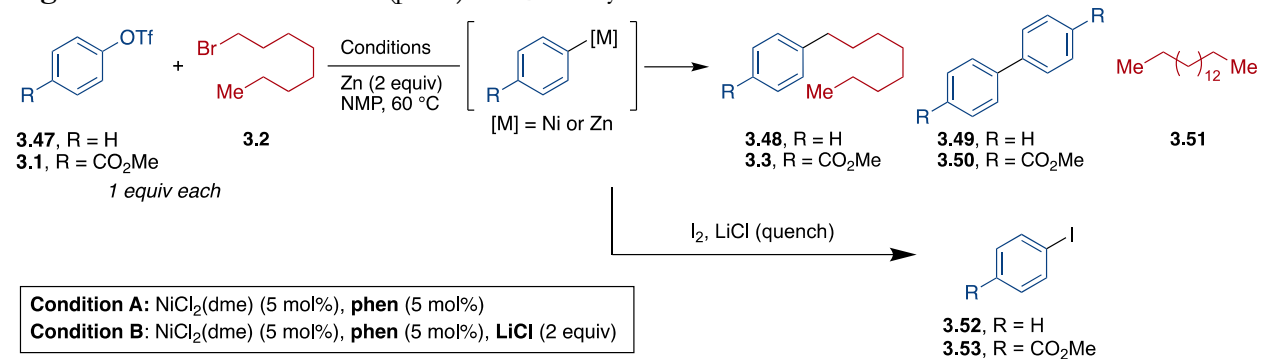


mmol calculated from GC calibrated yield against 1,3,5-trimethoxybenzene.

Figure 3.6 demonstrates the reactivity of phen ligated nickel with phenyl triflates (**3.47**) and 4-carbomethoxyphenyl triflate (**3.1**) with or without LiCl present. Iodine quenching experiments showed that 1) phen ligated nickel without LiCl additive generates significant quantities of arylzinc along with cross-coupled product, and 2) the addition of LiCl converts arylzinc to aryl dimers through acceleration of transmetalation (complete conversion to aryl dimer within 30 min of reaction). The ratio of arylzinc to cross-coupled product varies based on aryl electronics. Activated aryl triflates

generate less arylzinc (and thus more product) compared to unactivated aryl triflates. These experiments prompted us to question whether aryl zinc species were involved in product formation, as has been reported in some types of XEC-style reactions,²⁰ or unproductive side products.

Figure 3.6. Effect of LiCl on (phen)NiCl₂ Catalyzed Reaction.



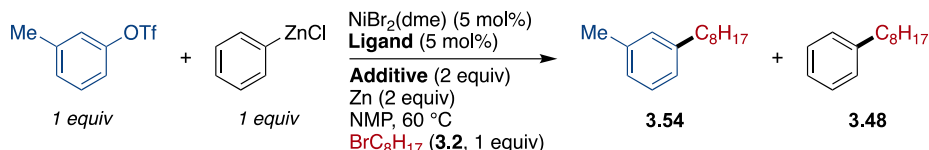
3.4.2. Role of the Aryl Zinc Species.

A series of control reactions were run to determine the conditions necessary for *in situ* formation of arylzinc halide and showed that: 1) no arylzinc was generated in the absence of a Ni catalyst, and 2) phen ligated nickel is required for phenylzinc formation, as neither nickel alone nor PyBCam^{CN} ligated nickel generated phenylzinc. These observations, along with work by Hintermann,²¹ suggest that phenylzinc is generated by transmetalation from arylnickel(II) to zinc salts present in

solution. Additionally, the reduced formation of arylzinc observed with 4-carbomethoxy phenyl triflate (**3.1**) suggests that the electronics of the arene can affect the rate of transmetalation.²² Notably, phenylzinc accumulated once alkyl bromide was depleted and only aryl triflate remained, suggesting that arylzinc formation occurs as a consequence of poor oxidative addition selectivity between coupling partners.

To further shed light upon the fate of arylzinc reagents in these XEC reactions, we conducted a series of competition experiments between electronically-matched aryl triflates and arylzinc halide reagents. Reaction of bromooctane with a 1:1 ratio of phenylzinc chloride and 3-methylphenyl triflate showed that the aryl triflate reacted faster than the phenylzinc chloride (Figure 3.7). When phen was used as the ligand, a 2:1 selectivity for coupling the triflate was observed despite the high concentration of phenylzinc present compared to the catalytic conditions. The same experiment with PyBCam^{CN} showed opposite selectivity of 1:6 of 3-octyltoluene (**i**) to octylbenzene (**ii**). When employing PyBCam^{CN} as the ligand, arylzinc does not form in an appreciable amount (less than 5 mol%), therefore the selectivity can be attributed to the reduced formation of arylzinc species. The possibility that alkyl zinc reagents are responsible for product formation was tested via a similar competition experiment between 1-bromooctane and dodecyl zinc bromide (Figure 3.8). Reactions with phen or PyBCam^{CN} both showed a 2:1 selectivity for coupling the alkyl bromide over the alkylzinc, suggesting that product formation is not occurring via an *in situ* Negishi coupling.

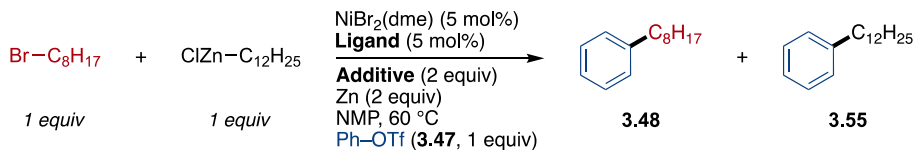
Figure 3.7. Competition Study Between Phenyl Zinc and Aryl Triflate.



Entry	Ligand/Additive	Yield 3.54 (%)	Yield 3.48 (%)	Ratio 3.54:3.48
1	phen (L1)	40	24	3:1
2	PyBCam ^{CN} (L9), LiCl	3	19	1:6

GC yield calibrated against 1,3,5-trimethoxybenzene as an internal standard is reported after 24 h.

Figure 3.8. Competition Study Between Alkyl Zinc and Alkyl Bromide.



Entry	Ligand/Additive	Ratio 3.48:3.55
1	phen (L1)	2:1
2	PyBCam ^{CN} (L9), LiCl	2:1

Ratio calculated from GC yield calibrated against 1,3,5-trimethoxybenzene as an internal standard.

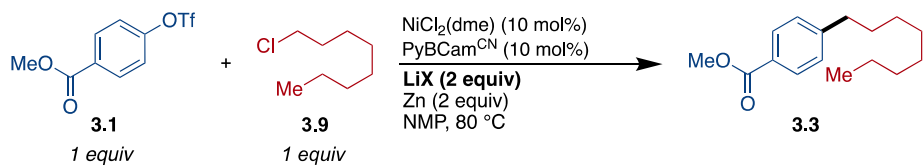
3.5. Complex Role of the Lithium Additives.

In related cross-electrophile coupling reactions, LiCl was shown to be effective at promoting the reduction of various Ni(II) species at the surface of zinc, while ZnCl₂ (which is necessarily formed under the reported XEC conditions) was shown to inhibit reduction of the same species suggesting that the cation is the key to this observed reactivity.¹⁶ Based on our previous work we hypothesized that we could use LiX salts to both accelerate the reduction of nickel at zinc and modulate the rate of radical generation through an *in situ* Finkelstein reaction.

In the cross-coupling of triflate **3.1** and alkyl chloride **3.9** with lithium chloride as a (super)stoichiometric additive, the cross-coupled product was only observed in 12% yield while the reduced aryl triflate and recovered alkyl chloride were seen in 21% and 50%, respectively. When LiBr

was used in place of LiCl the product was formed in 40% yield with 22% of the alkyl chloride recovered, supporting the hypothesis that halide identity in the salt additive is crucial for controlling reactivity of alkyl electrophiles (Figure 3.9). This was further demonstrated when LiI was employed, improving the yield to 86%. Employing lithium salts with non-halide counteranions afforded moderate conversion of the aryl triflate to the corresponding arene and recovered alkyl chloride. We observed that the added halide sources (bromide or iodide) has a strong correlation with the consumption of alkyl chloride (Figure 3.10).

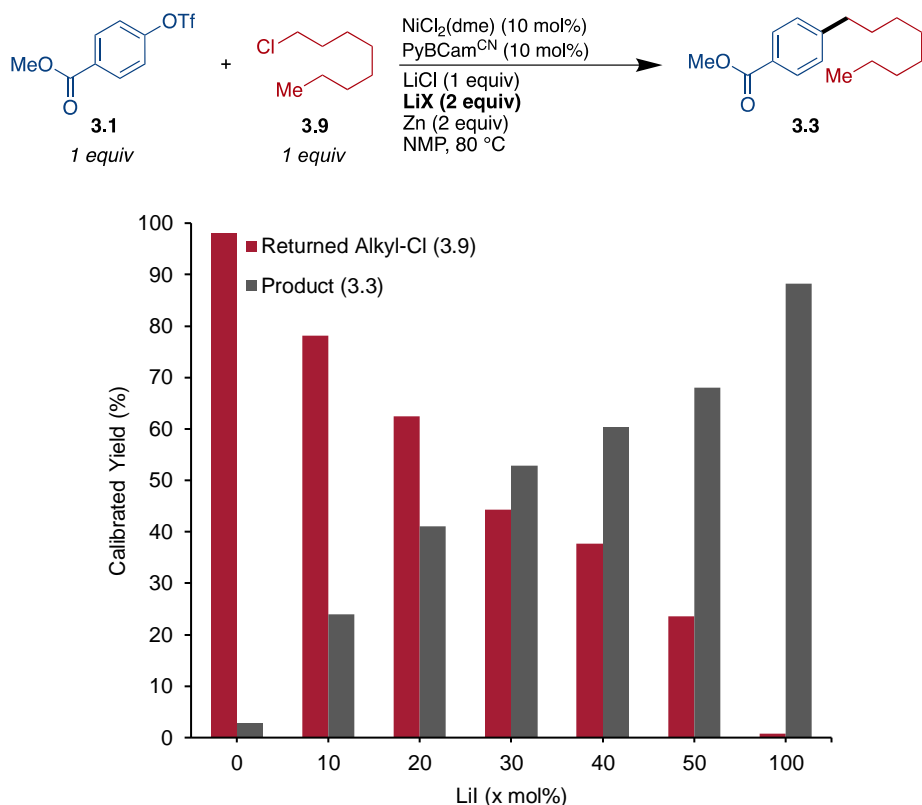
Figure 3.9. Effect of Li Additives on Product Formation.



Entry	Li Additive	3.3 (%)
1	LiCl	12
2	LiBr	40
3	LiI	>99
4	LiBF_4	2
5	LiOTf	3

Yields reported are calibrated against 1,3,5-trimethoxybenzene as an internal standard.

Figure 3.10. Correlation Between Lithium Iodide Amounts and Alkyl Chloride Consumption.



Yields reported are calibrated against 1,3,5-trimethoxybenzene as an internal standard.

3.6. Discussion.

The selectivity of a cross-coupling reaction is based upon the relative rates of each productive and unproductive elementary step, with the most selective reactions being ones in which the net productive pathway is faster than any side reaction. However, cross-electrophile coupling reactions mediated by a single catalyst have substrate activation steps (oxidative addition, SET, XAT, etc.) that are often governed by similar parameters, causing perturbations to reaction conditions to unpredictably effect multiple processes. Conversely, a scenario in which substrate activation steps are completely orthogonal to one another, would enable modular reaction conditions that can tune each step individually to decrease undesirable side reactivity. In our studies we found a synergistic effect

between ligand selection and halide exchange process, which was critical in achieving cross-selectivity between electronically diverse coupling partners.

3.6.1. Ligand Trends.

During our optimization, we found that judicious selection of ligand was necessary depending on coupling partners. We considered the following factors when developing the conditions: 1) arene electronics and 2) alkyl halide identity. Phen was effective for coupling electron deficient aryl triflates with alkyl bromides. One possible explanation is due to the decreased propensity of (phen)NiArX to undergo transmetalation to form arylzinc reagents when the aryl ligand is electron deficient (Figure 3.6, Condition A). PyBCam^{CN} outperformed phen in couplings with electron neutral and rich aryl triflates. In analogy to our previous report on the cross-electrophile coupling of aryl chlorides, PyBCam^{CN} is effective at the oxidative addition of traditionally inert aryl electrophiles. Notably, in comparison to phen, PyBCam^{CN} favors cross-coupling over homodimerization of the arene.

When coupling alkyl chlorides, PyBCam^{CN} was used regardless of arene electronics. Lithium salt additives are required to activate the alkyl chlorides via halide exchange. Since phen-ligated nickel generates arylzinc (Figure 3.6), the addition of LiCl accelerates transmetalation back to nickel, resulting in rapid aryl dimerization and decreased yields of cross-product. However, PyBCam^{CN} does not generate arylzinc species (Figure 3.5), and lithium salt additives should not promote undesired aryl dimerization.

3.6.2. Transmetalation as a Side Reaction.

Lithium salts have been shown to play multiple roles in cross-coupling reactions. Lithium chloride can accelerate the rate of transmetalation in Negishi reactions by solubilizing surface-bound organozinc species,²³ aiding in the formation of higher order zincates,²⁴ and increasing the dielectric

constant of the reaction medium.²⁵ Because of this literature precedent and the beneficial effect of LiCl in our reaction, we sought to investigate the potential intermediacy of organozinc species. This titration method¹⁹ quantifies any organometallic species that forms by conversion to the corresponding iodoarene. We note that a concentration of iodoarene greater than that of the nickel catalyst loading (5–10 mol%) would be indicative of the formation of an arylzinc intermediates. Control experiments support arylzinc formation occurs via transmetalation of arynickel onto an equivalent of ZnX_2 rather than direct insertion of the aryl triflate into zinc. PyBCam^{CN}-ligated nickel forms 3% iodoarene, which suggests no arylzinc intermediates are generated. However, phen-ligated nickel generates up to 67% iodoarene by the end of the reaction, leading us to consider the implications of arylzinc species on product formation.

Based on our mechanistic experiments with phen-ligated nickel, we hypothesize that cross-product does not form through arylzinc intermediates due to the following reasons: 1) increased amounts of iodobenzene was observed following consumption of the alkyl halide, suggesting that transmetalation is slower than radical capture and reductive elimination, and is not a pathway towards productive chemistry and 2) competition experiments (Figure 3.7) showed that phen-ligated nickel preferentially forms the cross-product from the aryl triflate rather than the arylzinc reagent. The addition of LiCl to these reactions accelerates transmetalation of arylzinc back onto the nickel catalyst and only forms aryl dimer, suggesting that an arylzinc is not a productive on-cycle intermediate. For PyBCam^{CN}, organozinc formation does not appear to occur under these conditions. However, if it did occur it would outcompete aryl triflate to form product and aryl dimer. Nonetheless, given the very low amount of biaryl observed in catalytic reactions, this suggests that arylzinc formation is not a viable pathway in reactions with PyBCam^{CN}.

3.6.3. Halide Exchange beyond Finkelstein.

The rate of oxidative addition of aryl electrophiles is impacted by the electronics, with increased electron density leading to slower oxidative addition. Cross-selectivity between two electrophiles requires the rates of each activation step to be matched (Figure 3.3). Tuning the reactivity of the alkyl coupling partner (radical generation) relative to the aryl partner (oxidative addition) enables cross-coupling across a broad range of electrophiles. Notably, this strategy allows for both increasing and decreasing the rate of alkyl radical generation through the selection of an appropriate lithium salt additive.

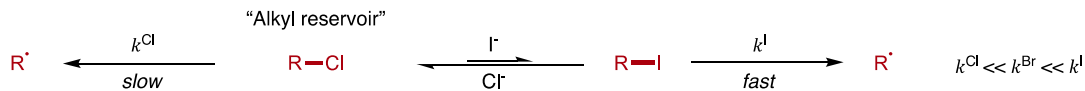
For electron-poor aryl triflates with alkyl bromides no salt additives were required as their intrinsic reactivity with nickel was already matched (Figure 3.4, Condition A). For electron-rich aryl triflates with alkyl bromides the intrinsic rate of radical generation was fast compared to oxidative addition, resulting in alkyl homodimerization and returned aryl triflate (Table 3.1, entry 6). To address this mismatch, we found the addition of LiCl promoted cross-selectivity over alkyl dimerization (Table 3.1, entry 7). We attribute this to an *in situ* halide exchange via an S_N2 reaction between the alkyl bromide and Cl^- , creating an equilibrium that favors the alkyl chloride. Direct radical generation from the alkyl chloride is significantly slower than from the alkyl bromide which slows down consumption of the alkyl coupling partner. We propose this halide exchange process to the chloride creates an “alkyl reservoir” that slowly releases the more reactive alkyl bromide at a rate that is well-matched with the oxidative addition of the aryl triflate.

When employing alkyl chlorides in our studies, we found that activation of C–Cl bond was necessary for achieving cross-selectivity. In the case of electron-poor aryl triflates a significant rate enhancement of radical generation was required to match with the faster rate of oxidative addition. We addressed this challenge through the addition of LiI, which promotes the *in situ* exchange to form the more reactive alkyl iodide. However, with electron-rich aryl triflates and alkyl chlorides, LiCl

additive with PyBCam^{CN} afforded satisfactory yields of product. Based on our previous studies, we hypothesize that increasing total chloride concentration makes available the catalytic bromide introduced through the nickel precatalyst. This is due to the chloride preferentially ligating to Zn²⁺ while the bromide can participate in halide exchange and activate the alkyl electrophile.

The halide identity of an alkyl halide has a significant effect on the rate of radical generation under cross-electrophile coupling conditions. Adding of lithium halide salts to a cross-electrophile coupling employing an alkyl halide that is susceptible to S_N2 allows for rapid equilibration of the lithium halide and alkyl halide (Figure 3.10). This strategy allows for facile tuning of radical generation through both the identity of the halide in (increased intrinsic reactivity of each halide), and the stoichiometry of the LiX salt (altering the relative concentration of each different alkyl-X). Importantly, the addition of LiCl minimizes alkyl dimerization by pushing equilibrium towards the alkyl chloride (Figure 3.11).

Figure 3.11. Identity of Halide and the Rate of Radical Generation.



In addition to halide exchange as a tuning strategy for alkyl radical generation, lithium salts have beneficial effects for nickel reduction.¹⁶ Firstly, we and others have observed that LiCl can overcome the inhibitory effect of ZnCl₂ that builds up throughout the reaction.(ref) Furthermore, Ni(OTf)₂ is challenging to reduce to Ni(0) (Figure 3.1a) but the addition of LiCl promotes this reduction and restores catalytic reactivity.

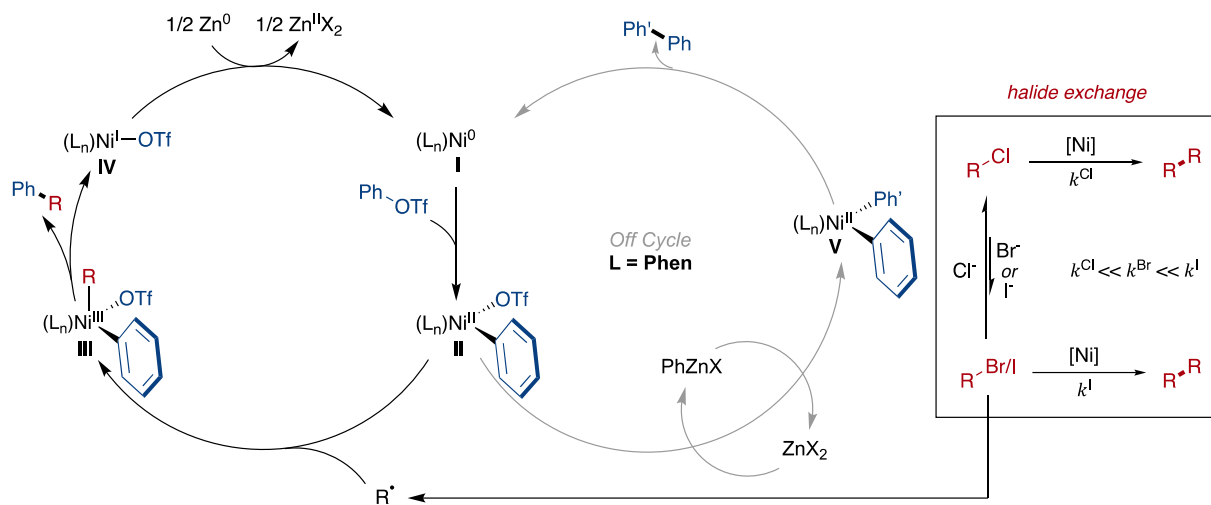
3.6.4. Proposed Mechanism.

Based on the data collected from our mechanistic studies, we proposed the following mechanism (Figure 3.12). Oxidative addition of aryl triflate into nickel(0) **I** results in the formation of arynickel(II) **II**. This is likely the nickel resting state, which then captures an alkyl radical to form a transient diorganonickel (III) **III**. This undergoes reductive elimination to generate the cross-coupled product and a nickel triflate salt **IV**. At this point we cannot rule out complex **IV** has a nickel(II) oxidation state. Zinc reduces this nickel salt to Ni(0) **I** for the complete catalytic cycle.

We have shown that PyBCam to be a proficient ligand for cross-coupling electron-rich aryl triflates with alkyl bromides and chlorides, while phen is well-suited for the cross-coupling of electron-poor aryl triflates with alkyl bromides, in analogy to work by Hosoya.¹⁴ In case of phen, our studies suggest that transmetalation between arynickel(II) and zinc salts generate arylzinc species. However, this species does not participate in product formation, instead this is an unproductive off-cycle pathway. The triflate derived byproducts (aryl–H and aryl–aryl) are likely a result of arylzinc formation.

The rate of alkyl radical formation is dictated by the identity of the halide salt additive. Through *in situ* S_N2, the identity of the alkyl halide in solution can be tuned to match the reactivity of aryl triflate oxidative addition. In this halide exchange equilibrium, conversion of the alkyl coupling partner into the alkyl chloride slows down the rate of radical generation. This equilibrium favors the alkyl chloride, which creates an alkyl reservoir effect and tunes the alkyl radical generation to better match with a slow oxidative addition. *In situ* generation of alkyl bromide/iodide enhances the rate of radical generation to match with a faster oxidative addition. Taken together, this halide exchange strategy enables cross-coupling across a broad range of aryl and alkyl coupling partners.

Figure 3.12. Proposed Mechanism for the Cross-Electrophile Coupling of Aryl Triflates with Alkyl Halides.



3.7. Conclusions.

We have demonstrated $C(sp^2)-C(sp^3)$ cross-electrophile coupling between aryl triflates and alkyl electrophiles. Notably, our strategy allows for the coupling of electronically diverse aryl triflates with alkyl bromides and chlorides. Key to achieving cross-selectivity was the selection of an appropriate ligand and lithium salt additive that tunes the alkyl reactivity by creating a halide exchange equilibrium. Mechanistic studies revealed nuanced effects of ligand and salts on tuning the rates of activation of each coupling partner. We anticipate this halide exchange strategy can be broadly applied to coupling different classes of electrophiles, especially in cases where coupling partners have inherently mismatched reactivity in nickel catalysis.

3.8. Experimental.

3.8.1. General Information.

3.8.1.1. Reagents.

Metals

Zinc flake (-325 mesh) was purchased from Alfa Aesar and activated according to the method reported by Everson *et al.*¹⁸ by washing with 1 M HCl for 1 minute followed by washing with water and diethyl ether. The resulting grey powder was flame dried under vacuum in a scintillation vial and stored under N₂.

Nickel(II) bromide ethylene glycol dimethyl ether [NiBr₂(dme)] was synthesized according to the literature procedure and analyzed by elemental analysis prior to use.²⁶ The resulting orange powder was stored under N₂.

Nickel(II) chloride ethylene glycol dimethyl ether [NiCl₂(dme)] was synthesized according to the literature procedure and analyzed by elemental analysis prior to use.²⁶ The resulting yellow powder was stored under N₂.

Bis(1,5-cyclooctadiene)nickel(0) [Ni(COD)₂] was purchased from Strem, stored in the glovebox, and used as received.

(2,2':6',2''-terpyridine)nickel(II)chloride [(terpy)NiCl₂] was synthesized according to the literature procedure and isolated as an air stable green solid.²⁷

Ligands

1,10-Phenanthroline (phen) was purchased from Sigma Aldrich, stored in a glovebox, and used as received.

4,7-Diphenyl-1,10-phenanthroline (BPhen) was purchased from Sigma Aldrich, stored in a glovebox,

and used as received.

2,2'-Bipyridine (bpy) was purchased from Sigma Aldrich, stored in a glovebox, and used as received.

4,4'-Di-tert-butyl-2,2'-bipyridine (dtbbpy) was purchased from Sigma Aldrich, stored in a glovebox, and used as received.

4,4'-Dimethoxy-2,2'-bipyridine (dmbpy) was purchased from Sigma Aldrich, stored in a glovebox, and used as received.

2,2':6',2''-Terpyridine (terpy) was purchased from Sigma Aldrich, stored in a glovebox, and used as received.

2,2'-Bipyridine-6-carboximidamide•HCl (BPyCam•HCl, L1) was synthesized according to the literature procedure.²⁸ The resulting white powder was dried under vacuum and stored in a glovebox.

Pyridine-2,6-bis(carboximidamide)•2HCl (PyBCam•2HCl, L2) was synthesized according to the literature procedure.²⁹ The resulting white powder was dried under vacuum and stored in a glovebox.

Pyridine-2,6-bis(N-cyanocarboxamidine) (PyBCam^{CN}, L3) was synthesized according to the literature procedure.³⁰ The resulting white powder was dried under vacuum and stored in a glovebox.

Solvents

Anhydrous N-methylpyrrolidone (NMP), N,N-dimethylformamide (DMF), and N,N-

dimethylacetamide (DMA), dimethylsulfoxide (DMSO) were purchased from Sigma Aldrich, stored in a glovebox, and used as received. For reactions outside of the glovebox the reagents were sparged with N₂ for >10 minutes prior to use. Acetonitrile (MeCN), tetrahydrofuran (THF), and toluene were obtained by passage through activated alumina and molecular sieves in a solvent purification system and stored in a glovebox.

Aryl Substrates

Methylparaben trifluoromethanesulfonate was synthesized according to the literature procedure.³¹ The resulting oil was stored in the glovebox.

4-Benzoylphenyl trifluoromethanesulfonate was synthesized according to the literature procedure.³² The resulting solid was stored in the glovebox.

4-(Trifluoromethyl)phenyl trifluoromethanesulfonate was synthesized according to the literature procedure.³¹ The resulting oil was stored in the glovebox.

Pyridin-3-yl trifluoromethanesulfonate was synthesized according to the literature procedure.³³ The resulting oil was stored in the glovebox.

Quinolin-6-yl trifluoromethanesulfonate was synthesized according to the literature procedure.³¹ The resulting oil was stored in the glovebox.

4-Chlorophenyl trifluoromethanesulfonate was synthesized according to the literature procedure.³³ The resulting oil was stored in the glovebox.

Phenyl trifluoromethanesulfonate was synthesized according to the literature procedure.³⁴ The resulting oil was stored in the glovebox.

4-Methoxyphenyl trifluoromethanesulfonate was synthesized according to the literature procedure.³¹ The resulting oil was stored in the glovebox.

2-Methoxyphenyl trifluoromethanesulfonate was synthesized according to the literature procedure.³⁵ The resulting oil was stored in the glovebox.

4-(Methylthio)phenyl trifluoromethanesulfonate was synthesized according to the literature procedure.³⁶ The resulting oil was stored in the glovebox.

2-Methylphenyl trifluoromethanesulfonate was synthesized according to the literature procedure.³⁷ The resulting oil was stored in the glovebox.

3-Methylphenyl trifluoromethanesulfonate was synthesized according to the literature procedure.³⁸ The resulting oil was stored in the glovebox.

2,3-Dihydro-1*H*-inden-5-yl trifluoromethanesulfonate was synthesized according to the literature procedure.³⁹ The resulting oil was stored in the glovebox.

4-Fluorophenyl trifluoromethanesulfonate was synthesized according to the literature procedure.⁴⁰ The resulting oil was stored in the glovebox.

4-Chloro-3-methylphenyl trifluoromethanesulfonate was synthesized according to the literature procedure.⁴¹ The resulting oil was stored in the glovebox.

Naphthalen-2-yl trifluoromethanesulfonate was synthesized according to the literature procedure.³¹ The resulting oil was stored in the glovebox.

2-Methylbenzo[d]thiazol-5-yl trifluoromethanesulfonate was synthesized according to the literature procedure.³⁶ The resulting oil was stored in the glovebox.

4-(4,4,5,5-Tetramethyl-1,3,2-dioxaborolan-2-yl)phenyl trifluoromethanesulfonate was synthesized according to the literature procedure.³⁵ The resulting oil was stored in the glovebox.

(8R,9S,13S,14S)-13-Methyl-17-oxo-7,8,9,11,12,13,14,15,16,17-deahydro-6H cyclopenta[a]phenanthren-3-yl trifluoromethanesulfonate (estrone triflate) was synthesized according to the literature procedure.³² The resulting solid was stored in the glovebox.

Methyl (S)-2-((tert-butoxycarbonyl)amino)-3-(4-(((trifluoromethyl)sulfonyl)oxy)phenyl)propanoate was synthesized according to the literature procedure.⁴² The resulting oil was stored in the glovebox.

Phenylzinc chloride was synthesized according to the literature procedure and obtained as a solution in THF.⁴³ This solution was stored in a glovebox and titrated with iodine prior to use. Error! Bookmark not defined.

Alkyl Halide Substrates

1-Bromoocetane was purchased from Sigma Aldrich and sparged with N₂ prior to use.

Ethyl 4-bromobutyrate was purchased from Sigma Aldrich and sparged with N₂ prior to use.

(Bromomethyl)cyclohexane was purchased from Sigma Aldrich and sparged with N₂ prior to use.

4-Bromo-1-chlorobutane was purchased from Sigma Aldrich and sparged with N₂ prior to use.

2-(3-Bromopropyl)-4,4,5,5-tetramethyl-1,3,2-dioxaborolane was purchased from Sigma Aldrich and sparged with N₂ prior to use.

(3-Chloropropyl)benzene was purchased from Sigma Aldrich and sparged with N₂ prior to use.

(2-Chloroethoxy)benzene was purchased from Sigma Aldrich and sparged with N₂ prior to use.

2-(Chloromethyl)tetrahydrofuran was purchased from Sigma Aldrich and sparged with N₂ prior to use.

4-(Chloromethyl)-2,2-dimethyl-1,3-dioxolane was purchased from Sigma Aldrich and sparged with N₂ prior to use.

3-Chloropropyl acetate was purchased from Sigma Aldrich and sparged with N₂ prior to use.

tert-Butyl (3-chloropropyl)carbamate was purchased from Sigma Aldrich and sparged with N₂ prior to

use.

Bromocyclopentane was purchased from Sigma Aldrich and sparged with N₂ prior to use.

Chlorocyclopentane was purchased from Sigma Aldrich and sparged with N₂ prior to use.

1-Bromo-2-isopropylbenzene was purchased from Alfa Aesar, sparged with N₂, and stored in the glovebox prior to use.

1-Chlorooctane was purchased from Sigma Aldrich and sparged with N₂ prior to use.

Dodecylzinc bromide was synthesized according to the literature procedure and obtained as a solution in DMA.⁴⁴ This solution was stored in a glovebox and titrated with iodine prior to use. Error! Bookmark not defined.

Other Reagents

Lithium chloride (LiCl) was purchased from Sigma Aldrich and dried under vacuum before being stored in a glovebox.

Lithium bromide (LiBr) was purchased from Sigma Aldrich and dried under vacuum before being stored in a glovebox.

Sodium chloride (NaCl) was purchased from Sigma Aldrich and dried under vacuum before being stored in a glovebox.

Dodecane was purchased from Sigma Aldrich and used as received.

Hexamethyldisiloxane was purchased from Sigma Aldrich and used as received.

n-Butyllithium (1.6 M in hexanes) was purchased from Sigma Aldrich and titrated with iodine to determine the concentration prior to use. Error! Bookmark not defined.

Potassium tert-butoxide was purchased from Sigma Aldrich, stored in the glovebox, and used as received.

3.8.1.2. Methods.

NMR Spectroscopy

^1H and ^{13}C NMR spectra were acquired on 400 and 500 MHz AVANCE spectrometer equipped with a DCH cryoprobe (Bruker), at a sample temperature of 25 °C. NMR spectra were recorded with TopSpin 3.5.6 (Bruker). The Bruker AVANCE 400 NMR spectrometer was supported by NSF grant CHE-1048642. The Bruker AVANCE 500 NMR spectrometer was supported by a generous gift from Paul J. and Margaret M. Bender.

Referencing and absolute referencing to TMS, apodization, Fourier transform, phase and baseline corrections, and spectral analyses were carried out with MestReNova 12.0.4 (Mestrelab Research). NMR chemical shifts are reported in ppm and are referenced to the residual solvent peak for CDCl_3 ($\delta = 7.26$ ppm, ^1H NMR; $\delta = 77.16$ ppm, ^{13}C NMR. Coupling constants (J) are reported in Hertz.

Gas Chromatography

GC analyses were performed on an Agilent 7890A GC equipped with dual DB-5 columns (20 m × 180 μ m × 0.18 μ m), dual FID detectors, and hydrogen as the carrier gas. A sample volume of 1 μ L was injected at a temperature of 300 °C and a 100:1 split ratio. The initial inlet pressure was 20.3 psi but varied as the column flow was held constant at 1.8 mL/min for the duration of the run. The initial oven temperature of 50 °C was held for 0.46 min followed by a temperature ramp of 65 °C/min up to 300 °C. The total run time was 5.0 min and the FID temperature was 325 °C.

GC/MS Analysis

GC/MS analyses were performed on a Shimadzu GCMS-QP2010 equipped with an RTX-XLB column (30 m × 0.25 mm × 0.28 μ m) with a quadrupole mass analyzer using helium as the carrier gas. The analysis method used in all cases was 1 μ L injection of sample, an injection temp of 225 °C, and a 25:1 split ratio. The initial inlet pressure was 7.8 psi, but varied as the column flow was held constant at 1.0 mL/min for the duration of the run. The interface temperature was held at 250 °C, and the ion source (EI+, 30 eV) was held at 250 °C. The initial oven temperature was held at 50 °C for 2 min with the detector off, followed by a temperature ramp, with the detector on, to 280 °C at 40 °C/min. The temperature was held at 280 °C for 3 min. Total run time was 11.75 min.

Chromatography

Chromatography was performed on silica gel (EMD, silica gel 60, particle size 0.040-0.063 mm) using standard flash techniques, on a Teledyne Isco CombiFlash instrument using pre-packaged cartridges, on a Teledyne Isco Rf-200 (detection at 210 nm and 280 nm), or on a Biotage Isolera One (detection at 210 nm and 400 nm, on Sfar Duo columns). Products were visualized by UV, KMnO₄ stain, PMA stain, or fractions were analyzed by GC.

Elemental Analysis

Microanalysis samples were weighed with a PerkinElmer Model AD6000 Autobalance and their compositions were determined with a PerkinElmer 2400 Series II Analyzer by the CENTC Elemental Analysis Facility at the University of Rochester, funded by NSF CHE-0650456.

Infrared Spectroscopy

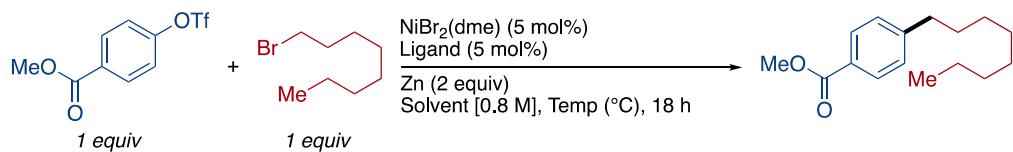
Solid state FT-IR spectroscopic data were collected in ATR mode using a Bruker TENSOR 27 spectrometer located in the Chemical Instrumentation Instructional Laboratory at the University of Wisconsin-Madison Department of Chemistry and are reported in wavenumbers (cm^{-1}).

High Resolution Mass Spectrometry

UW-Madison: High resolution mass spectra (HRMS). Mass spectrometry data was collected on a Thermo Q ExactiveTM Plus (thermofisher.com) via flow injection with electrospray ionization or via ASAPMSTM (asap-ms.com) by the chemistry mass spectrometry facility at the University of Wisconsin-Madison. The purchase of the Thermo Q ExactiveTM Plus in 2015 was funded by NIH Award 1S10 OD020022-1 to the Department of Chemistry.

3.8.2. General Procedures.

3.8.2.1. General Procedure for Reaction Optimization with Electron Poor Arenes.



Reactions were set up in a N_2 filled glove box. A catalyst solution was prepared by charging an oven-

dried 1-dram vial with a PTFE-coated stirbar, $\text{NiBr}_2(\text{dme})$ (3.1 mg, 0.01 mmol, 5 mol%), and the listed ligand (0.05 mmol, 5 mol%). The solids were dissolved in NMP (250 μL) and allowed to stir at rt for 10 min. To this solution methyl 4-(trifluoromethylsulfonyloxy)benzoate (56.8 mg, 0.20 mmol, 1.0 equiv), 1-bromooctane (38.6 mg, 0.20 mmol, 1.0 equiv), and zinc (activated zinc flake, 26.2 mg, 0.40 mmol, 2.0 equiv) were added, followed by dodecane (10 μL , 0.044 mmol) as an internal standard. The reaction vials were sealed with screw caps fitted with PTFE-faced silicone septa and removed from the glovebox. The reaction was allowed to stir (1250 RPM) at the listed temperature for 18 h.

NMR Analysis

The crude reaction mixture was filtered through silica gel (\sim 4 g) with a 3:1 mixture of pentane/EtOAc and the filtrate was concentrated by rotary evaporation. Hexamethydisiloxane (10 μL , 0.0471 mmol) was added as an external standard and the residue was diluted with CDCl_3 (\sim 500 μL). The resulting solution was analyzed by NMR and the spectra automatically phase and baseline corrected to provide a stable baseline. The integration of the hexamethydisiloxane diagnostic peak at 0.061 ppm was set to 18 protons and yields determined based on the integrated ratio of a characteristic product peak.

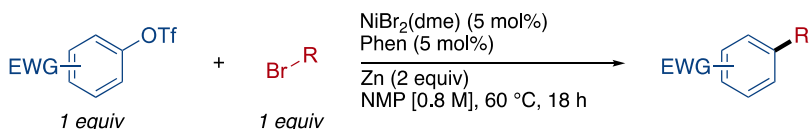
GC Analysis

The reaction was monitored by GC analysis by taking a 10 μL aliquot of the crude reaction mixture with a gas-tight syringe. The aliquot was diluted with EtOAc (0.50 mL), filtered through a 2-cm silica plug in a Pasteur pipette, and collected in a GC vial. The sample was analyzed by GC using our standard method and the yields were determined based on the peak area of the analyte compared to dodecane as an internal standard.

Isolation and Purification

Reactions were isolated on a 0.2 mmol scale of aryl triflate and alkyl bromide. In some cases isolated reactions were run without the addition of an internal standard to avoid difficulties in separating dodecane from the desired product. The crude reaction mixture was filtered through silica gel (4 cm silica plug in a thick-walled glass pipette) with EtOAc (~10 mL) and the filtrate was concentrated by rotary evaporation. The resulting material was purified by column chromatography on silica to provide the desired products.

3.8.2.2. General Procedure for Electron Poor Arenes.



Reactions were set up in a N_2 filled glove box. For a preparative-scale benchtop procedure, see **8.3.2.5 General Procedure for Preparative-Scale Benchtop Reactions**. An oven-dried 1-dram vial with a PTFE-coated stirbar was charged with $\text{NiBr}_2(\text{dme})$ (3.1 mg, 0.01 mmol, 5 mol%) and phen (1.8 mg, 0.01 mmol, 5 mol%). The solids were dissolved in NMP (250 μL) and allowed to stir at rt for >10 min resulting in a green solution. To this solution was added the listed aryl triflate (0.20 mmol, 1.0 equiv), the listed alkyl bromide (0.20 mmol, 1.0 equiv), and dodecane (10 μL , 0.044 mmol) as an internal standard. The zinc reductant (activated zinc flake, 26.2 mg, 0.40 mmol, 2.0 equiv) was added last, resulting in a slow color change from green to dark brown. The reaction vial was sealed with a screw cap fitted with a PTFE-faced silicone septum and removed from the glovebox. The reaction was allowed to stir (1250 RPM) at 60 $^\circ\text{C}$ for 18 h.

NMR Analysis

Same as **General Procedure** as noted above.

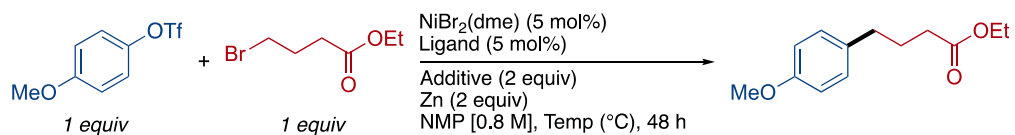
GC Analysis

Same as **General Procedure** as noted above.

Isolation and Purification

Same as **General Procedure** as noted above.

3.8.2.3. General Procedure for Reaction Optimization with Electron Rich Arenes.

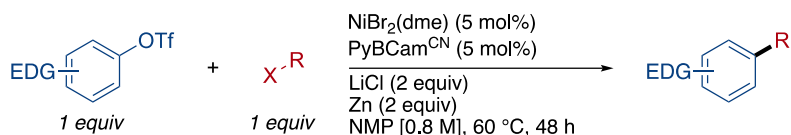


Reactions were set up in a N_2 filled glove box. A catalyst solution was prepared by charging an oven-dried 1-dram vial with a PTFE-coated stirbar, $\text{NiBr}_2(\text{dme})$ (3.1 mg, 0.01 mmol, 5 mol%), listed ligand (0.05 mmol, 5 mol%), and additive (0.40 mmol, 2.0 equiv). The solids were dissolved in NMP (250 μL) and allowed to stir at rt for 10 min. To this solution 4-(trifluoromethylsulfonyloxy)anisole (51.2 mg, 0.20 mmol, 1.0 equiv), ethyl 4-bromobutanoate (39.0 mg, 0.20 mmol, 1.0 equiv), and zinc (activated zinc flake, 26.2 mg, 0.40 mmol, 2.0 equiv) were added, followed by dodecane (10 μL , 0.044 mmol) as an internal standard. The reaction vials were sealed with screw caps fitted with PTFE-faced silicone septa and removed from the glovebox. The reaction was allowed to stir (1250 RPM) at the listed temperature for 48 h.

NMR Analysis

Same as **General Procedure** as noted above.

3.8.2.4. General Procedure for Electron Rich Arenes.



Reactions were set up in a N_2 filled glove box. For a preparative-scale benchtop procedure, see **3.8.2.5**

General Procedure for Preparative-Scale Benchtop Reactions. An oven-dried 1-dram vial with a PTFE-coated stirbar was charged with $\text{NiBr}_2(\text{dme})$ (3.1 mg, 0.01 mmol, 5 mol%), PyBCam^CN (2.1 mg, 0.01 mmol, 5 mol%), and LiCl (17.0 mg, 0.40 mmol, 2.0 equiv). The solids were dissolved in NMP (250 μL) and allowed to stir at rt for >10 min resulting in a light blue solution. To this solution was added the listed aryl triflate (0.20 mmol, 1.0 equiv), the listed alkyl halide (0.20 mmol, 1.0 equiv), and dodecane (10 μL , 0.044 mmol) as an internal standard. The zinc reductant (activated zinc flake, 26.2 mg, 0.40 mmol, 2.0 equiv) was added last, resulting in a slow color change from blue to dark brown. The reaction vial was sealed with a screw cap fitted with a PTFE-faced silicone septum and removed from the glovebox. The reaction was allowed to stir (1250 RPM) at 60 °C for 48 h.

NMR Analysis

Same as **General Procedure** as noted above.

GC Analysis

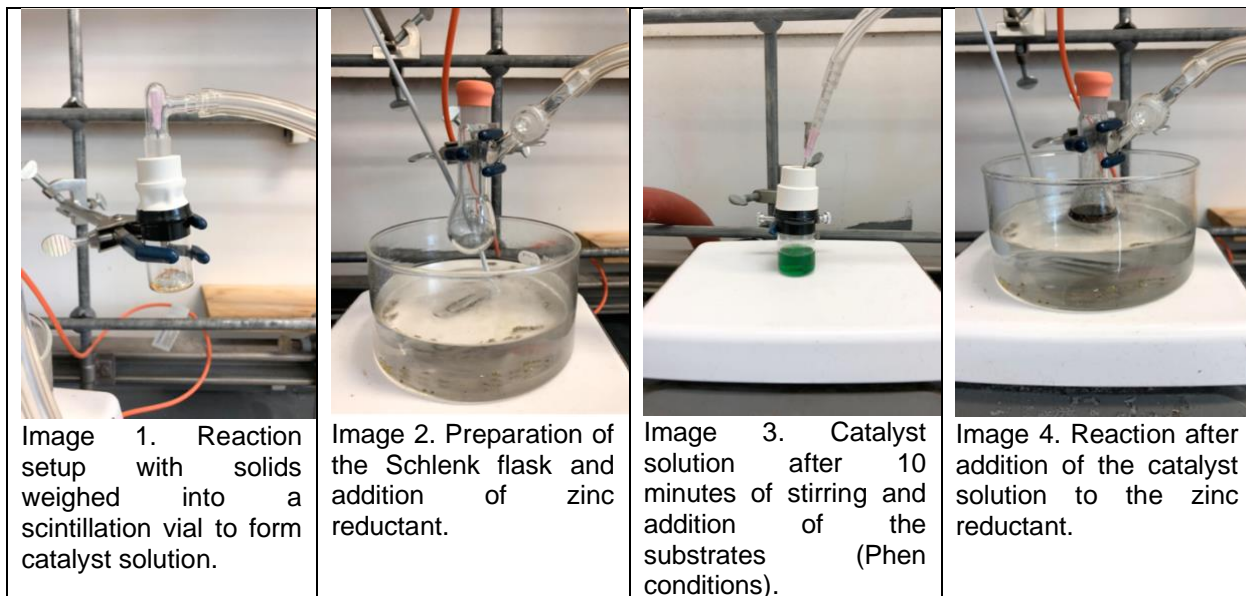
Same as **General Procedure** as noted above.

Isolation and Purification

Same as **General Procedure** as noted above.

3.8.2.5. General Procedure for Preparative-Scale Benchtop Reactions.

A catalyst solution was prepared on the benchtop by charging a scintillation vial with a PTFE-coated stirbar, $\text{NiBr}_2(\text{dme})$ (63.3 mg, 0.205 mmol, 5 mol%), and either Phen (36.9 mg, 0.205 mmol, 5 mol%) or PyBCam^{CN} (43.7 mg, 0.205 mmol, 5 mol%) and LiCl (348 mg, 8.20 mmol, 2.0 equiv). The scintillation vial was capped with a septa and evacuated before being backfilled with N_2 . N_2 sparged NMP (5.13 mL) was added to the scintillation vial and the solution was allowed to stir at rt for 10 min. A Schlenk flask was charged with a stir bar and activated zinc (536 mg, 8.20 mmol, 2.0 equiv) before being flame dried under vacuum, backfilled with N_2 , and allowed to cool. The listed aryl triflate (4.10 mmol, 1.0 equiv) and alkyl halide (4.10 mmol, 1.0 equiv) were sparged with N_2 and added via syringe under N_2 to the catalyst solution. The catalyst suspension was then cannula transferred to the Schlenk flask via syringe under N_2 . The reaction flask was added to a pre-heated 60 °C oil bath and allowed to stir (500 RPM) for 24 or 48 h for reactions with Phen or PyBCam^{CN}, respectively.



Isolation and Purification

The reaction was cooled to rt and diluted with Et₂O (60 mL) before being washed with a solution of saturated brine (60 mL). The Et₂O layer was collected and the aqueous layer was extracted with Et₂O (3 × 30 mL). The combined organic layers were dried over MgSO₄, filtered, and the filtrate was concentrated by rotary evaporation. The resulting crude material was diluted with EtOAc and made into a slurry with silica gel before the volatile solvents were removed by rotary evaporation. The resulting dry-loaded product was purified by column chromatography on silica.

3.8.3. Product Characterization.



Methyl 4-octylbenzoate (3.3) [CAS: 54256-51-8]

The general procedure for reaction optimization with electron poor arenes was followed using the conditions from Entry 1 in Table 3.1 with methyl 4-(((trifluoromethyl)sulfonyl)oxy)benzoate (56.8 mg, 0.20 mmol, 1.0 equiv) and 1-bromooctane (38.6 mg, 0.20 mmol, 1.0 equiv) as substrates. After 18 h, the crude reaction mixture was loaded onto silica gel and purified by column chromatography (40:1 hexanes/Et₂O) to afford the product (40.4 mg, 81% yield) as a colorless oil. This procedure was repeated to establish its reproducibility and the second reaction provided the product (44.9 mg, 0.181 mmol, 90% yield) in similar yield. Characterization data matched those reported in the literature.⁴

¹H NMR (400 MHz, CDCl₃) δ 7.96 – 7.93 (m, 2H), 7.26 – 7.23 (m, 2H), 3.90 (s, 3H), 2.65 (t, *J* = 7.7 Hz, 2H), 1.62 (q, *J* = 7.3 Hz, 2H), 1.30 – 1.26 (m, 10H), 0.89 – 0.86 (m, 3H).

¹³C{¹H} NMR (126 MHz, CDCl₃) δ 167.4, 148.7, 129.7, 128.6, 127.7, 52.1, 36.2, 32.0, 31.3, 29.6, 29.4, 29.4, 22.8, 14.2.

MS (EI) [M]⁺ m/z calcd for C₁₆H₂₄O₂⁺ 248.18; a solution in ethyl acetate found: 248.15.

IR (cm⁻¹) 2924, 2855, 1720, 1609, 1277, 1177, 1107.



(4-octylphenyl)(phenyl)methanone (3.10) [CAS: 64357-43-3]

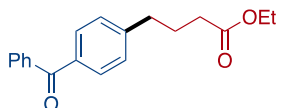
The general procedure for electron poor arenes was followed with 4-benzoylphenyl trifluoromethanesulfonate (66.1 mg, 0.20 mmol, 1.0 equiv) and 1-bromoocetane (38.6 mg, 0.20 mmol, 1.0 equiv) as substrates. After 18 h, the crude reaction mixture was loaded onto silica gel and purified by column chromatography (40:1 hexanes/Et₂O) to afford the product (43.9 mg, 75% yield) as a colorless oil. This procedure was repeated to establish its reproducibility and the second reaction provided the product (49.2 mg, 84% yield) in similar yield. Synthesis of this compound is reported, however, no spectra have been reported to date.

¹H NMR (500 MHz, CDCl₃) δ 7.79 (d, *J* = 7.6 Hz, 2H), 7.74 (d, *J* = 7.8 Hz, 2H), 7.58 (t, *J* = 7.4 Hz, 1H), 7.48 (t, *J* = 7.6 Hz, 2H), 7.29 – 7.26 (m, 3H), 2.69 (t, *J* = 7.8 Hz, 2H), 1.65 (quint, *J* = 7.5 Hz, 2H), 1.34 – 1.27 (m, 10H), 0.88 (t, *J* = 6.7 Hz, 3H).

¹³C{¹H} NMR (126 MHz, CDCl₃) δ 196.7, 148.4, 138.1, 135.2, 132.3, 130.5, 130.1, 128.5, 128.3, 36.2, 32.0, 31.3, 29.6, 29.5, 29.4, 22.8, 14.3.

MS (EI) [M]⁺ m/z calcd for C₂₁H₂₆O⁺ 294.20; a solution in ethyl acetate found: 294.20.

IR (cm⁻¹) 2924, 2855, 1659, 1600, 1277, 700.



Ethyl 4-(4-benzoylphenyl)butanoate (3.11) [CAS: 1220102-02-2]

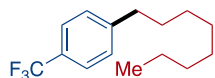
The general procedure for preparative-scale benchtop reactions was followed using Phen (36.9 mg, 0.21 mmol, 5 mol%) as a ligand and 4-benzoylphenyl trifluoromethanesulfonate (1.35 g, 4.10 mmol, 1.0 equiv) and ethyl 4-chlorobutyrate (587 μL, 4.10 mmol, 1.0 equiv) as substrates. After 18 h, the

crude reaction mixture was extracted with Et_2O (3×30 mL) and washed with brine (3×100 mL). The resulting organic solution was dried over sodium sulfate, filtered, and concentrated to a yellow oil. The oil was purified by column chromatography (gradient from 10:1 pentane/EtOAc to 3:1 pentane/EtOAc) to afford the product (894.7 mg, 74% yield) as a slightly yellow oil. Characterization data matched those reported in the literature.⁴⁵

^1H NMR (500 MHz, CDCl_3) δ 7.78 (d, $J = 6.8$ Hz, 1H), 7.74 (d, $J = 8.2$ Hz, 2H), 7.55 (t, $J = 7.4$ Hz, 1H), 7.45 (t, $J = 7.7$ Hz, 2H), 7.29 (d, $J = 8.2$ Hz, 2H), 4.13 (q, $J = 7.1$ Hz, 2H), 2.73 (t, $J = 7.7$ Hz, 2H), 2.34 (t, $J = 7.4$ Hz, 2H), 2.02 – 1.96 (m, 2H), 1.25 (t, $J = 7.1$ Hz, 3H).

$^{13}\text{C}\{^1\text{H}\}$ NMR (126 MHz, CDCl_3) δ 196.2, 173.1, 146.6, 137.7, 135.4, 132.2, 130.3, 129.9, 128.4, 128.2, 60.2, 35.0, 33.4, 26.1, 14.2.

HRMS (ESI $^+$) $[\text{M}+\text{H}]^+$ m/z calcd for $\text{C}_{19}\text{H}_{21}\text{O}_3^+$ 297.1485, $[\text{M}+\text{NH}_4]^+$ m/z calcd for $\text{C}_{19}\text{H}_{24}\text{NO}_3^+$ 314.1751, $[\text{M}+\text{Na}]^+$ m/z calcd for $\text{C}_{19}\text{H}_{20}\text{O}_3\text{Na}^+$ 319.1305; a solution in acetonitrile with 10 mM NH_4OAc found: 297.1482, 314.1747, 319.1298.



1-octyl-4-(trifluoromethyl)benzene (3.12) [CAS: 725251-79-6]

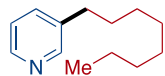
The general procedure for electron poor arenes was followed with 4-(trifluoromethyl)phenyl trifluoromethanesulfonate (58.8 mg, 0.20 mmol, 1.0 equiv) and 1-bromoocetane (38.6 mg, 0.20 mmol, 1.0 equiv) as substrates. After 18 h, the crude reaction mixture was loaded onto silica gel and purified by column chromatography (100% hexanes) to afford the product (31.9 mg, 62% yield) as a colorless oil. This procedure was repeated to establish its reproducibility and the second reaction provided the product (33.8 mg, 65% yield) in similar yield. Characterization data matched those reported in the literature.⁴⁶

¹H NMR (500 MHz, CDCl₃) δ 7.52 (d, *J* = 8.0 Hz, 2H), 7.28 (d, *J* = 8.0 Hz, 2H), 2.65 (t, *J* = 7.8 Hz, 2H), 1.62 (q, *J* = 7.4 Hz, 2H), 1.31 – 1.26 (m, 10H), 0.90 – 0.87 (m, 3H).

¹³C{¹H} NMR (126 MHz, CDCl₃) δ 147.0, 128.6, 128.0, 127.6, 125.1 (q, *J* = 3.7 Hz), 35.8, 31.8, 31.2, 29.4, 29.2, 29.2, 22.6, 14.0.

HRMS (ESI+) [M]⁺ m/z calcd for C₁₅H₂₁F₃⁺ 258.1590; ASAP-MS found: 258.1587.

IR (cm⁻¹) 2926, 2857, 1323, 1118, 1067, 1019.



3-octylpyridine (3.13) [CAS: 58069-37-7]

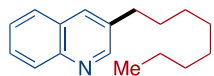
The general procedure for electron poor arenes was followed with 3-pyridinyl trifluoromethanesulfonate (45.4 mg, 0.20 mmol, 1.0 equiv) and 1-bromooctane (38.6 mg, 0.20 mmol, 1.0 equiv) as substrates. After 18 h, the crude reaction mixture was loaded onto silica gel and purified by column chromatography (20:1 pentane/Et₂O) to afford the product (37.2 mg, 97% yield) as a yellow oil. This procedure was repeated to establish its reproducibility and the second reaction provided the product (31.7 mg, 83% yield) in similar yield. Characterization data matched those reported in the literature.⁴⁷

¹H NMR (500 MHz, CDCl₃) δ 8.43 – 8.41 (m, 2H), 7.47 (dt, *J* = 7.8, 2.0 Hz, 1H), 7.18 (dd, *J* = 7.8, 4.8 Hz, 1H), 2.60 – 2.52 (m, 2H), 1.63 – 1.57 (m, 2H), 1.30 – 1.25 (m, 10H), 0.87 (t, *J* = 6.9 Hz, 3H).

¹³C{¹H} NMR (126 MHz, CDCl₃) δ 150.1, 147.3, 138.1, 135.9, 123.3, 33.1, 32.0, 31.3, 29.5, 29.3, 29.3, 22.8, 14.2.

HRMS (ESI+) [M+H]⁺ m/z calcd for C₁₅H₂₁N⁺ 192.1747; a solution in acetonitrile with 10 mM NH₄OAc found: 192.1748.

IR (cm⁻¹) 2955, 2924, 2854, 1422, 1026, 712.



3-octylquinoline (3.14)

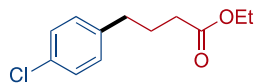
The general procedure for electron poor arenes was followed with 3-quinolinyl trifluoromethanesulfonate (55.4 mg, 0.20 mmol, 1.0 equiv) and 1-bromooctane (38.6 mg, 0.20 mmol, 1.0 equiv) as substrates. After 18 h, the crude reaction mixture was loaded onto silica gel and purified by column chromatography (gradient from 20:1 pentane/Et₂O to 10:1 pentane/Et₂O) to afford the product (13.6 mg, 28% yield) as a yellow oil. Characterization data matched those reported in the literature.⁴⁸

¹H NMR (500 MHz, CDCl₃) δ 8.78 (d, *J* = 2.2 Hz, 1H), 8.07 (d, *J* = 8.4 Hz, 1H), 7.91 (d, *J* = 2.1 Hz, 1H), 7.76 (dd, *J* = 8.1, 1.4 Hz, 1H), 7.65 (ddd, *J* = 8.4, 6.8, 1.5 Hz, 1H), 7.52 (ddd, *J* = 8.1, 6.8, 1.2 Hz, 1H), 2.79 (t, *J* = 7.7 Hz, 2H), 1.75 – 1.70 (m, 2H), 1.49 – 1.25 (m, 10H), 0.88 (t, *J* = 6.9 Hz, 3H).

¹³C{¹H} NMR (126 MHz, CDCl₃) δ 152.3, 146.9, 135.6, 134.2, 129.3, 128.6, 128.3, 127.4, 126.6, 33.4, 32.0, 31.3, 29.6, 29.4, 29.3, 22.8, 14.2.

HRMS (ESI⁺) [M+H]⁺ m/z calcd for C₁₇H₂₄N⁺ 242.1903; a solution in acetonitrile with 10 mM NH₄OAc found: 242.1898.

IR (cm⁻¹) 2924, 2853, 1495, 749.



Ethyl 4-(4-chlorophenyl)butanoate (3.15) [CAS: 3435-98-1]

The general procedure for electron rich arenes was followed with 4-chlorophenyl trifluoromethanesulfonate (52.1 mg, 0.20 mmol, 1.0 equiv) and ethyl 4-bromobutyrate (39.0 mg, 0.20 mmol, 1.0 equiv) as substrates. After 48 h, the crude reaction mixture was loaded onto silica gel and

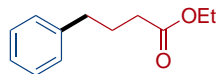
purified by column chromatography (50:1 pentane/EtOAc) to afford the product (17.0 mg, 37% yield) as a colorless oil. Characterization data matched those reported in the literature.⁴⁹

¹H NMR (500 MHz, CDCl₃) δ 7.26 – 7.24 (m, 2H), 7.12 – 7.10 (m, 2H), 4.12 (q, *J* = 7.1 Hz, 2H), 2.62 (t, *J* = 7.6 Hz, 2H), 2.30 (t, *J* = 7.5 Hz, 2H), 1.93 (quint, *J* = 7.5 Hz, 2H), 1.25 (t, *J* = 7.2 Hz, 3H).

¹³C{¹H} NMR (126 MHz, CDCl₃) δ 173.5, 140.0, 131.9, 130.0, 128.6, 60.5, 34.6, 33.7, 26.6, 14.4.

HRMS (ESI⁺) [M+H]⁺ m/z calcd for C₁₂H₁₆ClO₂⁺ 227.0833, [M+NH₄]⁺ m/z calcd for C₁₂H₁₉ClNO₂⁺ 244.1099, [M+Na]⁺ m/z calcd for C₁₂H₁₅ClO₂Na⁺ 249.0653; a solution in acetonitrile with 10 mM NH₄OAc found: 227.0828, 244.1094, 249.0647.

IR (cm⁻¹) 2980, 2935, 2870, 1730, 1492, 1246, 1092, 799.



Ethyl 4-phenylbutanoate (3.16) [CAS: 10031-93-3]

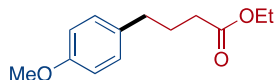
The general procedure for electron rich arenes was followed with phenyl trifluoromethanesulfonate (45.2 mg, 0.20 mmol, 1.0 equiv) and ethyl 4-bromobutyrate (39.0 mg, 0.20 mmol, 1.0 equiv) as substrates. After 48 h, the crude reaction mixture was loaded onto silica gel and purified by column chromatography (40:1 pentane/Et₂O) to afford the product (29.4 mg, 76% yield) as a colorless oil. This procedure was repeated to establish its reproducibility and the second reaction provided the product (29.9 mg, 78% yield) in similar yield. Characterization data matched those reported in the literature.⁵⁰

¹H NMR (400 MHz, CDCl₃) δ 7.31 – 7.27 (m, 2H), 7.21 – 7.17 (m, 3H), 4.13 (q, *J* = 7.2 Hz, 2H), 2.66 (t, *J* = 7.6 Hz, 2H), 2.32 (t, *J* = 7.5 Hz, 2H), 1.97 (quint, *J* = 7.6 Hz, 2H), 1.26 (t, *J* = 7.1 Hz, 3H).

¹³C{¹H} NMR (101 MHz, CDCl₃) δ 173.7, 141.6, 128.6, 128.5, 126.1, 60.4, 35.3, 33.8, 26.7, 14.4.

MS (EI) [M]⁺ m/z calcd for C₁₂H₁₆O₂⁺ 192.12; a solution in ethyl acetate found: 192.10.

IR (cm⁻¹) 2932, 1732, 1200, 700.



Ethyl 4-(4-methoxyphenyl)butanoate (3.7) [CAS: 4586-89-4]

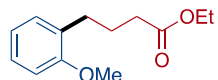
The general procedure for electron rich arenes was followed with 4-methoxyphenyl trifluoromethanesulfonate (51.2 mg, 0.20 mmol, 1.0 equiv) and ethyl 4-bromobutyrate (39.0 mg, 0.20 mmol, 1.0 equiv) as substrates. After 48 h, the crude reaction mixture was loaded onto silica gel and purified by column chromatography (gradient from 100% pentane to 40:1 pentane/Et₂O) to afford the product (28.9 mg, 65% yield) as a colorless oil. This procedure was repeated to establish its reproducibility and the second reaction provided the product (30.8 mg, 69% yield) in similar yield. Characterization data matched those reported in the literature.⁴

¹H NMR (500 MHz, CDCl₃) δ 7.09 (d, *J* = 8.4 Hz, 2H), 6.83 (d, *J* = 8.2 Hz, 2H), 4.12 (q, *J* = 7.1 Hz, 2H), 3.79 (s, 3H), 2.59 (t, *J* = 7.6 Hz, 2H), 2.30 (t, *J* = 7.5 Hz, 2H), 1.92 (quint, *J* = 7.5 Hz, 2H), 1.25 (t, *J* = 7.1 Hz, 3H).

¹³C{¹H} NMR (126 MHz, CDCl₃) δ 173.7, 158.0, 133.7, 129.5, 113.9, 60.4, 55.4, 34.4, 33.8, 26.9, 14.4.

MS (EI) [M]⁺ m/z calcd for C₁₃H₁₈O₃⁺ 222.13; a solution in ethyl acetate found: 222.10.

IR (cm⁻¹) 2936, 1732, 1512, 1246, 1177, 1038, 737.



Ethyl 4-(2-methoxyphenyl)butanoate (3.17) [CAS: 33209-76-6]

The general procedure for electron rich arenes was followed with 2-methoxyphenyl trifluoromethanesulfonate (51.2 mg, 0.20 mmol, 1.0 equiv) and ethyl 4-bromobutyrate (39.0 mg, 0.20 mmol, 1.0 equiv) as substrates. After 48 h, the crude reaction mixture was loaded onto silica gel and

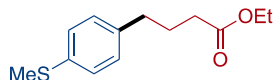
purified by column chromatography (20:1 pentane/Et₂O) to afford the product (26.8 mg, 60% yield) as a colorless oil. This procedure was repeated to establish its reproducibility and the second reaction provided the product (27.2 mg, 61% yield) in similar yield. Characterization data matched those reported in the literature.⁵¹

¹H NMR (500 MHz, CDCl₃) δ 7.18 (td, *J* = 7.8, 1.8 Hz, 1H), 7.12 (dd, *J* = 7.3, 1.7 Hz, 1H), 6.88 (td, *J* = 7.4, 1.1 Hz, 1H), 6.84 (dd, *J* = 8.1, 1.1 Hz, 1H), 4.12 (q, *J* = 7.1 Hz, 2H), 3.81 (s, 3H), 2.67 – 2.64 (m, 2H), 2.32 (t, *J* = 7.6 Hz, 2H), 1.92 (quint, *J* = 7.6 Hz, 2H), 1.25 (t, *J* = 7.2 Hz, 3H).

¹³C{¹H} NMR (126 MHz, CDCl₃) δ 173.9, 157.6, 130.2, 130.0, 127.3, 120.5, 110.4, 60.3, 55.3, 34.1, 29.7, 25.2, 14.4.

HRMS (ESI⁺) [M+H]⁺ m/z calcd for C₁₃H₁₉O₃⁺ 223.1329, [M+NH₄]⁺ m/z calcd for C₁₃H₂₂NO₃⁺ 240.1594, [M+Na]⁺ m/z calcd for C₁₃H₁₈O₃Na⁺ 245.1148; a solution in acetonitrile with 10 mM NH₄OAc found: 223.1327, 240.1591, 245.1145.

IR (cm⁻¹) 2938, 2836, 1730, 1494, 1241, 1031, 751.



Ethyl 4-(4-(methylthio)phenyl)butanoate (3.18)

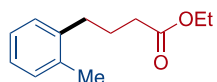
The general procedure for electron rich arenes was followed with 4-methylthiophenyl trifluoromethanesulfonate (54.5 mg, 0.20 mmol, 1.0 equiv) and ethyl 4-bromobutyrate (39.0 mg, 0.20 mmol, 1.0 equiv) as substrates. After 48 h, the crude reaction mixture was loaded onto silica gel and purified by column chromatography (gradient from 100% pentane to 40:1 pentane/Et₂O) to afford the product (28.9 mg, 65% yield) as a colorless oil. This procedure was repeated to establish its reproducibility and the second reaction provided the product (30.8 mg, 69% yield) in similar yield. Characterization data matched those reported in the literature.⁵²

¹H NMR (500 MHz, CDCl₃) δ 7.21 – 7.19 (m, 2H), 7.10 (d, *J* = 8.2 Hz, 2H), 4.13 (q, *J* = 7.1 Hz, 2H), 2.61 (t, *J* = 7.6 Hz, 2H), 2.47 (s, 3H), 2.30 (t, *J* = 7.4 Hz, 2H), 1.93 (quint, *J* = 7.5 Hz, 2H), 1.25 (t, *J* = 7.1 Hz, 3H).

¹³C{¹H} NMR (126 MHz, CDCl₃) δ 173.6, 138.7, 135.7, 129.2, 127.3, 60.4, 34.7, 33.7, 26.6, 16.5, 14.4.

MS (EI) [M]⁺ m/z calcd for C₁₃H₁₈O₂S⁺ 238.10; a solution in ethyl acetate found: 238.10.

IR (cm⁻¹) 2924, 2880, 1732, 1512, 1390, 1204, 1146, 737.



Ethyl 4-(*o*-tolyl)butanoate (3.19) [CAS: 105986-51-4]

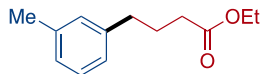
The general procedure for electron rich arenes was followed with *o*-tolyl trifluoromethanesulfonate (48.0 mg, 0.20 mmol, 1.0 equiv) and ethyl 4-bromobutyrate (39.0 mg, 0.20 mmol, 1.0 equiv) as substrates. After 48 h, the crude reaction mixture was loaded onto silica gel and purified by column chromatography (40:1 hexanes/Et₂O) to afford the product (21.3 mg, 52% yield) as a colorless oil. This procedure was repeated to establish its reproducibility and the second reaction provided the product (20.6 mg, 50% yield) in similar yield. Characterization data matched those reported in the literature.⁵¹

¹H NMR (500 MHz, CDCl₃) δ 7.16 – 7.10 (m, 4H), 4.14 (q, *J* = 7.1 Hz, 2H), 2.66 – 2.63 (m, 2H), 2.37 (t, *J* = 7.4 Hz, 2H), 2.32 (s, 3H), 1.92 (quint, *J* = 7.5 Hz, 2H), 1.27 (t, *J* = 7.1 Hz, 3H).

¹³C{¹H} NMR (126 MHz, CDCl₃) δ 173.6, 139.8, 136.1, 130.4, 129.1, 126.2, 126.1, 60.4, 34.1, 32.7, 25.5, 19.3, 14.4.

HRMS (ESI⁺) [M+Na]⁺ m/z calcd for C₁₃H₁₈O₂Na⁺ 229.1199; a solution in acetonitrile with 10 mM NH₄OAc found: 229.1199.

IR (cm⁻¹) 2937, 2870, 1731, 1247, 1147, 732.



Ethyl 4-(*m*-tolyl)butanoate (3.20)

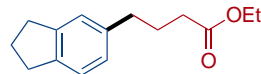
The general procedure for electron rich arenes was followed with *m*-tolyl trifluoromethanesulfonate (48.0 mg, 0.20 mmol, 1.0 equiv) and ethyl 4-bromobutyrate (39.0 mg, 0.20 mmol, 1.0 equiv) as substrates. After 48 h, the crude reaction mixture was loaded onto silica gel and purified by column chromatography (40:1 hexanes/Et₂O) to afford the product (25.8 mg, 63% yield) as a colorless oil. This procedure was repeated to establish its reproducibility and the second reaction provided the product (27.2 mg, 61% yield) in similar yield. Characterization data matched those reported in the literature.⁵¹

¹H NMR (500 MHz, CDCl₃) δ 7.19 – 7.16 (m, 1H), 7.02 – 6.97 (m, 3H), 4.13 (q, *J* = 7.1 Hz, 2H), 2.63 – 2.60 (m, 2H), 2.33 – 2.30 (m, 5H), 1.95 (quint, *J* = 7.6 Hz, 2H), 1.26 (t, *J* = 7.1 Hz, 3H).

¹³C{¹H} NMR (126 MHz, CDCl₃) δ 173.7, 141.5, 138.1, 129.5, 128.4, 126.8, 125.6, 60.4, 35.2, 33.9, 26.7, 21.5, 14.4.

HRMS (ESI⁺) [M+H]⁺ m/z calcd for C₁₃H₁₉O₂⁺ 207.1380, [M+NH₄]⁺ m/z calcd for C₁₃H₂₂NO₂⁺ 224.1645, [M+Na]⁺ m/z calcd for C₁₃H₁₈O₂Na⁺ 229.1200; a solution in acetonitrile with 10 mM NH₄OAc found: 207.1379, 224.1644, 229.1198.

IR (cm⁻¹) 2981, 2930, 2868, 1732, 1027, 699.



Ethyl 4-(2,3-dihydro-1*H*-inden-5-yl)butanoate (3.21) [CAS: 34704-33-1]

The general procedure for electron rich arenes was followed with 2,3-dihydro-1*H*-inden-5-yl trifluoromethanesulfonate (53.2 mg, 0.20 mmol, 1.0 equiv) and ethyl 4-bromobutyrate (39.0 mg, 0.20

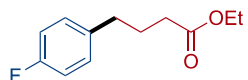
mmol, 1.0 equiv) as substrates. After 48 h, the crude reaction mixture was loaded onto silica gel and purified by column chromatography (40:1 hexanes/Et₂O) to afford the product (29.9 mg, 64% yield) as a colorless oil. This procedure was repeated to establish its reproducibility and the second reaction provided the product (25.6 mg, 55% yield) in similar yield.

¹H NMR (500 MHz, CDCl₃) δ 7.15 (d, *J* = 7.6 Hz, 1H), 7.06 (s, 1H), 6.96 (dd, *J* = 7.6, 1.6 Hz, 1H), 4.14 (q, *J* = 7.1 Hz, 2H), 2.88 (td, *J* = 7.4, 4.2 Hz, 4H), 2.62 (t, *J* = 7.6 Hz, 2H), 2.33 (t, *J* = 7.5 Hz, 2H), 2.07 (quint, *J* = 7.5 Hz, 2H), 1.95 (quint, *J* = 7.5 Hz, 2H), 1.26 (t, *J* = 7.1 Hz, 3H).

¹³C{¹H} NMR (126 MHz, CDCl₃) δ 173.7, 144.6, 141.9, 139.4, 126.4, 124.6, 124.3, 60.3, 35.1, 33.9, 32.9, 32.6, 27.0, 25.7, 14.4.

HRMS (ESI⁺) [M+H]⁺ m/z calcd for C₁₅H₂₁O₂⁺ 233.1536, [M+NH₄]⁺ m/z calcd for C₁₅H₂₄NO₂⁺ 250.1802, [M+Na]⁺ m/z calcd for C₁₅H₂₀O₂Na⁺ 255.1356; a solution in acetonitrile with 10 mM NH₄OAc found: 233.1534, 250.1800, 255.1352.

IR (cm⁻¹) 2941, 2846, 1731, 1144, 909, 729.



Ethyl 4-(4-fluorophenyl)butanoate (3.22) [CAS: 1693-05-6]

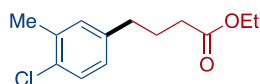
The general procedure for electron rich arenes was followed with 4-fluorophenyl trifluoromethanesulfonate (48.8 mg, 0.20 mmol, 1.0 equiv) and ethyl 4-bromobutyrate (39.0 mg, 0.20 mmol, 1.0 equiv) as substrates. After 48 h, the crude reaction mixture was loaded onto silica gel and purified by column chromatography (gradient from 100% pentane to 40:1 pentane/Et₂O) to afford the product (30.6 mg, 73% yield) as a colorless oil. This procedure was repeated to establish its reproducibility and the second reaction provided the product (27.5 mg, 65% yield) in similar yield. Characterization data matched those reported in the literature.⁵¹

¹H NMR (500 MHz, CDCl₃) δ 7.13 (dd, *J* = 8.4, 5.4 Hz, 2H), 6.96 (dd, *J* = 10.0, 7.4 Hz, 2H), 4.12 (q, *J* = 7.1 Hz, 2H), 2.62 (t, *J* = 7.6 Hz, 2H), 2.30 (t, *J* = 7.4 Hz, 2H), 1.93 (quint, *J* = 7.5 Hz, 2H), 1.25 (t, *J* = 7.1 Hz, 3H).

¹³C{¹H} NMR (126 MHz, CDCl₃) δ 173.5, 161.4 (d, *J* = 243.3 Hz), 137.2 (d, *J* = 3.4 Hz), 129.9 (d, *J* = 7.6 Hz), 115.2 (d, *J* = 21.2 Hz), 60.4, 34.4, 33.7, 26.8, 14.4.

MS (EI) [M]⁺ m/z calcd for C₁₂H₁₅FO₂⁺ 210.10; a solution in ethyl acetate found: 210.10.

IR (cm⁻¹) 2982, 2936, 2866, 1732, 1508, 1219, 1146, 737.



Ethyl 4-(4-chloro-3-methylphenyl)butanoate (3.23)

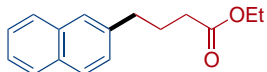
The general procedure for electron rich arenes was followed with 4-chloro-3-methylphenyl trifluoromethanesulfonate (54.9 mg, 0.20 mmol, 1.0 equiv) and ethyl 4-bromobutyrate (39.0 mg, 0.20 mmol, 1.0 equiv) as substrates. After 48 h, the crude reaction mixture was loaded onto silica gel and purified by column chromatography (40:1 pentane/Et₂O) to afford the product (23.9 mg, 50% yield) as a colorless oil. This procedure was repeated to establish its reproducibility and the second reaction provided the product (23.9 mg, 50% yield) in similar yield.

¹H NMR (500 MHz, CDCl₃) δ 7.16 (d, *J* = 1.7 Hz, 1H), 7.13 (d, *J* = 7.8 Hz, 1H), 6.96 (dd, *J* = 7.6, 1.8 Hz, 1H), 4.13 (q, *J* = 7.1 Hz, 2H), 2.59 (t, *J* = 7.6 Hz, 2H), 2.33 (s, 3H), 2.30 (t, *J* = 7.5 Hz, 2H), 1.93 (quint, *J* = 7.5 Hz, 2H), 1.26 (t, *J* = 7.1 Hz, 3H).

¹³C{¹H} NMR (126 MHz, CDCl₃) δ 173.5, 140.8, 134.3, 133.6, 131.0, 129.1, 126.9, 60.5, 34.5, 33.7, 26.5, 19.7, 14.4.

HRMS (ESI⁺) [M+Na]⁺ m/z calcd for C₁₃H₁₇ClO₂⁺ 263.0809; a solution in acetonitrile with 10 mM NH₄OAc found: 263.0808.

IR (cm⁻¹) 2980, 2932, 2864, 1731, 1497, 1147, 1051, 819.



Ethyl 4-(naphthalen-2-yl)butanoate (3.24) [CAS: 6326-90-5]

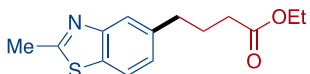
The general procedure for electron rich arenes was followed with naphthalen-2-yl trifluoromethanesulfonate (55.2 mg, 0.20 mmol, 1.0 equiv) and ethyl 4-bromobutyrate (39.0 mg, 0.20 mmol, 1.0 equiv) as substrates. After 48 h, the crude reaction mixture was loaded onto silica gel and purified by column chromatography (20:1 pentane/Et₂O) to afford the product (29.8 mg, 61% yield) as a colorless oil. This procedure was repeated to establish its reproducibility and the second reaction provided the product (32.2 mg, 66% yield) in similar yield. Characterization data matched those reported in the literature.⁵¹

¹H NMR (500 MHz, CDCl₃) δ 7.80 (dd, *J* = 14.3, 7.7 Hz, 3H), 7.63 (s, 1H), 7.44 (dd, *J* = 14.5, 8.2, 6.9, 1.5 Hz, 2H), 7.34 (dd, *J* = 8.4, 1.7 Hz, 1H), 4.13 (q, *J* = 7.1 Hz, 2H), 2.83 (t, *J* = 7.6 Hz, 2H), 2.36 (t, *J* = 7.5 Hz, 2H), 2.06 (quint, *J* = 7.5, 7.1 Hz, 2H), 1.26 (t, *J* = 7.1 Hz, 3H).

¹³C{¹H} NMR (126 MHz, CDCl₃) δ 173.6, 139.1, 133.7, 132.2, 128.1, 127.7, 127.6, 127.4, 126.7, 126.1, 125.3, 60.4, 35.4, 33.8, 26.5, 14.4.

MS (EI) [M]⁺ m/z calcd for C₁₆H₁₈O₂⁺ 242.13; a solution in ethyl acetate found: 242.15.

IR (cm⁻¹) 3055, 2982, 2936, 1728, 1373, 1265, 733.



Ethyl 4-(2-methylbenzo[d]thiazol-5-yl)butanoate (3.25)

The general procedure for electron rich arenes was followed with 2-methylbenzo[d]thiazol-5-yl trifluoromethanesulfonate (59.5 mg, 0.20 mmol, 1.0 equiv) and ethyl 4-bromobutyrate (39.0 mg, 0.20

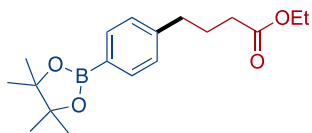
mmol, 1.0 equiv) as substrates. After 48 h, the crude reaction mixture was loaded onto silica gel and purified by column chromatography (gradient from 20:1 pentane/EtOAc to 5:1) to afford the product (27.9 mg, 53% yield) as a yellow oil.

¹H NMR (500 MHz, CDCl₃) δ 7.75 (d, *J* = 1.5 Hz, 1H), 7.72 (d, *J* = 8.1 Hz, 1H), 7.18 (dd, *J* = 8.1, 1.6 Hz, 1H), 4.12 (q, *J* = 7.1 Hz, 2H), 2.82 (s, 3H), 2.81 (t, *J* = 7.6 Hz, 2H), 2.33 (t, *J* = 7.4 Hz, 2H), 2.01 (quint, *J* = 7.5 Hz, 2H), 1.25 (t, *J* = 7.1 Hz, 3H).

¹³C{¹H} NMR (126 MHz, CDCl₃) δ 173.6, 167.4, 153.9, 139.8, 133.3, 125.8, 122.1, 121.3, 60.4, 35.2, 33.7, 26.9, 20.3, 14.4.

HRMS (ESI⁺) [M+H]⁺ m/z calcd for C₁₄H₁₈NO₂S⁺ 264.1053; a solution in acetonitrile with 10 mM NH₄OAc found: 264.1048.

IR (cm⁻¹) 2980, 2933, 2868, 1729, 1552, 1246, 1172, 1026, 813.



Ethyl 4-(4-(4,4,5,5-tetramethyl-1,3,2-dioxaborolan-2-yl)phenyl)butanoate (3.26) [CAS: 1365610-75-8]

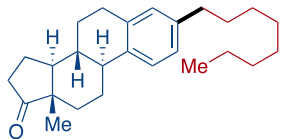
The general procedure for electron rich arenes was followed with 4-(4,4,5,5-tetramethyl-1,3,2-dioxaborolan-2-yl)phenyl trifluoromethanesulfonate (70.4 mg, 0.20 mmol, 1.0 equiv) and ethyl 4-bromobutyrate (39.0 mg, 0.20 mmol, 1.0 equiv) as substrates. After 48 h, the crude reaction mixture was loaded onto silica gel and purified by column chromatography (40:1 pentane/EtOAc) to afford the product (42.6 mg, 67% yield) as a colorless oil. Characterization data matched those reported in the literature.⁴

¹H NMR (500 MHz, CDCl₃) δ 7.74 – 7.73 (m, 2H), 7.19 (d, *J* = 7.5 Hz, 2H), 4.12 (q, *J* = 7.1 Hz, 2H), 2.66 (t, *J* = 7.6 Hz, 2H), 2.30 (t, *J* = 7.5 Hz, 2H), 1.98 – 1.92 (m, 2H), 1.33 (s, 12H), 1.25 (t, *J* = 7.2 Hz, 3H).

¹³C{¹H} NMR (126 MHz, CDCl₃) δ 173.6, 145.0, 135.1, 128.1, 83.8, 60.4, 35.4, 33.8, 26.5, 25.0, 14.4.

HRMS (ESI⁺) [M+H]⁺ *m/z* calcd for C₁₈H₂₈BO₄⁺ 319.2075, [M+NH₄]⁺ *m/z* calcd for C₁₈H₃₁BNO₄⁺ 336.2341, [M+Na]⁺ *m/z* calcd for C₁₈H₂₇BO₄Na⁺ 341.1895; a solution in acetonitrile with 10 mM NH₄OAc found: 319.2067, 336.2337, 341.883.

IR (cm⁻¹) 2979, 1732, 1612, 1358, 1214, 1142, 1089, 859.



(8*R*,9*S*,13*S*,14*S*)-13-methyl-3-octyl-6,7,8,9,11,12,13,14,15,16-decahydro-17*H*-cyclopenta[*a*]phenanthren-17-one (3.27)

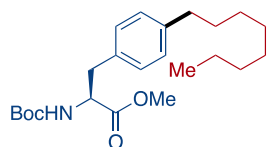
The general procedure for electron rich arenes was followed with (8*R*,9*S*,13*S*,14*S*)-13-methyl-17-oxo-7,8,9,11,12,13,14,15,16,17-decahydro-6*H*-cyclopenta[*a*]phenanthren-3-yl trifluoromethanesulfonate [estrone trifluoromethanesulfonate] (80.5 mg, 0.20 mmol, 1.0 equiv) and 1-bromo octane (38.6 mg, 0.20 mmol, 1.0 equiv) as substrates. After 48 h, the crude reaction mixture was loaded onto silica gel and purified by column chromatography (gradient from 40:1 pentane/Et₂O to 20:1 pentane/Et₂O) to afford the product (53.8 mg, 73% yield) as a colorless oil. This procedure was repeated to establish its reproducibility and the second reaction provided the product (50.7 mg, 69% yield) in similar yield.

¹H NMR (500 MHz, CDCl₃) δ 7.23 (d, *J* = 7.9 Hz, 1H), 7.01 (dd, *J* = 8.0, 1.9 Hz, 1H), 6.95 (d, *J* = 1.8 Hz, 1H), 3.03 – 2.83 (m, 2H), 2.60 – 2.49 (m, 3H), 2.48 – 2.41 (m, 1H), 2.32 (td, *J* = 11.0, 4.0 Hz, 1H), 2.22 – 1.92 (m, 4H), 1.71 – 1.41 (m, 8H), 1.41 – 1.22 (m, 10H), 0.94 (s, 3H), 0.91 (t, *J* = 7.1 Hz, 3H).

$^{13}\text{C}\{\text{H}\}$ NMR (126 MHz, CDCl_3) δ 220.9, 140.4, 136.9, 136.2, 129.0, 125.8, 125.2, 50.5, 48.0, 44.3, 38.2, 35.8, 35.4, 31.9, 31.6, 31.5, 29.5, 29.4, 29.2, 26.6, 25.7, 22.6, 21.6, 14.1, 13.8.

HRMS (ESI+) $[\text{M}+\text{H}]^+$ m/z calcd for $\text{C}_{26}\text{H}_{39}\text{O}^+$ 367.2995; ASAP-MS found: 367.2995.

IR (cm^{-1}) 2923, 2853, 1737, 1612, 1500, 821.



(S)-2-((tert-butoxycarbonyl)amino)-3-(4-octylphenyl)propanoic acid (3.28)

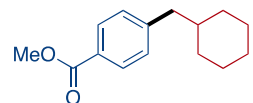
The general procedure for electron rich arenes was followed with (S)-2-((tert-butoxycarbonyl)amino)-3-((trifluoromethyl)sulfonyl)oxyphenylpropanoic acid [L-tyrosine trifluoromethanesulfonate] (85.5 mg, 0.20 mmol, 1.0 equiv) and 1-bromoocetane (38.6 mg, 0.20 mmol, 1.0 equiv) as substrates. After 48 h, the crude reaction mixture was loaded onto silica gel and purified by column chromatography (gradient from 20:1 pentane/EtOAc to 10:1 pentane/EtOAc) to afford the product (30.2 mg, 39% yield) as a colorless oil in 39% ee based on chiral SFC-MS. This procedure was repeated to establish its reproducibility and the second reaction provided the product (43.0 mg, 55% yield) in similar yield.

^1H NMR (500 MHz, CDCl_3) δ 7.10 (d, $J = 8.0$ Hz, 2H), 7.02 (d, $J = 7.8$ Hz, 2H), 4.95 (d, $J = 8.4$ Hz, 1H), 4.56 (q, $J = 6.6$ Hz, 1H), 3.71 (s, 3H), 3.04 (qd, $J = 13.9, 6.0$ Hz, 2H), 2.56 (dd, $J = 8.8, 6.7$ Hz, 2H), 1.61 – 1.57 (m, 3H), 1.41 (s, 9H), 1.32 – 1.21 (m, 10H), 0.88 (t, $J = 6.9$ Hz, 3H). Note: Minor rotameric peaks are present in the ^1H , but only peaks from the major compound are reported.

$^{13}\text{C}\{\text{H}\}$ NMR (126 MHz, CDCl_3) δ 172.6, 155.3, 141.8, 133.2, 129.3, 128.7, 80.0, 61.4, 54.6, 52.3, 38.1, 35.7, 32.0, 31.6, 29.6, 29.5, 29.4, 28.4, 22.8, 14.2.

HRMS (ESI⁺) [M+H]⁺ m/z calcd for C₂₃H₃₈NO₄⁺ 392.2795, [M+Na]⁺ m/z calcd for C₂₃H₃₇NO₄Na⁺ 414.2615; a solution in acetonitrile with 10 mM NH₄OAc found: 392.2791, 414.2611.

IR (cm⁻¹) 3347, 2952, 2917, 2849, 1736, 1690, 1527, 1164, 1061, 831.



Methyl 4-(cyclohexylmethyl)benzoate (3.29)

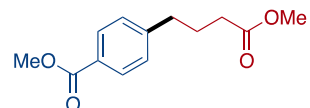
The general procedure for electron poor arenes was followed with methyl 4-(((trifluoromethyl)sulfonyl)oxy)benzoate (56.8 mg, 0.20 mmol, 1.0 equiv) and (bromomethyl)cyclohexane (27.9 μ L, 0.20 mmol, 1.0 equiv) as substrates. The alkyl bromide was sparged with nitrogen for 10 min prior to being added outside the glovebox by syringe. After 18 h, the crude reaction mixture was loaded onto silica gel and purified by column chromatography (100:1 pentane/EtOAc) to afford the product (22.7 mg, 49% yield) as a colorless oil. Characterization data matched those reported in the literature.⁵³

¹H NMR (500 MHz, CDCl₃) δ 7.95 – 7.93 (m, 2H), 7.21 – 7.19 (m, 2H), 3.90 (s, 3H), 2.53 (d, *J* = 7.1 Hz, 2H), 1.71 – 1.62 (m, 5H), 1.32 – 1.12 (m, 4H), 0.98 – 0.93 (m, 2H).

¹³C{¹H} NMR (126 MHz, CDCl₃) δ 167.4, 147.2, 129.6, 129.3, 127.8, 52.1, 44.3, 39.8, 33.2, 26.6, 26.4.

HRMS (ESI⁺) [M+NH₄]⁺ m/z calcd for C₁₅H₂₄NO₂⁺ 250.1802, [M+Na]⁺ m/z calcd for C₁₅H₂₀O₂Na⁺ 255.1356; a solution in acetonitrile with 10 mM NH₄OAc found: 250.1800, 255.1353.

IR (cm⁻¹) 2922, 2850, 1719, 1274, 1177, 1109, 102, 757.



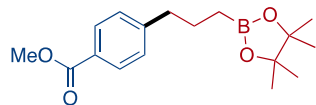
Methyl 4-(4-methoxy-4-oxobutyl)benzoate (3.30)

The general procedure for electron poor arenes was followed with 4-carbomethoxyphenyl triflate (142.1 mg, 0.50 mmol, 1.0 equiv) and methyl 4-bromobutyrate (90.5 mg, 0.50 mmol, 1.0 equiv) as substrates. After 24 h, the crude reaction mixture was loaded onto silica gel and purified by column chromatography (gradient from 100 hexanes to 100 dichloromethane) to afford the product (76.7 mg, 65% yield) as a colorless oil. Characterization data matched those reported in the literature.⁵⁴

¹H NMR (500 MHz, CDCl₃) δ 7.91 – 7.86 (m, 2H), 7.17 (d, *J* = 8.0 Hz, 2H), 3.83 (s, 3H), 3.59 (s, 3H), 2.63 (t, *J* = 7.7 Hz, 2H), 2.26 (t, *J* = 7.4 Hz, 2H), 1.90 (quint, *J* = 7.5 Hz, 2H).

¹³C{¹H} NMR (126 MHz, CDCl₃) δ 173.7, 167.1, 146.9, 129.8, 128.5, 128.1, 52.0, 51.6, 35.1, 33.3, 26.1.

IR (cm⁻¹) 2943, 1712, 1605, 1431, 1271, 1173, 1101, 760, 702.



Methyl 4-(3-(4,4,5,5-tetramethyl-1,3,2-dioxaborolan-2-yl)propyl)benzoate (3.31)

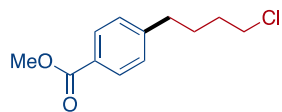
The general procedure for electron poor arenes was followed with methyl 4-(((trifluoromethyl)sulfonyl)oxy)benzoate (56.8 mg, 0.20 mmol, 1.0 equiv) and 2-(3-bromopropyl)-4,4,5,5-tetramethyl-1,3,2-dioxaborolane (42.3 μL, 0.20 mmol, 1.0 equiv) as substrates. The alkyl bromide was sparged with nitrogen for 10 min prior to being added outside the glovebox by syringe. After 18 h, the crude reaction mixture was loaded onto silica gel and purified by column chromatography (gradient from 40:1 pentane/EtOAc to 20:1 pentane/EtOAc) to afford the product (28.0 mg, 46% yield) as a colorless oil. ¹H NMR matched those reported in the literature,⁵⁵ however, the reported ¹³C NMR has 9 signals.

¹H NMR (500 MHz, CDCl₃) δ 7.93 (d, *J* = 8.3 Hz, 2H), 7.23 (d, *J* = 8.2 Hz, 2H), 3.89 (s, 3H), 2.67 – 2.64 (m, 2H), 1.74 (quint, *J* = 7.7 Hz, 2H), 1.24 (s, 12H), 0.82 (t, *J* = 7.9 Hz, 2H).

$^{13}\text{C}\{\text{H}\}$ NMR (126 MHz, CDCl_3) δ 167.4, 148.4, 129.7, 128.7, 127.7, 83.2, 52.1, 38.7, 25.9, 25.0.

HRMS (ESI $^+$) $[\text{M}+\text{H}]^+$ m/z calcd for $\text{C}_{17}\text{H}_{26}\text{BO}_4^+$ 305.1919, $[\text{M}+\text{NH}_4]^+$ m/z calcd for $\text{C}_{17}\text{H}_{29}\text{BO}_4\text{N}^+$ 322.2184, $[\text{M}+\text{Na}]^+$ m/z calcd for $\text{C}_{17}\text{H}_{25}\text{BO}_4\text{Na}^+$ 327.1738; a solution in acetonitrile with 10 mM NH_4OAc found: 305.1911, 322.2180, 327.1732.

IR (cm^{-1}) 2977, 2935, 1720, 1610, 1273, 1144, 1108, 967.



Methyl 4-(4-chlorobutyl)benzoate (3.32)

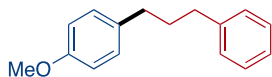
The general procedure for electron poor arenes was followed with methyl 4-((trifluoromethyl)sulfonyloxy)benzoate (56.8 mg, 0.20 mmol, 1.0 equiv) and 1-bromo-4-chlorobutane (23.0 μL , 0.20 mmol, 1.0 equiv) as substrates. The alkyl bromide was sparged with nitrogen for 10 min prior to being added outside the glovebox by syringe. After 18 h, the crude reaction mixture was loaded onto silica gel and purified by column chromatography (40:1 pentane/EtOAc) to afford the product (21.8 mg, 48% yield) as a colorless oil. Characterization data matched those reported in the literature.⁵⁶

^1H NMR (500 MHz, CDCl_3) δ 7.97 – 7.95 (m, 2H), 7.25 (d, $J = 8.2$ Hz, 2H), 3.90 (s, 3H), 3.56 – 3.54 (m, 2H), 2.71 – 2.68 (m, 2H), 1.81 – 1.79 (m, 4H).

$^{13}\text{C}\{\text{H}\}$ NMR (126 MHz, CDCl_3) δ 167.2, 147.5, 129.9, 128.6, 128.1, 52.1, 44.9, 35.3, 32.1, 28.3.

HRMS (ESI $^+$) $[\text{M}+\text{H}]^+$ m/z calcd for $\text{C}_{12}\text{H}_{16}\text{ClO}_2^+$ 227.0833, $[\text{M}+\text{NH}_4]^+$ m/z calcd for $\text{C}_{12}\text{H}_{19}\text{ClO}_2\text{N}^+$ 244.1099, $[\text{M}+\text{Na}]^+$ m/z calcd for $\text{C}_{12}\text{H}_{15}\text{ClO}_2\text{Na}^+$ 249.0653; a solution in acetonitrile with 10 mM NH_4OAc found: 227.0829, 244.1094, 249.0648.

IR (cm^{-1}) 2950, 2862, 1716, 1610, 1434, 1274, 1178, 1020, 762.



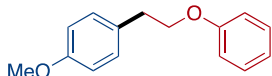
1-methoxy-4-(3-phenylpropyl)benzene (3.33) [CAS: 40715-68-2]

The general procedure for electron rich arenes was followed with 4-methoxyphenyl trifluoromethanesulfonate (51.2 mg, 0.20 mmol, 1.0 equiv) and (3-chloropropyl)benzene (30.9 mg, 0.20 mmol, 1.0 equiv) as substrates. After 48 h, the crude reaction mixture was loaded onto silica gel and purified by column chromatography (100:1 pentane/EtOAc) to afford the product (37.0 mg, 82% yield) as a colorless oil. Characterization data matched those reported in the literature.⁴

¹H NMR (500 MHz, CDCl₃) δ 7.30 – 7.27 (m, 2H), 7.20 – 7.17 (m, 3H), 7.12 – 7.09 (m, 2H), 6.85 – 6.82 (m, 2H), 3.80 (s, 3H), 2.65 (t, *J* = 7.7 Hz, 2H), 2.60 (t, *J* = 7.5 Hz, 2H), 1.97 – 1.91 (m, 2H).
¹³C{¹H} NMR (126 MHz, CDCl₃) δ 157.9, 142.5, 134.5, 129.4, 128.6, 128.4, 125.8, 113.9, 55.4, 35.5, 34.7, 33.3.

HRMS (ESI+) [M+H]⁺ m/z calcd for C₁₆H₁₈O⁺ 227.1430; ASAP-MS found: 227.1429.

IR (cm⁻¹) 3026, 2934, 2856, 1611, 1511, 1243, 1036, 698.



1-methoxy-4-(2-phenoxyethyl)benzene (3.34) [CAS: 127294-20-6]

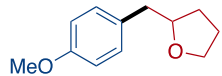
The general procedure for electron rich arenes was followed with 4-methoxyphenyl trifluoromethanesulfonate (51.2 mg, 0.20 mmol, 1.0 equiv) and (2-chloroethoxy)benzene (31.3 mg, 0.20 mmol, 1.0 equiv) as substrates. After 48 h, the crude reaction mixture was loaded onto silica gel and purified by column chromatography (gradient from 100% pentane to 50:1 pentane/Et₂O) to afford the product (21.0 mg, 46% yield) as a colorless oil. Characterization data matched those reported in the literature.⁴

¹H NMR (500 MHz, CDCl₃) δ 7.30 – 7.26 (m, 2H), 7.23 – 7.20 (m, 2H), 6.94 (tt, *J* = 7.4, 1.1 Hz, 1H), 6.92 – 6.89 (m, 2H), 6.88 – 6.85 (m, 2H), 4.14 (t, *J* = 7.1 Hz, 2H), 3.80 (s, 3H), 3.05 (t, *J* = 7.2 Hz, 2H).

¹³C{¹H} NMR (126 MHz, CDCl₃) δ 159.0, 158.4, 130.4, 130.1, 129.6, 120.8, 114.7, 114.1, 69.0, 55.4, 35.1.

HRMS (ESI+) [M+H]⁺ m/z calcd for C₁₅H₁₇O₂⁺ 229.1223; ASAP-MS found: 229.1222.

IR (cm⁻¹) 3031, 2935, 2869, 2834, 1612, 1512, 1239, 1174, 1032, 752.



2-(4-methoxybenzyl)tetrahydrofuran (3.35) [CAS: 859999-32-9]

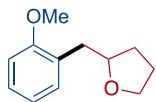
The general procedure for electron rich arenes was followed with 4-methoxyphenyl trifluoromethanesulfonate (51.2 mg, 0.20 mmol, 1.0 equiv) and 2-(chloromethyl)tetrahydrofuran (24.1 mg, 0.20 mmol, 1.0 equiv) as substrates. After 48 h, the crude reaction mixture was loaded onto silica gel and purified by column chromatography (gradient from 40:1 pentane/EtOAc to 10:1 pentane/EtOAc) to afford the product (30.1 mg, 78% yield) as a colorless oil. Characterization data matched those reported in the literature.⁴

¹H NMR (500 MHz, CDCl₃) δ 7.16 – 7.13 (m, 2H), 6.85 – 6.82 (m, 2H), 4.05 – 3.99 (m, 1H), 3.91 – 3.86 (m, 1H), 3.79 (s, 3H), 3.75 – 3.71 (m, 1H), 2.85 (dd, *J* = 13.7, 6.4 Hz, 1H), 2.69 (dd, *J* = 13.7, 6.5 Hz, 1H), 1.94 – 1.79 (m, 3H), 1.58 – 1.51 (m, 1H).

¹³C{¹H} NMR (126 MHz, CDCl₃) δ 158.2, 131.2, 130.3, 113.9, 80.4, 68.1, 55.4, 41.1, 31.0, 25.8.

HRMS (ESI+) [M+H]⁺ m/z calcd for C₁₂H₁₇O₂⁺ 193.1223; ASAP-MS found: 193.1222.

IR (cm⁻¹) 2934, 2860, 2835, 1612, 1512, 1244, 1059, 1034, 833.



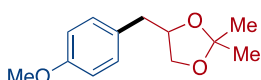
2-(2-methoxybenzyl)tetrahydrofuran (3.36)

The general procedure for preparative-scale benchtop reactions was followed using PyBCam^{CN} (43.7 mg, 0.21 mmol, 5 mol%) as a ligand and 2-methoxyphenyl trifluoromethanesulfonate (1.05 g, 4.10 mmol, 1.0 equiv) and 2-(chloromethyl)tetrahydrofuran (445 μ L, 4.10 mmol, 1.0 equiv) as substrates. After 48 h, the crude reaction mixture was extracted with Et₂O (3 \times 30 mL) and washed with brine (3 \times 100 mL). The resulting organic solution was dried over sodium sulfate, filtered, and concentrated to a slightly yellow oil. The oil was purified by column chromatography (gradient from 10:1 pentane/EtOAc to 8:1 pentane/EtOAc) to afford the product (385.2 mg, 49% yield) as a colorless oil. Characterization data matched those reported in the literature.⁵⁷

¹H NMR (500 MHz, CDCl₃) δ 7.22 (t, *J* = 7.1 Hz, 2H), 6.92 (td, *J* = 7.4, 1.1 Hz, 1H), 6.88 (dd, *J* = 8.6, 1.1 Hz, 1H), 4.17 (quint, *J* = 6.5 Hz, 1H), 3.99 – 3.89 (m, 1H), 3.84 (s, 3H), 3.77 (td, *J* = 7.8, 5.8 Hz, 1H), 2.96 (dd, *J* = 13.4, 6.4 Hz, 1H), 2.81 (dd, *J* = 13.4, 6.8 Hz, 1H), 2.00 – 1.80 (m, 3H), 1.67 – 1.54 (m, 1H).

¹³C{¹H} NMR (126 MHz, CDCl₃) δ 157.5, 130.8, 127.4, 127.4, 120.4, 110.2, 78.7, 67.8, 55.2, 36.1, 31.0, 25.6.

HRMS (ESI⁺) [M+H]⁺ m/z calcd for C₁₂H₁₇O₂⁺ 193.1223, [M+Na]⁺ m/z calcd for C₁₂H₁₆O₂Na⁺ 215.1043; a solution in acetonitrile with 10 mM NH₄OAc found: 193.1224, 215.1041.



4-(4-methoxybenzyl)-2,2-dimethyl-1,3-dioxolane (3.37)

The general procedure for electron rich arenes was followed with 4-methoxyphenyl

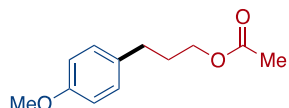
trifluoromethanesulfonate (51.2 mg, 0.20 mmol, 1.0 equiv) and 4-(chloromethyl)-2,2-dimethyl-1,3-dioxolane (28.3 μ L, 0.20 mmol, 1.0 equiv) as substrates. After 48 h, the crude reaction mixture was loaded onto silica gel and purified by column chromatography (20:1 pentane/EtOAc) to afford the product (23.0 mg, 52% yield) as a colorless oil. 1 H NMR matched those reported in the literature,⁴ however, our report is missing one 13 C NMR signal.

1 H NMR (500 MHz, CDCl₃) δ 7.14 – 7.11 (m, 2H), 6.85 – 6.82 (m, 2H), 4.31 – 4.26 (m, 1H), 3.95 (dd, *J* = 8.1, 5.9 Hz, 1H), 3.79 (s, 3H), 3.63 (dd, *J* = 8.1, 7.0 Hz, 1H), 2.95 (dd, *J* = 13.7, 6.1 Hz, 1H), 2.72 (dd, *J* = 13.8, 7.2 Hz, 1H), 1.43 (s, 3H), 1.35 (s, 3H).

13 C{ 1 H} NMR (126 MHz, CDCl₃) δ 158.4, 130.3, 129.7, 114.0, 109.2, 69.1, 55.4, 39.3, 27.1, 25.9.

HRMS (ESI⁺) [M+H]⁺ m/z calcd for C₁₃H₁₉O₃⁺ 223.1329, [M+NH₄]⁺ m/z calcd for C₁₃H₂₂NO₃⁺ 240.1594, [M+Na]⁺ m/z calcd for C₁₃H₁₈O₃Na⁺ 245.1148; a solution in acetonitrile with 10 mM NH₄OAc found: 223.1326, 240.1588, 245.1142.

IR (cm⁻¹) 2986, 2936, 2836, 1613, 1513, 1245, 1058, 1035, 731.



3-(4-methoxyphenyl)propyl acetate (3.38) [CAS: 125092-37-7]

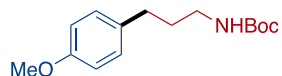
The general procedure for electron rich arenes was followed with 4-methoxyphenyl trifluoromethanesulfonate (51.2 mg, 0.20 mmol, 1.0 equiv) and 3-chloropropyl acetate (27.3 mg, 0.20 mmol, 1.0 equiv) as substrates. After 48 h, the crude reaction mixture was loaded onto silica gel and purified by column chromatography (gradient from 20:1 pentane/EtOAc to 10:1 pentane/EtOAc) to afford the product (29.6 mg, 71% yield) as a colorless oil. Characterization data matched those reported in the literature.⁴

¹H NMR (500 MHz, CDCl₃) δ 7.10 (d, *J* = 8.6 Hz, 2H), 6.83 (d, *J* = 8.6 Hz, 2H), 4.07 (t, *J* = 6.6 Hz, 2H), 3.79 (s, 3H), 2.63 (t, *J* = 7.7 Hz, 2H), 2.06 (s, 3H), 1.95 – 1.89 (m, 2H).

¹³C{¹H} NMR (126 MHz, CDCl₃) δ 171.3, 158.0, 133.4, 129.4, 114.0, 64.0, 55.4, 31.4, 30.5, 21.1.

HRMS (ESI⁺) [M+Na]⁺ *m/z* calcd for C₁₂H₁₆O₃Na⁺ 231.0992; a solution in acetonitrile with 10 mM NH₄OAc found: 231.0992.

IR (cm⁻¹) 2953, 2836, 1735, 1512, 1235, 1034, 810.



***tert*-butyl (3-(4-methoxyphenyl)propyl)carbamate (3.39) [CAS: 1227797-33-2]**

The general procedure for electron rich arenes was followed with 4-methoxyphenyl trifluoromethanesulfonate (51.2 mg, 0.20 mmol, 1.0 equiv) and *tert*-butyl (3-chloropropyl)carbamate (38.7 mg, 0.20 mmol, 1.0 equiv) as substrates. After 48 h, the crude reaction mixture was loaded onto silica gel and purified by column chromatography (gradient from 20:1 pentane/EtOAc to 10:1 pentane/EtOAc) to afford the product (31.1 mg, 59% yield) as a colorless oil. ¹H NMR matched those reported in the literature,⁵⁸ however, ¹³C NMR has not been reported.

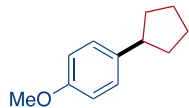
¹H NMR (500 MHz, CDCl₃) δ 7.09 (d, *J* = 8.6 Hz, 2H), 6.82 (d, *J* = 8.6 Hz, 2H), 4.53 (s, 1H), 3.78 (s, 3H), 3.14 (q, *J* = 6.7 Hz, 2H), 2.58 (t, *J* = 7.6 Hz, 2H), 1.77 (quint, *J* = 7.4 Hz, 2H), 1.44 (s, 9H).

Reported peaks are for the major Boc rotamer. A minor rotamer is present, but too low in concentration to effectively characterize.

¹³C{¹H} NMR (126 MHz, CDCl₃) δ 158.0, 156.1, 133.7, 129.4, 114.0, 79.2, 55.4, 40.3, 32.3, 32.1, 28.6.

HRMS (ESI⁺) [M+H]⁺ *m/z* calcd for C₁₅H₂₄NO₃⁺ 266.1751, [M+NH₄]⁺ *m/z* calcd for C₁₅H₂₇N₂O₃⁺ 283.2016, [M+Na]⁺ *m/z* calcd for C₁₅H₂₃NO₃Na⁺ 288.1570; a solution in acetonitrile with 10 mM NH₄OAc found: 266.1743, 283.2009, 288.1562.

IR (cm⁻¹) 3349, 2976, 2933, 1688, 1511, 1243, 1165, 1036.



1-cyclopentyl-4-methoxybenzene (3.40) [CAS: 1507-97-7]

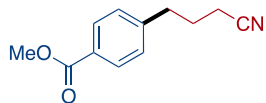
The general procedure for electron rich arenes was followed with 4-methoxyphenyl trifluoromethanesulfonate (51.2 mg, 0.20 mmol, 1.0 equiv) and chlorocyclopentane (20.9 mg, 0.20 mmol, 1.0 equiv) as substrates. After 48 h, the crude reaction mixture was loaded onto silica gel and purified by column chromatography (100:1 pentane/EtOAc) to afford the product (14.2 mg, 40% yield) as a colorless oil. Characterization data matched those reported in the literature.⁴

¹H NMR (500 MHz, CDCl₃) δ 7.16 (d, *J* = 8.5 Hz, 2H), 6.84 (d, *J* = 8.7 Hz, 2H), 3.79 (s, 3H), 2.97 – 2.90 (m, 1H), 2.07 – 2.01 (m, 2H), 1.83 – 1.75 (m, 2H), 1.71 – 1.62 (m, 2H), 1.58 – 1.50 (m, 2H).

¹³C{¹H} NMR (126 MHz, CDCl₃) δ 157.8, 138.7, 128.1, 113.8, 55.4, 45.3, 34.9, 25.6.

HRMS (ESI+) [M+H]⁺ m/z calcd for C₁₂H₁₇O⁺ 177.1274; ASAP-MS found: 177.1272.

IR (cm⁻¹) 2950, 2867, 2834, 1612, 1512, 1242, 1177, 1038, 824.



Methyl 4-(3-cyanopropyl)benzoate (3.41)

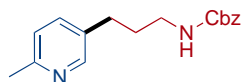
The general procedure for electron rich arenes was followed with methyl 4-(((trifluoromethyl)sulfonyl)oxy)benzoate (142.1 mg, 0.50 mmol, 1.0 equiv) and 4-chlorobutanenitrile (51.8 mg, 0.50 mmol, 1.0 equiv) as substrates. After 48 h, the crude reaction mixture was loaded onto silica gel and purified by column chromatography (10:1 hexanes/EtOAc) to afford the product (84.3 mg, 83% yield) as a white solid. Characterization data matched those reported in the literature.⁵⁹

¹H NMR (500 MHz, CDCl₃) δ 7.97 – 7.95 (m, 2H), 7.24 (dd, *J* = 8.4, 2.3 Hz, 2H), 3.88 (s, 3H), 2.81 (t, *J* = 7.3 Hz, 2H), 2.31 (t, *J* = 7.1 Hz, 2H), 2.01 – 1.94 (m, 2H).

¹³C{¹H} NMR (126 MHz, CDCl₃) δ 166.9, 145.1, 130.0, 128.6, 128.5, 119.2, 52.1, 34.4, 26.6, 16.5.

HRMS (ESI+) [M+H]⁺ m/z calcd for C₁₂H₁₄NO₂⁺ 204.1019, [M+NH₄]⁺ m/z calcd for C₁₂H₁₇N₂O₂⁺ 221.1285; a solution in acetonitrile with 10 mM NH₄OAc found: 204.1016, 221.1281.

IR (cm⁻¹) 2928, 2235, 1706, 1604, 1431, 1270, 1173, 1098, 757, 701.



Benzyl (3-(6-methylpyridin-3-yl)propyl)carbamate (3.42)

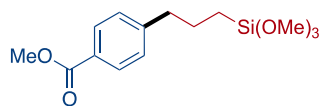
The general procedure for electron rich arenes was followed with 6-methylpyridin-3-yl trifluoromethanesulfonate (120.6 mg, 0.50 mmol, 1.0 equiv) and benzyl (3-chloropropyl)carbamate (113.8 mg, 0.50 mmol, 1.0 equiv) as substrates. After 24 h, the crude reaction mixture was loaded onto silica gel and purified by column chromatography (70:30 hexanes/EtOAc) to afford the product (86.7 mg, 61% yield) as a colorless oil.

¹H NMR (500 MHz, DMSO) δ 8.28 (s, 1H), 7.50 (dd, *J* = 7.9, 2.3 Hz, 1H), 7.39 – 7.29 (m, 6H), 7.15 (d, *J* = 7.9 Hz, 1H), 5.02 (s, 2H), 3.01 (q, *J* = 6.6 Hz, 2H), 2.54 (t, *J* = 7.7 Hz, 2H), 2.42 (s, 3H), 1.74 – 1.64 (m, 2H).

¹³C{¹H} NMR (126 MHz, DMSO) δ 156.6, 155.6, 149.2, 137.7, 136.6, 134.3, 128.8, 128.2, 128.2, 123.1, 65.6, 31.4, 29.4, 24.0.

HRMS (ESI+) [M+H]⁺ m/z calcd for C₁₇H₂₁N₂O₂⁺ 285.1598; a solution in acetonitrile with 10 mM NH₄OAc found: 285.1591.

IR (cm⁻¹) 3420, 1706, 1252, 1047, 1021, 1000, 819, 757.



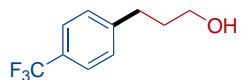
Methyl 4-(3-(trimethoxysilyl)propyl)benzoate (3.43)

The general procedure for electron rich arenes was followed with methyl 4-((trifluoromethyl)sulfonyl)oxy)benzoate (142.1 mg, 0.50 mmol, 1.0 equiv) and (3-chloropropyl)trimethoxysilane (99.4 mg, 0.50 mmol, 1.0 equiv) as substrates. After 24 h, the crude reaction mixture was loaded onto silica gel and purified by column chromatography (60:40 hexanes/EtOAc) to afford the product (28.3 mg, 19% yield) as a viscous colorless oil.

¹H NMR (500 MHz, CDCl₃) δ 7.98 – 7.95 (m, 2H), 7.27 – 7.25 (m, 2H), 3.92 (s, 3H), 3.58 (s, 9H), 2.71 (t, *J* = 7.6 Hz, 2H), 1.81 – 1.74 (m, 2H), 0.71 – 0.67 (m, 2H).

¹³C{¹H} NMR (126 MHz, CDCl₃) δ 167.2, 147.8, 129.6, 128.6, 127.8, 51.9, 50.5, 39.0, 24.3, 8.9.

IR (cm⁻¹) 2927, 1711, 1280, 1110, 901, 720, 647.



3-(4-(Trifluoromethyl)phenyl)propan-1-ol (3.44) [CAS: 180635-74-9]

The general procedure for electron rich arenes was followed with 4-(trifluoromethyl)phenyl trifluoromethanesulfonate (147.1 mg, 0.50 mmol, 1.0 equiv) and 3-chloropropan-1-ol (47.3 mg, 0.50 mmol, 1.0 equiv) as substrates. After 24 h, the crude reaction mixture was loaded onto silica gel and purified by column chromatography (70:30 hexanes/EtOAc) to afford the product (51.2 mg, 50% yield) as a colorless oil. Characterization data matched those reported in the literature.⁶⁰

¹H NMR (400 MHz, CDCl₃) δ 7.53 (d, *J* = 8.0 Hz, 2H), 7.30 (d, *J* = 8.0 Hz, 2H), 3.67 (t, *J* = 6.4 Hz, 2H), 2.81 – 2.73 (m, 2H), 1.98 – 1.80 (m, 2H), 1.75 (s, 1H).

$^{13}\text{C}\{^1\text{H}\}$ NMR (101 MHz, CDCl_3) δ 146.0 (q, $J = 1.5$ Hz), 128.8, 128.3 (q, $J = 32.4$ Hz), 125.3 (q, $J = 3.8$ Hz) 124.4 (q, $J = 271.8$ Hz), 61.9, 33.8, 31.9.

$^{19}\text{F}\{^1\text{H}\}$ NMR (377 MHz, CDCl_3) δ -62.3.

3.9. References

- (1) Weix, D. J. Methods and Mechanisms for Cross-Electrophile Coupling of Csp^2 Halides with Alkyl Electrophiles. *Acc. Chem. Res.* **2015**, *48*, 1767–1775.
- (2) Gu, J.; Wang, X.; Xue, W.; Gong, H. Nickel-catalyzed reductive coupling of alkyl halides with other electrophiles: concept and mechanistic considerations. *Org. Chem. Front.* **2015**, *2*, 1411–1421.
- (3) Wang, X.; Dai, Y.; Gong, H. Nickel-Catalyzed Reductive Couplings. *Top. Curr. Chem.* **2016**, *374*, 43.
- (4) Kim, S.; Goldfogel, M. J.; Gilbert, M. M.; Weix, D. J. Nickel-Catalyzed Cross-Electrophile Coupling of Aryl Chlorides with Primary Alkyl Chlorides. *J. Am. Chem. Soc.* **2020**, *142*, 9902–9907.
- (5) Chi, B. K.; Widness, J. K.; Gilbert, M. M.; Salgueiro, D. C.; Garcia, K. J.; Weix, D. J. In-Situ Bromination Enables Formal Cross-Electrophile Coupling of Alcohols with Aryl and Alkenyl Halides. *ACS Catal.* **2022**, *12*, 580–586.
- (6) Komeyama, K.; Ohata, R.; Kiguchi, S.; Osaka, I. Highly nucleophilic vitamin B12-assisted nickel-catalysed reductive coupling of aryl halides and non-activated alkyl tosylates. *Chem. Commun.* **2017**, *53*, 6401–6404.
- (7) Molander, G. A.; Traister, K. M.; O'Neill, B. T. Engaging Nonaromatic, Heterocyclic Tosylates in Reductive Cross-Coupling with Aryl and Heteroaryl Bromides. *J. Org. Chem.* **2015**, *80*, 2907–2911.
- (8) Huihui, K. M. M.; Caputo, J. A.; Melchor, Z.; Olivares, A. M.; Spiewak, A. M.; Johnson, K. A.; DiBenedetto, T. A.; Kim, S.; Ackerman, L. K. G.; Weix, D. J. Decarboxylative Cross-Electrophile Coupling of N-Hydroxyphthalimide Esters with Aryl Iodides. *J. Am. Chem. Soc.* **2016**, *138*, 5016–5019.
- (9) Salgueiro, D. C.; Chi, B. K.; Guzei, I. A.; Garcia-Reynaga, P.; Weix, D. J. Control of Redox-Active Ester Reactivity Enables a General Cross-Electrophile Approach to Access Arylated Strained Rings. *Angew. Chem., Int. Ed.* **2022**, *61*, e202205673.
- (10) Wang, J.; Ehehalt, L. E.; Huang, Z. D.; Beleh, O. M.; Guzei, I. A.; Weix, D. J. Formation of $\text{C}(\text{sp}^2)\text{-C}(\text{sp}^3)$ Bonds Instead of Amide C-N Bonds from Carboxylic Acid and Amine Substrate Pools by Decarbonylative Cross-Electrophile Coupling. *J. Am. Chem. Soc.* **2023**, *145*, 9951–9958.
- (11) Zarate, C.; van Gemmeren, M.; Somerville, R. J.; Martin, R. Chapter Four - Phenol Derivatives: Modern Electrophiles in Cross-Coupling Reactions. In *Adv. Organomet. Chem.*, Pérez, P. J. Ed.; Vol. 66; Academic Press, 2016; pp 143–222.
- (12) Joshi-Pangu, A.; Wang, C.-Y.; Biscoe, M. R. Nickel-Catalyzed Kumada Cross-Coupling Reactions of Tertiary Alkylmagnesium Halides and Aryl Bromides/Triflates. *J. Am. Chem. Soc.* **2011**, *133*, 8478–8481.

(13) Huang, X.; Teng, S.; Chi, Y. R.; Xu, W.; Pu, M.; Wu, Y.-D.; Zhou, J. S. Enantioselective Intermolecular Heck and Reductive Heck Reactions of Aryl Triflates, Mesylates, and Tosylates Catalyzed by Nickel. *Angew. Chem., Int. Ed.* **2021**, *60*, 2828–2832.

(14) Sumida, Y.; Sumida, T.; Hosoya, T. Nickel-Catalyzed Reductive Cross-Coupling of Aryl Triflates and Nonaflates with Alkyl Iodides. *Synthesis* **2017**, *49*, 3590–3601.

(15) Duan, J. C.; Du, Y. F.; Pang, X. B.; Shu, X. Z. Ni-catalyzed cross-electrophile coupling between vinyl/aryl and alkyl sulfonates: synthesis of cycloalkenes and modification of peptides. *Chem. Sci.* **2019**, *10*, 8706–8712.

(16) Huang, L. B.; Ackerman, L. K. G.; Kang, K.; Parsons, A. M.; Weix, D. J. LiCl-Accelerated Multimetallic Cross-Coupling of Aryl Chlorides with Aryl Triflates. *J. Am. Chem. Soc.* **2019**, *141*, 10978–10983.

(17) Kang, K.; Huang, L. B.; Weix, D. J. Sulfonate Versus Sulfonate: Nickel and Palladium Multimetallic Cross-Electrophile Coupling of Aryl Triflates with Aryl Tosylates. *J. Am. Chem. Soc.* **2020**, *142*, 10634–10640.

(18) Everson, D. A.; Jones, B. A.; Weix, D. J. Replacing Conventional Carbon Nucleophiles with Electrophiles: Nickel-Catalyzed Reductive Alkylation of Aryl Bromides and Chlorides. *J. Am. Chem. Soc.* **2012**, *134*, 6146–6159.

(19) Krasovskiy, A.; Knochel, P. Convenient Titration Method for Organometallic Zinc, Magnesium, and Lanthanide- Reagents. *Synthesis* **2006**, 890–891.

(20) (a) Czaplik, W. M.; Mayer, M.; Jacobi von Wangenheim, A. Domino Iron Catalysis: Direct Aryl-Alkyl Cross-Coupling. *Angew. Chem., Int. Ed.* **2009**, *48*, 607–610. (b) Krasovskiy, A.; Duplais, C.; Lipshutz, B. Zn-Mediated, Pd-Catalyzed Cross-Couplings in Water at Room Temperature Without Prior Formation of Organozinc Reagents. *J. Am. Chem. Soc.* **2009**, *131*, 15592–15593.

(21) Klein, P.; Lechner, V. D.; Schimmel, T.; Hintermann, L. Generation of Organozinc Reagents by Nickel Diazadiene Complex Catalyzed Zinc Insertion into Aryl Sulfonates. *Chem.–Eur. J.* **2020**, *26*, 176–180.

(22) This was observed to a lesser extent in the work of Hintermann (reference 21), where 4-carboxymethylphenyl tosylate provided a lower yield of arylzinc reagent than electron neutral or electron-rich substrates.

(23) Feng, C.; Cunningham, D. W.; Easter, Q. T.; Blum, S. A. Role of LiCl in Generating Soluble Organozinc Reagents. *J. Am. Chem. Soc.* **2016**, *138*, 11156–11159.

(24) McCann, L. C.; Organ, M. G. On The Remarkably Different Role of Salt in the Cross-Coupling of Arylzincs From That Seen With Alkylzincs. *Angew. Chem., Int. Ed.* **2014**, *53*, 4386–4389.

(25) Eckert, P.; Sharif, S.; Organ, M. G. Salt to Taste: The Critical Roles Played by Inorganic Salts in Organozinc Formation and in the Negishi Reaction. *Angew. Chem., Int. Ed.* **2021**, *60*, 12224–12241.

(26) Kermagoret, A.; Braunstein, P. Mono- and Dinuclear Nickel Complexes with Phosphino-, Phosphinito-, and Phosphonitopyridine Ligands: Synthesis, Structures, and Catalytic Oligomerization of Ethylene. *Organometallics* **2008**, *27*, 88–99.

(27) Judge, J. S.; Reiff, W. M.; Intille, G. M.; Ballway, P.; Baker, W. A. Five-Co-Ordinate Complexes of First Transition Series Ions with 2,2',2"-Terpyridine. *J. Inorg. Nucl. Chem.* **1967**, *29*, 1711–1716.

(28) Bejan, E.; Aït-Haddou, H.; Daran, J.-C.; Balavoine, G. G. A. Enaminones in the Synthesis of New Polyaza Heterocycles. *Eur. J. Org. Chem.* **1998**, *12*, 2907–2912.

(29) Hansen, E. C.; Pedro, D. J.; Wotal, A. C.; Gower, N. J.; Nelson, J. D.; Caron, S.; Weix, D. J. New Ligands for Nickel Catalysis from Diverse Pharmaceutical Heterocycle Libraries. *Nat. Chem.* **2016**, *8*, 1126–1130.

(30) Hansen, E. C.; Li, C.; Yang, S.; Pedro, D.; Weix, D. J. Coupling of Challenging Heteroaryl Halides with Alkyl Halides via Nickel-Catalyzed Cross-Electrophile Coupling. *J. Org. Chem.* **2017**, *82*, 7085–7092.

(31) Yu, P.; Morandi, B. Nickel-Catalyzed Cyanation of Aryl Chlorides and Triflates Using Butyronitrile: Merging Retro-Hydrocyanation with Cross-Coupling. *Angew. Chem. Int. Ed.* **2017**, *56*, 15693–15697.

(32) Dürr, A. B.; Yin, G.; Kalvet, I.; Napol, F.; Schoenebeck, F. Nickel-Catalyzed Trifluoromethylthiolation of Csp^2 -O Bonds. *Chem. Sci.* **2016**, *7*, 1076–1081.

(33) Lovering, G. J.; Aparece, M. D.; Morken, J. P. Pd-Catalyzed Conjunctive Cross-Coupling between Grignard-Derived Boron “Ate” Complexes and $C(sp^2)$ Halides or Triflates: NaOTf as a Grignard Activator and Halide Scavenger. *J. Am. Chem. Soc.* **2017**, *139*, 3153–3160.

(34) Cho, S.; Wang, Q. Ortho-Difunctionalization of Arynes by $LiZnEt_2$ (TMP)-Mediated Deprotonative Zincation/Elimination of Aryl Triflates. *Tetrahedron* **2018**, *74*, 3325–3328.

(35) Zhang, K.-F.; Christoffel, F.; Baudoin, O. Barbier–Negishi Coupling of Secondary Alkyl Bromides with Aryl and Alkenyl Triflates and Nonaflates. *Angew. Chem. Int. Ed.* **2018**, *57*, 1982–1986.

(36) Vinogradova, E. V.; Park, N. H.; Fors, B. P.; Buchwald, S. L. Palladium-Catalyzed Synthesis of N-Aryl Carbamates. *Org. Lett.* **2013**, *15*, 1394–1397.

(37) Hackenberger, D.; Song, B.; Grünberg, M. F.; Farsadpour, S.; Menges, F.; Kelm, H.; Groß, C.; Wolff, T.; Niedner-Schatteburg, G.; Thiel, W. R.; et al. Bimetallic Cu/Pd Catalysts with Bridging Aminopyrimidinyl Phosphines for Decarboxylative Cross-Coupling Reactions at Moderate Temperature. *ChemCatChem.* **2015**, *7*, 3579–3588.

(38) Muto, K.; Yamaguchi, J.; Itami, K. Nickel-Catalyzed C–H/C–O Coupling of Azoles with Phenol Derivatives. *J. Am. Chem. Soc.* **2012**, *134*, 169–172.

(39) Jolly, P. I.; Fleary-Roberts, N.; O’Sullivan, S.; Doni, E.; Zhou, S.; Murphy, J. A. Reactions of Triflate Esters and Triflamides with an Organic Neutral Super-Electron-Donor. *Org. Biomol. Chem.* **2012**, *10*, 5807–5810.

(40) Kendall, A. J.; Salazar, C. A.; Martino, P. F.; Tyler, D. R. Direct Conversion of Phosphonates to Phosphine Oxides: An Improved Synthetic Route to Phosphines Including the First Synthesis of Methyl JohnPhos. *Organometallics* **2014**, *33*, 6171–6178.

(41) Cui, L.-C.; Zhang, Z.-Q.; Lu, X.; Xiao, B.; Fu, Y. Pd-Catalyzed Cross-Coupling of 1,1-Diborylalkanes with Aryl Triflates. *RSC Adv.* **2016**, *6*, 51932–51935.

(42) Cong, F.; Wei, Y.; Tang, P. Combining Photoredox and Silver Catalysis for Azidotrifluoromethoxylation of Styrenes. *Chem. Commun.* **2018**, *54*, 4473–4476.

(43) Shi, S.; Szostak, M. Efficient Synthesis of Diaryl Ketones by Nickel-Catalyzed Negishi Cross-Coupling of Amides by Carbon–Nitrogen Bond Cleavage at Room Temperature Accelerated by a Solvent Effect. *Chem.–Eur. J.* **2016**, *22*, 10420–10424.

(44) Lin, X.; Qing, F.-L. Palladium-Catalyzed Anti-Markovnikov Hydroalkylation of Homoallylic Alcohols Bearing β -Fluorines. *Org. Lett.* **2013**, *15*, 4478–4481.

(45) Ejiri, S.; Odo, S.; Takahashi, H.; Nishimura, Y.; Gotoh, K.; Nishihara, Y.; Takagi, K. Negishi Alkyl–Aryl Cross-Coupling Catalyzed by Rh: Efficiency of Novel Tripodal 3-Diphenylphosphino-2-(diphenylphosphino)methyl-2-methylpropyl Acetate Ligand. *Org. Lett.* **2010**, *12*, 1692–1695.

(46) Everson, D. A.; Shrestha, R.; Weix, D. J. Nickel-Catalyzed Reductive Cross-Coupling of Aryl Halides with Alkyl Halides. *J. Am. Chem. Soc.* **2010**, *132*, 3636–3636.

(47) Vechorkin, O.; Proust, V.; Hu, X. Functional Group Tolerant Kumada–Corriu–Tamao Coupling of Nonactivated Alkyl Halides with Aryl and Heteroaryl Nucleophiles: Catalysis by a Nickel Pincer Complex Permits the Coupling of Functionalized Grignard Reagents. *J. Am. Chem. Soc.* **2009**, *131*, 9756–9766.

(48) He, Y.; Han, B.; Zhu, S. Terminal-Selective C(sp³)–H Arylation: NiH-Catalyzed Remote Hydroarylation of Unactivated Internal Olefins. *Organometallics* **2021**, *40*, 2253–2264.

(49) Johnson, K. A.; Biswas, S.; Weix, D. J. Cross-Electrophile Coupling of Vinyl Halides with Alkyl Halides. *Chem.–Eur. J.* **2016**, *22*, 7399–7402.

(50) Treacy, S. M.; Rovis, T. Copper Catalyzed C(sp³)–H Bond Alkylation via Photoinduced Ligand-to-Metal Charge Transfer. *J. Am. Chem. Soc.* **2021**, *143*, 2729–2735.

(51) Nani, R. R.; Reisman, S. E. α -Diazo- β -ketonitriles: Uniquely Reactive Substrates for Arene and Alkene Cyclopropanation. *J. Am. Chem. Soc.* **2013**, *135*, 7304–7311.

(52) Miao, P.; Li, R.; Lin, X.; Rao, L.; Sun, Z. Visible-light induced metal-free cascade Wittig/hydroalkylation reactions. *Green Chemistry* **2021**, *23*, 1638–1641.

(53) Liu, Z.; Cao, S.; Yu, W.; Wu, J.; Yi, F.; Anderson, E. A.; Bi, X. Site-Selective C–H Benzylation of Alkanes with N-Triftosylhydrazones Leading to Alkyl Aromatics. *Chem* **2020**, *6*, 2110–2124.

(54) Luo, S.; Peng, M.; Querard, P.; Li, C.-C.; Li, C.-J. Copper-Catalyzed Conjugate Addition of Carbonyls as Carbanion Equivalent via Hydrazones. *J. Org. Chem.* **2021**, *86*, 13111–13117.

(55) Sun, B.; Zheng, S.; Mo, F. Transition metal- and light-free radical borylation of alkyl bromides and iodides using silane. *Chem. Commun.* **2021**, *57*, 5674–5677.

(56) Dohle, W.; Lindsay, D. M.; Knochel, P. Copper-Mediated Cross-Coupling of Functionalized Arylmagnesium Reagents with Functionalized Alkyl and Benzylic Halides. *Org. Lett.* **2001**, *3*, 2871–2873.

(57) Rigoulet, M.; Thillary du Boullay, O.; Amgoune, A.; Bourissou, D. Gold(I)/Gold(III) Catalysis that Merges Oxidative Addition and π -Alkene Activation. *Angew. Chem. Int. Ed.* **2020**, *59*, 16625–16630.

(58) Tsui, G. C.; Menard, F.; Lautens, M. Regioselective Rhodium(I)-Catalyzed Hydroarylation of Protected Allylic Amines with Arylboronic Acids. *Org. Lett.* **2010**, *12*, 2456–2459.

(59) Rathnayake, M. D.; Weaver, J. D., III. Coupling Photocatalysis and Substitution Chemistry to Expand and Normalize Redox-Active Halides. *Org. Lett.* **2021**, *23*, 2036–2041.

(60) Kobayashi, M.; Itoh, S.; Yoshimura, K.; Tsukamoto, Y.; Obora, Y. Iridium Complex-Catalyzed C2-Extension of Primary Alcohols with Ethanol via a Hydrogen Autotransfer Reaction. *J. Org. Chem.* **2020**, *85*, 11952–11958.

